A THEORETICAL AND EXPERIMENTAL INVESTIGATION OF STEADY AND UNSTEADY LAMINAR FLOW OF AIR IN TUBES SUBJECTED TO HIGH INLET TEMPERATURES

A THESIS

Presented to

The Faculty of the Graduate Division

by

Arthur Chilton Bruce

In Partial Fulfillment

of the Requirements for the Degree

Doctor of Philosophy in the

School of Aerospace Engineering

Georgia Institute of Technology

October, 1967

In presenting the dissertation as a partial fulfillment of the requirements for an advanced degree from the Georgia Institute of Technology, I agree that the Library of the Institute shall make it available for inspection and circulation in accordance with its regulations governing materials of this type. I agree that permission to copy from, or to publish from, this dissertation may be granted by the professor under whose direction it was written, or, in his absence, by the Dean of the Graduate Division when such copying or publication is solely for scholarly purposes and does not involve potential financial gain. It is understood that any copying from, or publication of, this dissertation which involves potential financial gain will not be allowed without written permission:

3/17/65
b

A THEORETICAL AND EXPERIMENTAL INVESTIGATION OF STEADY AND UNSTEADY LAMINAR FLOW OF AIR IN TUBES SUBJECTED TO HIGH INLET TEMPERATURES

Approved:

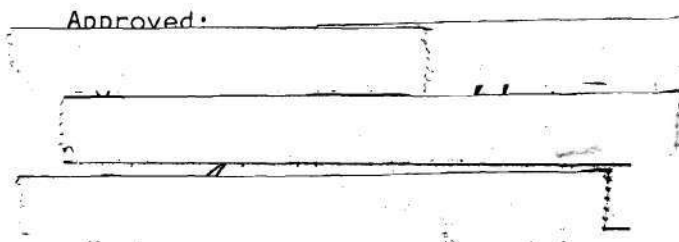

Date approved by Chairman: 5/8/68

ACKNOWLEDGEMENTS

The author wishes to express his sincere appreciation to his thesis advisors, Dr. A. L. Ducoffe, Director of the School of Aerospace Engineering, and Dr. F. M. White, Jr., formerly Associate Professor of Aerospace Engineering, for suggesting this research and for their interest and many valuable suggestions during its progress.

The author is also indebted to Professor J. E. Hubbart and Dr. J. C. Wu for their review, helpful criticism, and discussion of this work.

Indebtedness to the personnel of the Aerospace Engineering Shop and the many graduate students who so generously assisted in the experimental phase of this work is gratefully acknowledged.

Finally, the author wishes to express his gratitude to his wife, Joyce Clementine, and his family for their enduring patience and sacrifice demonstrated during the course of this work. This thesis is dedicated to them with love.

TABLE OF CONTENTS

LIST OF TABLES

LIST OF ILLUSTRATIONS

LIST OF ILLUSTRATIONS (Continued)

NOMENCLATURE

A_1	internal tube cross-section area
A_2	internal tube wetted surface area
A_j	coefficient, equation (91)
a	empirical friction factor parameter, equation (74)
B_j	coefficient, equation (92)
C_j	coefficient, equation (93)
$C_{1,2,3}$	constants, equation (105)
c_p	fluid specific heat at constant pressure
c_w	wall material specific heat
D, D_i	tube internal diameter
D_j	coefficient, equation (94)
D_o	tube outside diameter
dA	differential area element
dV	differential volume element
E_j	coefficient, equation (97)
e	fluid specific internal energy
F_j	coefficient, equation (97)
f	friction factor
G	mass flux at tube exit
Gr_o	Grashof number, equation (56)
g	gravitational constant
h_i	forced convection heat transfer coefficient
h_o	free convection heat transfer coefficient

K	Poiseuille tube calibration constant
$K_{1,2,3,4}$	constants, equation (81)
k	fluid conductivity
k_w	wall conductivity
L	tube length
M	Mach number
Nu_i	forced convection Nusselt number
Nu_o	free convection Nusselt number
n_i	unit normal vector
P	Langhaar pressure function
Pr	Prandtl number
p	pressure
$p_{1,2,3,4}$	experimental pressures, Figure 1
q	dynamic pressure
q_w	heat flux vector
R	gas constant or tube internal radius
R_o	tube external radius
Rey	local Reynolds number
Rey_a	Reynolds number based on ambient temperature $\frac{GD}{\mu a}$
r	tube radial coordinate
T, T_g	gas temperature
T_a	ambient temperature
T_o	mean temperature, equation (53)
T_w	wall temperature
t	time or wall thickness
t/D_i	wall thickness to tube internal diameter ratio

U	one-dimensional fluid velocity
u	longitudinal component of fluid velocity
x	longitudinal position
x/D_i	dimensionless longitudinal position
α_w	wall thermal diffusivity
β	reciprocal mean temperature $1/T_o$
γ	gas specific heat ratio
Δp, Δp_1	test tube pressure drop $p_1 - p_E$
Δp_2	Poiseuille tube pressure drop
δ_{ik}	Kronecker delta
ϵ	tube wall emissivity
Θ	positive constant, equation (83)
μ	fluid dynamic viscosity coefficient
ν	fluid kinematic viscosity coefficient
ρ	fluid density
ρ_w	wall material density
σ	Stephan-Boltzmann constant or dimensionless longitudinal position variable
τ_w	wall shear stress

Subscripts

a	ambient conditions
E	at tube exit
1	at tube entrance
j	position index, j = 0,1,2, . . . M,M+1
o	with reference to mean temperature, equation (53)
p	Poiseuille tube

w	wall property

Superscripts

*	nondimensionalized with reference to ambient temperature

Other

$( )_j^n$	n^{th} time step, j^{th} position step
$\overline{( )}$	average cross-section property

SUMMARY

The compressible unsteady laminar flow of air in long slender tubes subjected to a step function increase in the inlet air temperature is considered in terms of both an experimental investigation and the formulation of an appropriate theoretical analysis to supplement the experiment. The experiments deal with flow in copper tubes of fixed diameter with length to internal diameter ratios of 400, 600, 800, and 1000, a wall thickness to internal diameter ratio of 0.3, and with the tube external surface free to cool to its surroundings by natural convection and radiation. It was found that laminar flow in the tubes could be obtained for Reynolds numbers less than 1250. A suitably designed furnace at the tube inlet provided inlet gas temperatures up to approximately 1000 ^{o}F. Each of the test tubes was instrumented to obtain results for the centerline gas and tube wall temperature distributions from entrance to exit and the experimental setup was designed to allow measurements of the tube overall pressure drop. The mass flow through the test tube was measured by means of the pressure drop across a calibrated Poiseuille tube attached to the exit end of the test tube.

Execution of the experimental investigation was divided into two essential parts. First, each test tube was utilized in a series of runs with cold flow (flow at the temperature of the ambient surroundings) that encompassed the range of Reynolds numbers from 100 to 1250 in order to provide accurate details of the pressure drop that could be expected for cold flow. The second portion of the experiments for each tube

consisted of hot flow runs for Reynolds numbers of approximately 850 and 1200 with gas inlet temperatures of approximately 600, 800, and 950 ^{o}F, the highest temperature being attainable only for the high Reynolds number flow. Each hot flow run was initiated by allowing the air at elevated temperature from the furnace to flow through the test tube which was initially at a temperature equal to that of its ambient (room temperature) surroundings, thus, with ensuing time the tube heats up, the gas temperatures increase, and the tube pressure drop is increased. During the course of the run the gas inlet temperature and the mass flow through the tube, as measured by the Poiseuille tube downstream of the test tube, were held constant insofar as manual control of these variables allowed.

These hot flow runs provided measurements of pressure drop and gas and wall temperatures during the time interval between initiation of the run and approximate attainment of equilibrium flow. The experiment was not, however, designed to provide detailed measurements of the small time transients occuring immediately following the beginning of a run and pertaining to the movement through the tube of a thermal contact discontinuity which originates at the tube entrance. These initial transients should be of a duration of the order of a second, whereas the significant time increments pertinent to the experiments were considered to be of the order of one-half minute or larger.

The experimental results indicate that the tube pressure drop is significantly influenced by the gas inlet temperature and that this dependence is more pronounced at the higher Reynolds numbers. The experimental temperature distributions likewise are dependent on the gas

inlet temperature and Reynolds number but show, within experimental accuracy, no dependence on the tube length. Correspondingly, the change in the tube pressure drop showed no significant dependence on tube length for the lengths of tube utilized. In all cases the tube lengths were sufficiently long to ensure that the gas temperature at the tube exit was for all practical purposes equal to the ambient temperature of the tube surroundings. Evaluation of the experimental results in terms of precise observations of the dependence of the flow variables on the various parameters of the problem was made difficult by the limited number of experiments that could be conducted in a reasonable time and the inability to closely control the mass flow and inlet temperature both during a run and for purposes of repeating a run at the same value of these parameters.

A theoretical analysis of the flow problem defined by the experimental phase of the investigation is presented together with comparisons with the experiment and predictions of the dependence of the tube pressure drop on time, length to diameter ratio, mass flow, inlet temperature, and thickness to diameter ratio. The theory is based on a derivation of the governing equations for the flow and a tube wall thermal energy balance which follow from application of the general integral equations for conservation of mass, momentum, and energy. In this derivation the problem is formulated in terms of a one-dimensional representation of all variables as dependent upon only the longitudinal position. The fluid flow difference equations appropriate to this description are then simplified by noting that the flow can be assumed to be quasi-steady and that the Mach number is essentially zero. The wall

thermal energy equation is given in terms of a one-dimensional representation of a heat balance which includes forced convection heating from the gas, longitudinal conduction in the wall, and cooling due to natural convection and radiation to the external ambient surroundings. With the application of flow boundary conditions corresponding to a constant inlet temperature, exit mass flow, and exit pressure, together with the assumption that the ends of the tube are insulated, the complete problem is presented in a form suitable for numerical computation. As a consequence of the quasi-steady nature of the fluid flow the difference equations for the fluid are ordinary equations but are coupled to the wall equation through the wall temperature. Thus the wall equation, which is of a parabolic nature, provides the essential mechanism for unsteadiness in the problem.

A solution of the system of difference equations is effected by utilizing a six-point implicit difference scheme for the wall energy equation together with a standard Runge-Kutta method for integration of the fluid equations. In order to carry out the solution information pertaining to the fluid flow friction factor and Nusselt number are required as inputs. Accordingly, a friction factor formula is postulated by representing the analytical results of Langhaar (J. Appl. Mech., 2, 55, 1942) in terms of a hyperbola with a friction factor parameter which is determined empirically from the cold flow experimental results for each test tube. A constant value of the Nusselt number that matches the theoretical predictions to the hot flow pressure drop results obtained experimentally for the short test tube is found and utilized for all theoretical predictions.

The theoretical computation procedure is applied for the hot flow conditions pertaining to each experiment and a comparison of theory and experiment shows good agreement for the range of the parameters investigated. Based on this agreement the theory is utilized to investigate the dependence of the tube pressure drop on the various parameters involved; it is found that the dependence of the tube pressure drop on the primary parameter, the gas inlet temperature, is linear over the range of temperatures investigated. Whereas the tube length shows no appreciable influence on the change in the pressure drop due to hot flow, the tube wall thickness is found to possess significant influence. For small values of the wall thickness to diameter ratio, corresponding to thin walled tubes, the time response of the flow is shorter and the pressure drop effects are larger corresponding to the higher gas temperatures attained. An essential limitation of the validity of the theory is encountered for very thin walled tubes due to violation of the quasi-steady assumption. On the other hand, the theory is also limited to tube walls that are not too thick due to neglect of radial variations of the wall temperatures.

Based on the experimental and theoretical findings, it is concluded that the major portion of the hot flow influence on the tube pressure drop arises from effects in the flow development region near the tube entrance.

CHAPTER I

INTRODUCTION

The consideration of laminar flow in tubes has its origin in the classical literature of the past century. In its simplest formulation it is one of the relatively few viscous flow problems that produce an exact solution. In terms of a less restrictive formulation, such as may be demanded in modern applications, it is, at best, a formidable problem which is not amenable to exact analytical solution and which doubtfully can be handled by numerical techniques on even the most capable of present day computers. In view of the magnitude of the general problem it is obvious that a great deal of pertinent research would be directed toward consideration of various smaller facets of a complicating nature to the general problem. Whereas some of this work, which will be reviewed briefly in subsequent sections, is instructive, it is generally not applicable piecewise to the general problem due to the restrictive assumptions that are necessary to make these analyses tractable. On the other hand, there exists the possibility that a general analysis may be formulated by approximate means if one is willing to forego extreme details of the problem in favor of an overall or averaged result. Such an analysis may be referred to as an "engineering approach" and it is the intent of the present work to present such an approach to a fairly general problem dealing with the laminar flow of air in tubing.

Review of the Literature

The problem of flow in tubes, although undoubtedly an early consideration in the subject of hydraulics, first appears in the literature in serious form during the first half of the nineteenth century. Since that time the accumulation of literature dealing specifically with the problem has become extensive. While much of the literature is old, it is interesting to note many new additions in recent years, which serve to increase our understanding of the general tube flow problem and to point out the shortcomings of our present state of knowledge with regards to it.

The first appearance in the literature of any concrete investigation of the tube flow problem is usually credited to Hagen (1)*. In an experimental investigation he successfully correlated the flow rate of water through narrow tubes to the tube pressure drop, length, and radius. Almost simultaneously, Poiseuille (2), in dealing with capillar tubes, arrived at similar conclusions. The result of these investigations is the well-known fundamental law for fully developed laminar flow in tubes, the Hagen-Poiseuille law. The work of Reynolds (3) added essential details to a more general understanding of the problem with definitive experiments on transition to turbulence and the importance of the Reynold's number in both transition studies as well as correlation of experimental results.

The restrictions, as evidenced by experiment, on the applicability of the Hagen-Poiseuille law to only a fully developed laminar flow

* Numbers in parentheses refer to references appearing in the Literature Cited.

were well known prior to the twentieth century. The character of the development of the flow from an initially uniform velocity distribution at the tube inlet was, likewise, at least partially understood, having been accounted for by Hagen as a kinetic energy term in his correlation of experimental results. Poiseuille, on the other hand, only noted that his correlation formula did not work for short tubes. Subsequent work, dealing with the flow development due to friction downstream of the tube inlet is summarized by Goldstein (4). He credits Boussinesq (5) with the first theoretical treatment of the inlet development and gives details of the boundary-layer-like approaches to the development region due to Schiller (6) and the unpublished work of Atkinson and Goldstein. The latter works are generally conceded to be somewhat superior to Boussinesq's results very near the tube inlet when compared to the experimental results of Nikuradse presented by Prandtl and Tietjens (7).

Typical of the development problem, the preceding works yield results for the longitudinal pressure distribution, the longitudinal velocity distribution across a tube section, and an estimate of the development length. They are, however, somewhat unwieldy in that they utilize a boundary layer approach with subsequent series solutions. A fairly recent analysis by Langhaar (8) circumvents this difficulty by a linearizing approximation to the Navier-Stokes equation and subsequent authors have favored Langhaar's results for both comparative purposes and extensions of the development problem to include thermodynamic considerations. Without the use of Langhaar's linearization, Hornbeck (9) has presented an interesting numerical solution which essentially verifies Langhaar's results for the pressure distribution but seems to

indicate that the linearization is not well justified for the generation of velocity profiles. It may be fairly stated that a typical characteristic of the inlet development problem at this point is its essentially parabolic nature as evidenced by the success of the boundary-layer-like approach. On the other hand the preceding work is restricted to steady, laminar, incompressible flow without heat transfer at the tube walls.

A natural extension or generalization of the hydrodynamic problem is the consideration, in addition to viscous effects, of the effects of heat transfer through the tube wall. An early result for heat transfer in fully developed laminar flow with constant wall temperature was given by Graetz (10) with the same solution rediscovered twenty-five years later by Nusselt (11). An excellent evaluation of this work is given by Jakob (12) who also summarizes the small amount of available experimental data and notes that the neglect of radial flow components may be a probable source for the discrepancy between experiment and the analytical results of Graetz. A more recent review is given by Sellars, Tribus, and Klein (13).

In an attempt to extend the thermodynamic problem to include the development region, Kays (14) has presented a numerical solution for the laminar flow heat transfer with simultaneously developing velocity and temperature profiles. He, however, neglects radial velocity components and utilizes Langhaar's results for the velocity profiles in order to solve for the temperature profiles from a parabolic boundary-layer-like energy equation. That is, longitudinal conduction is considered negligible in comparison to convection. He obtains solutions for the

heat transfer in terms of Nusselt numbers for the conditions of constant wall temperature, constant heat flux, and constant temperature difference between the tube wall and the flowing fluid, and illustrates good comparisons with experimental results (15). A refinement of Kays' work to include the radial component of velocity in the entrance region by utilizing Langhaar velocity profiles together with the continuity equation is given by Ulrichson and Schmitz (16). Their results indicate a significant over-estimate of the Nusselt number in the development region due to the neglect, as in Kays' work, of the radial velocity component.

The obvious restrictions of the previous work are their common assumption of constant physical properties and consideration of only highly specialized thermal boundary conditions at the tube wall. Extensions to discard these restrictions have been presented. Tribus and Klein (17) give a review of the problem of dealing with the thermal boundary conditions and present an incompressible, constant properties analysis for non-isothermal surfaces. With large radial temperature gradients, the effects of variable properties are discussed by Deissler (18) who considers fully developed flow, by Sze (19) who neglects radial velocity components but considers flow development, and by Davenport and Leppert (20) who postulate a radial velocity component and by numerical solutions give results which indicate that the effects of radial velocity components are significant to estimates of the local friction factor.

Without regard to transient phenomena, it is evident that a detailed treatment of the general steady-state laminar tube flow problem

is a very difficult one. Even with the assumptions of a boundary-layer-like system of governing equations and restrictions to certain specified simple thermal boundary conditions at the tube wall, accurate treatment of the development region, variable properties, and radial flow effects seem to demand utilization of rather complicated numerical schemes. When the additional complications of unsteadiness due to either varying flow conditions or coupling with a tube wall of finite thickness and heat capacity are introduced, even the numerical approach begins to appear unrealistic in its magnitude. As in the extension of the tube flow problem to include the effects of heat transfer, first attempts at incorporating the complication of unsteadiness are made with the simplest possible realistic flow model.

In an attempt to provide practical calculation tools for consideration of transient temperature problems, Dusinberre (21) has presented a compact numerical method with example applications to three typical types of problems. By means of a heat balance between the flowing fluid and the tube wall and finite difference approximations he provides formulae for calculation of the time dependent tube wall and gas temperatures. His approach is essentially a one-dimensional formulation in that variations of the problem variables with radial position are not specified. Further, inasmuch as the hydrodynamics of the problem are specified, no flow response, that is, the effect of the changing temperatures upon flow variables, is investigated. His analysis, however, lays the ground rules for the calculation of the unsteady flow problem in terms of a formulation of a realistic magnitude.

Following the Dusinberre method, Rooks (22) has examined the more complicated problem including the coupling of the flow with the transient heat balance between the fluid and tube wall. In addition, Rooks specifies natural boundary conditions exterior to the tube wall, allowing the tube wall to be cooled by natural convection and radiation to the surrounding ambient atmosphere. The coupling considered by Rooks is provided only through the friction factor term in a steady one-dimensional fluid momentum equation, inasmuch as he assumes the flow is essentially incompressible and fully developed insofar as the tube pressure drop is concerned. Further, a natural simplification is employed in assuming that the fluid flow energy equation is representable in terms of a quasi-steady heat balance whereas the tube wall heat balance dictates the unsteadiness in the problem.

Nature of the Investigation

The present investigation is concerned with the response of a laminar flow of air through long slender tubes to an appreciable step function increase of inlet air temperature. The tube wall is made of conducting material and is free to absorb heat from the internal tube flow as well as to be cooled externally in a natural manner by natural convection and radiation to the surrounding atmosphere.

Inherently, the response problem is a compressible unsteady flow problem. The unsteady effects which dictate the response may, however, be described in terms of three separate mechanisms. These are the initial transient effects connected with the movement of a thermal contact discontinuity down the tube following the elevation of inlet air

temperature, the unsteadiness induced by the changing wall temperatures, and any unsteadiness incorporated in the flow boundary conditions. In the present work the initial transients are of very short duration and the boundary conditions placed on the tube flow are independent of time, so that the only unsteadiness effects to be considered are the large-time effects due to heating up of the tube wall.

The boundary conditions stipulated for the flow provide that the temperature of the air at the tube inlet after the initial step function increase, the mass flow rate at the tube exit, and the pressure at the tube exit all remain constant during the course of each experiment. The initial conditions describe the flow before the step function increase of inlet air temperature to consist of a "cold" flow through a "cold" tube. The "cold" flow designation is utilized to imply a flow at the same temperature as the ambient surroundings as opposed to the "hot" flow which ensues as a result of the inlet temperature increase.

Purpose of the Research

The purpose of the present investigation is to formulate a simplified approach to the laminar, compressible, unsteady flow of air in tubes which are subjected to natural thermal boundary conditions and which involve unsteadiness due to changes in temperature at the tube inlet.

A specific objective of the experimental portion of this work is to provide a limited amount of experimental data involving consideration of three primary parameters of the tube flow problem. These are the mass flow rate, the tube length to diameter ratio, and the inlet air temperature.

The specific objectives of the analytical work contained in this thesis are, first, to formulate the approximate governing equations for the tube and the flow in the tube within the framework of a one-dimensional description, second, to consider solutions to these equations subject to further simplifying assumptions, and finally, to examine the theoretical effects of variations in the three primary tube flow parameters plus an additional parameter, the tube wall thickness to diameter ratio.

The problem as described and treated in the present work originated from studies concerned with flow in tubes conducted in the School of Aerospace Engineering at The Georgia Institute of Technology (22, 23, 24). Emphasis in these studies has been placed on the need for good engineering estimates of the overall performance of tube systems. Due to the utility of its application, an adequate simple analysis is considered superior in this respect to a more detailed analysis which generally would be more cumbersome in its application to complicated systems. This philosophy is not only desirable but is practically demanded in the present work if answers for the generalized tube flow problem are desired.

CHAPTER II

EXPERIMENTAL EQUIPMENT AND INSTRUMENTATION

Complete Experimental Setup

The basic experimental apparatus and instrumentation are shown in the schematic representation of Figure 1. Air at a line pressure of approximately 125 psig. is regulated to 30 psig. in the surge tank and the subsequent air flow into the furnace is metered by means of a fine micro-needle valve. After leaving the furnace the hot air is fed directly into a small air reservoir and then into the test tube. Downstream of the test tube is positioned a calibrated Poiseuille tube for accurate measurement of the mass flow rate of air passing through the test tube. The air exits from the Poiseuille tube into the atmosphere.

Air Furnace

The details of construction of the furnace used to heat the air prior to entry into the test tube are shown in Figure 2. It would be desirable for stability purposes during constant temperature operation to construct a furnace of heavy, high heat capacity material. It was found, however, that such a furnace, which was initially employed, required excessive times to reach equilibrium and to effect changes in temperature for subsequent experiments. The furnace used therefore represents a compromise between stability and the ability to change operation to a different temperature without wasted time.

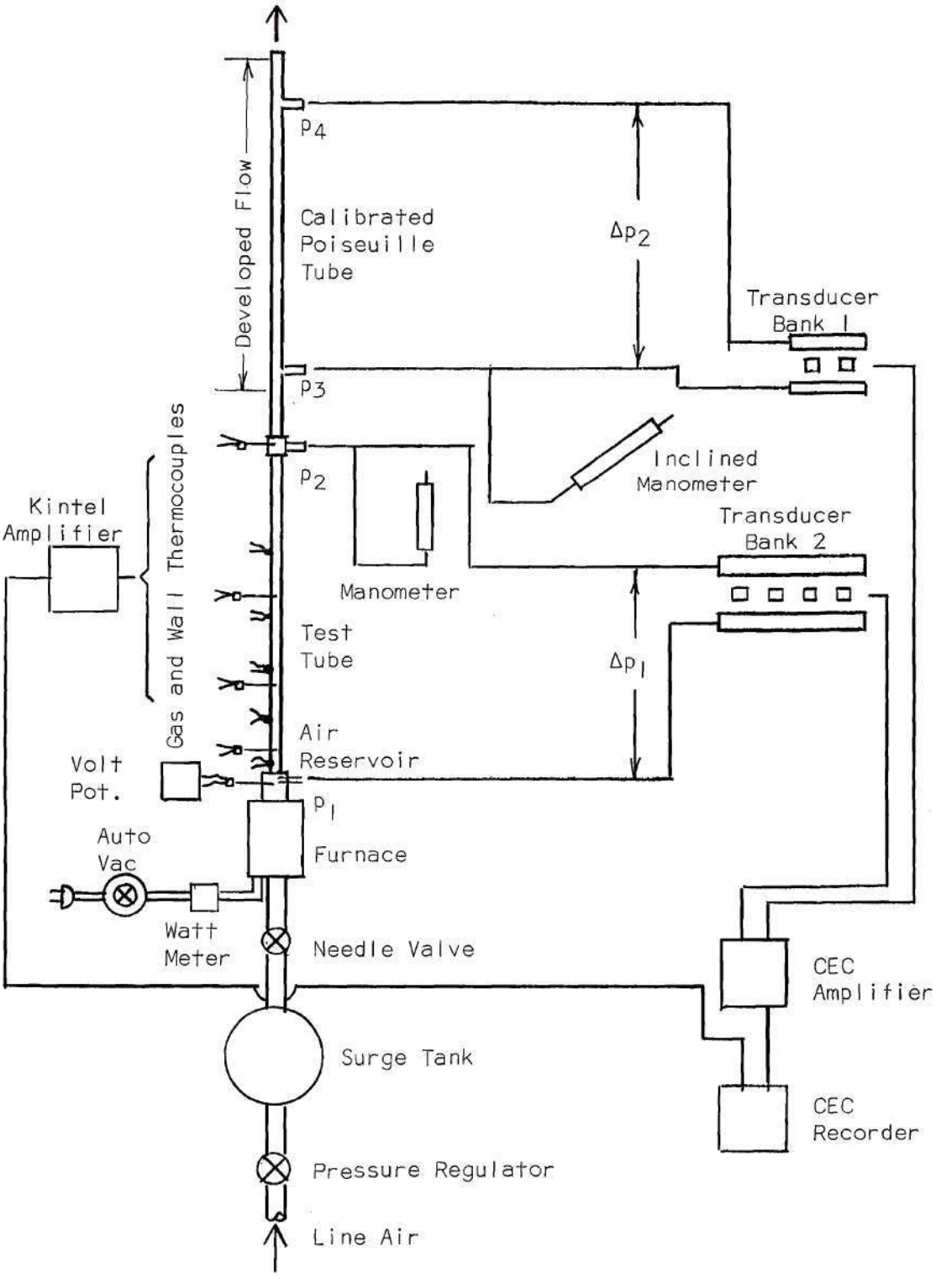

Figure 1. Overall Experimental Setup

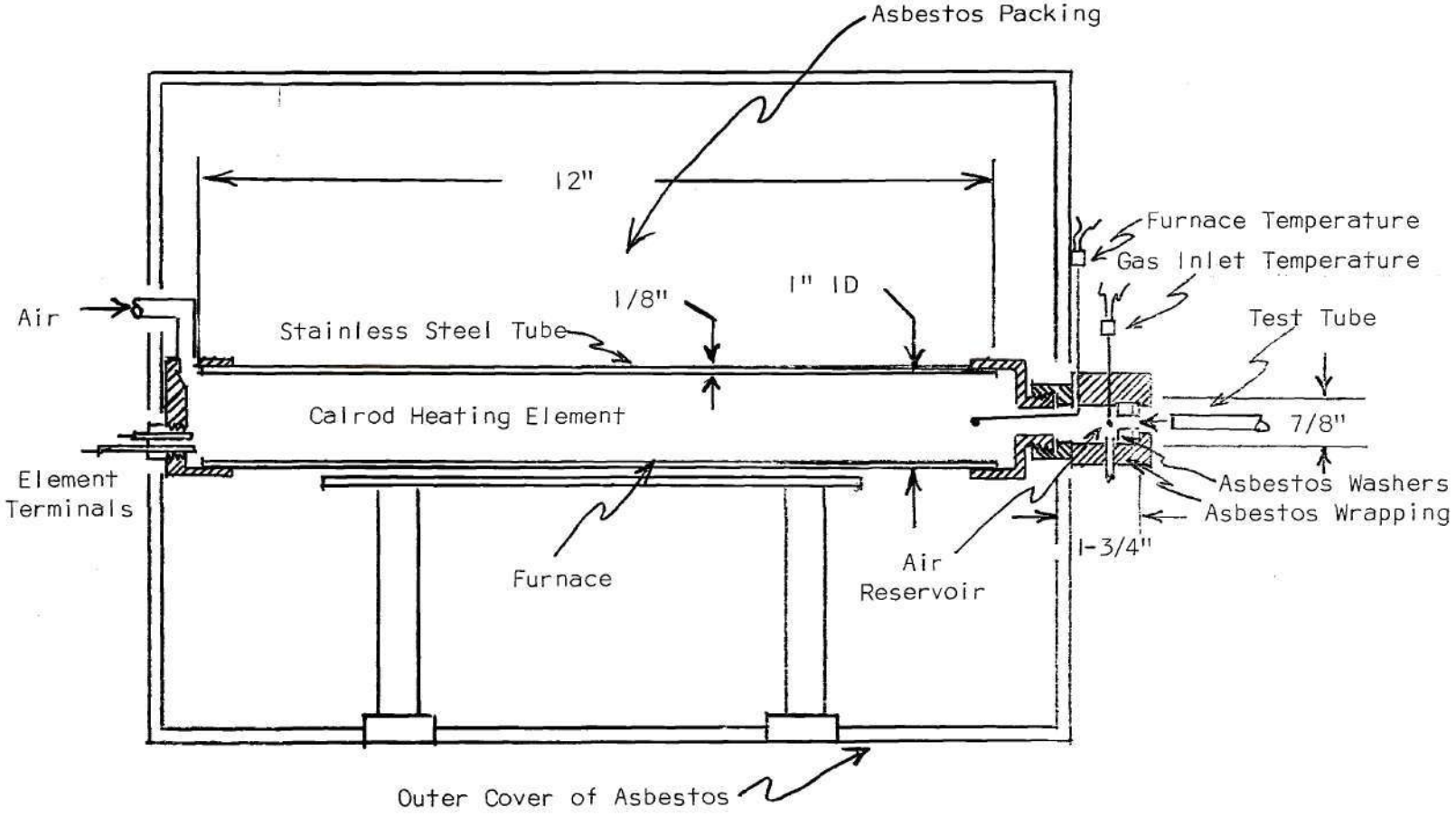

Figure 2. Details of Furnace Construction

The basic ingredient of the furnace is a 1500 watt General Electric Calrod heating element capable of continuous operation at temperatures up to 1500 ^{o}F. This Calrod element, which may be bent without internal damage to a radius of bend equal to the rod sheath diameter (0.260 in.), was wound upon itself to yield a cylinder of active element approximately 12 inches long and something under one inch in diameter. This unit was inserted into a stainless steel tube and sealed at both ends by steel caps. The rear cap contains provisions for a sealed extension of the Calrod terminals and admission of air from the metering valve. The forward cap provides for exit of the hot air into an affixed air reservoir constructed of lightweight steel and insulated on the outside with approximately 3/8 inches of asbestos wrapping. Interior to the reservoir and at its forward end are provided two 1/4 inch thick asbestos washers which provide a fairly snug fit for insertion of the test tube. Small leaks at this junction are considered negligible inasmuch as the tube mass flow is measured downstream of the test tube, and are preferred to a heat-conducting sealed joint which would be contrary to the objective of the experiment. After assembly the entire furnace body was packed in granulated asbestos to a minimum depth of three inches on any side within an outer cover of asbestos board.

Test Tubes

The test tubes were constructed of hard drawn copper with an internal diameter of 0.00975 feet, a thickness to internal diameter ratio of 0.3, and length to internal diameter ratios of 400, 600, 800, and

1000. Appropriate physical properties, dimensions, and locations for both gas and wall temperature thermocouples are given in Table I.

Instrumentation

The instrumentation employed in the experiments may be broken down into the required components for measurement of pressures and temperatures.

Pressure Measuring System

The pressure drop across the test tube was measured, as indicated in Figure 1, by means of a manifolded bank of four differential pressure transducers with linear ranges of ± 0.01, ± 0.05, ± 0.20, and ± 0.50 psid, respectively. Clamps were provided for the high and low sides of each of the first three transducers in order to isolate them from the system if the operating differential pressure exceeded their capacity. A similar bank of two differential pressure transducers with ranges of ± 0.01 and ± 0.05 psid was employed to measure the pressure drop across the calibrated Poiseuille tube. Transducer signals were amplified by a Consolidated Electrodynamics Type 5-114 recording oscillograph. Also as shown in Figure 1, the pressure p_2 at the downstream end of the test tube and the pressure p_3 at the first tap of the Poiseuille tube were measured by means of vertical and inclined Alcohol manometers with respective sensitivities of 4.3200 and 0.4026 psf/in. Al.

Temperature Measuring System

Gas and tube wall temperatures were measured by means of chromel-alumel thermocouples. The gas thermocouples were of a shielded variety

Table I. Test Tube Physical Properties and Characteristic Dimensions

Physical Properties *

Material: copper

Density: $\rho_w = 559$ lb/ft^3

Conductivity: $k_w = 222$ Btu/hr ft ^oF

Specific Heat: $c_w = 0.0915$ Btu/lb ^oF

Thermal Diffusivity: $\alpha_w = 4.353$ ft^2/hr

Emissivity (oxidized): $\epsilon = 0.725$

Geometrical Dimensions

Diameter, inside: $D_i = 0.00975$ ft

Diameter, outside: $D_o = 0.01562$ ft

Thickness to Internal Diameter Ratio: $t/D_i = 0.3$

Lengths: L = 46.875 in., 70.125 in., 93.562 in., 117.000 in.

Length to Diameter Ratios: L/D = 400, 600, 800, 1000

Thermocouple Locations from Tube Entrance

Gas Thermocouples		L/D = 400	L/D = 600	L/D = 800	L/D = 1000
T_1	x/D_i =	-1.00	-1.00	-1.00	-1.00
T_{g_1}		19.24	19.02	19.52	19.70
T_{g_2}		48.24	48.54	49.36	49.10
T_{g_3}		146.80	147.42	147.20	147.40
T_{g_4}		400.00	600.00	800.00	1000.00
Wall Thermocouples					
T_{w_1}	x/D_i =	5.97	5.98	4.48	6.60
T_{w_2}		29.48	28.86	29.44	29.40
T_{w_3}		58.94	58.80	58.96	59.40
T_{w_4}		98.36	98.40	98.00	98.30
T_{w_5}		196.00	197.22	196.24	196.00

* Reference (25), p. 498

(Baldwin-Lima-Hamilton HT micro-miniature, Type TCA-IP-200) and were inserted through the tube wall to a depth such that the tip was located on the tube centerline. They were then silver soldered in this position. The wall thermocouples were fabricated from chromel-alumel thermocouple wire and were seated into the tube wall to half the wall thickness. These were likewise silver soldered in place. All thermocouple signals were amplified by means of Kintel DC amplifiers and recorded along with the pressure signals. The only exception was the gas inlet temperature which was read by means of a Leeds Northrup 8687 volt potentiometer.

Control

Only two provisions for control of the experiment were provided. The first of these was the manual micro-needle valve for air flow control and the second was a variable voltage AC transformer to control the power input to the furnace. The latter was likewise manually operated.

Calibration

A complete calibration of the pressure drop and temperature instrumentation was found to be necessary at the beginning of each day's operation. Calibration of the pressure drop system consisted of utilizing the Poiseuille tube to generate successively higher pressure drops which were fed to both transducer banks and recorded while making simultaneous measurements with the vertical and inclined manometers.

The instrumentation channels for temperature measurement were calibrated by using the Leeds Northrup volt potentiometer to generate

accurate digital voltages which were applied to each temperature channel and recorded.

Experimental Accuracy

An evaluation of the overall accuracy of the experimental measurements must entail consideration not only of the instrumentation utilized to obtain the pressure drops and temperatures but also of the method of control provided for the unsteady flow experiments. With regards to the instrumentation, care was exercised in the choice of transducers, amplifiers, and recorder to provide a high degree of potential accuracy for the measurement of both pressure drops and temperatures. Likewise, the calibration of these systems was carefully carried out.

The accuracy of the pressure drop measurements, including calibration, zero drifts, and interpretation of oscillograph records is estimated to be well within an experimental accuracy of 5 per cent. For a sufficiently large number of carefully controlled runs all of these errors would enter in a random fashion and the steady cold flow runs, which by their nature are closely controlled, demonstrate very good accuracy well within the 5 per cent estimate.

The accuracy of measurement of the temperatures may be discussed in two parts corresponding to the tube wall temperatures and the gas temperatures. The tube wall temperatures are estimated to be within 3 per cent generally. It is difficult, however, to estimate the accuracy of the gas temperature measurements inasmuch as the thermocouples utilized for these measurements are of a shielded variety and are

exposed along their length to the radial temperature distribution of the tube fluid flow. As a consequence, the accuracy of measurement of the gas temperatures should not be considered to be better than approximately 5 per cent. Aside from accuracy of measurement, the gas temperatures obtained represent the tube centerline values as opposed to the theoretical bulk temperatures utilized for the analytical study of one-dimensional flow in Chapter V. Strictly speaking then the measured gas temperatures are not to be interpreted as an accurate experimental representation of the theoretically computed temperatures.

An occasional possible exception to the above statements of accuracy for the temperatures may be due to exceeding the linear range of the DC amplifiers utilized in the temperature measurement system. In the course of the calibration these amplifiers were found to perform to only approximately 70 per cent of their specified linear range and even though an attempt was made to compensate for this in the selection of appropriate gain settings, some overshoot would be possible due to the multiplicity of readings made.

The method of manual control provided for the furnace temperature and the mass flow rate introduces a possible source of significant error in the unsteady hot flow experiments. As mentioned previously, the furnace temperature was not perfectly stable and compensation for drift had to be effected manually. Also, inasmuch as the test tube pressure drop increases with time during the course of each hot flow run, the mass flow rate through the tube system, as observed on the inclined manometer, tends to decrease unless proper compensation is provided by means of the manual mass flow control needle valve. This compensation

was hindered by the slow response of the inclined manometer and is deemed to be the major significant error incorporated in the hot flow experiments. A certain degree of skill was accomplished in handling this compensation procedure; uncertainty, however, requires that an estimate of accuracy for the hot flow runs be set at approximately 10 per cent maximum error in pressure drop.

CHAPTER III

EXPERIMENTAL PROCEDURE

The procedure of the experiments performed in the present investigation may be explained in terms of the two different types of experimental runs conducted. The first of these, referred to as cold flow runs, corresponds to the flow of air at ambient temperature through the tubes. The second type of experiment, the hot flow runs, deals with flow at elevated inlet temperatures.

Cold Flow

The cold flow experiments, which are steady state flows, were designed to provide a description of the pressure drop and friction factor which could be expected from each of the test tubes, L/D_i = 400, 600, 800, and 1000, for the range of laminar flow investigated as represented by the flow Reynolds number. Preliminary trial runs on each test tube allowed a calibration of the inclined manometer (as shown in Figure 1 to measure p_3) readings which correspond to the flow Reynolds number or the mass flow through the system. This calibration, which did not include provision for ambient temperature changes, was utilized to select approximately a series of five flow rates descriptive of and restricted to laminar flow, as well as to predict which of the transducers in each of the two manifolded banks would be applicable to any mass flow setting.

The cold flow tests were then conducted by recording the two pressure drops and two pressures, as described previously in the description of the experimental setup, corresponding to each mass flow setting on the inclined manometer for each test tube. Simultaneous readings of ambient temperature and pressure were also made and repetitive runs were performed to insure repeatability of the results.

Hot Flow

The hot flow experiments utilized the same experimental setup as employed for the cold flow, with the exception of the added instrumentation for gas and wall temperatures. In these experiments the time history or response of the test tube pressure drop, gas temperatures, and wall temperatures are recorded following the introduction of hot air into an initially cold tube. The procedure followed to accomplish this consisted of first adjusting the manual mass flow and furnace temperature controls to give a steady flow through the test tube corresponding to the selected mass flow rate and inlet air temperature of the run. Without change in these control settings the test tube was then pulled out from its snug seat in the air reservoir on the forward end of the furnace and a short length of substitute tubing was inserted. This piece of substitute tube was pinched down to represent a restriction to the flow similar to that provided by the actual test tube. In its disconnected state the test tube was then cooled to ambient conditions with the aid of a sponge, cold water, and a time lapse of approximately 10 minutes. At this time the mass flow control was turned down slightly to correspond to the lower pressure drop anticipated initially for the

hot flow run and the run was commenced by starting the recording oscillograph and inserting the cold test tube into its seat in the air reservoir. The duration of each run was limited to 5.5 minutes, such time being sufficient to approximately reach an equilibrium steady state hot flow.

Inasmuch as the pressure drop across the test tube changes with time due to increasing gas temperatures, it was necessary to visually monitor the flow rate by means of the inclined manometer and make necessary adjustments in the flow rate with the needle valve upstream of the furnace. Simultaneously, any drift in the furnace temperature, as evidenced by changes in the inlet temperature, were manually opposed by adjustment of the furnace power transformer. Due to the method of commencing the hot flow runs and the manual control of mass flow rates for small times, the experiments inherently afforded measurements corresponding only to the quasi-steady flow ensuing after initial transients. Recordings of pressure drops and temperatures during the run interval were thus obtained on the oscillograph while simultaneously reading the two appropriate pressures and the gas inlet temperature at preselected time intervals corresponding to 0.25, 0.50, 0.75, 1.0, 1.25, 3.5, and 5.5 minutes. This procedure was then repeated for each of the selected mass flow rates, inlet temperatures, and test tubes.

CHAPTER IV

EXPERIMENTAL RESULTS

The experimental results obtained for the cold flow and hot flow runs with the four test tubes are shown in Table A-I and Table A-2, respectively, of Appendix A. Comments pertinent to these tables, sample graphical presentations, and a discussion of general observations regarding the results are presented separately in the present section for the cold and hot flow experiments. Further discussion of the specific physical behavior characteristics of the results will be included in Chapter VII, Presentation and Discussion of Results.

Cold Flow

The cold flow pressure drops for the four test tubes, L/D = 400, 600, 800, and 1000, are given in Table A-I. For each tube length the series of pressure drops, corresponding to the five selected mass flow rates, were repeated four times as shown in the table. Corresponding to each pressure drop the Reynolds number and the friction factor, based on ambient conditions, were calculated and are likewise shown in the table. For details of these calculations the reader is referred to Appendix B.

As a representative example of the experimental cold flow results, Figure 3 illustrates a plot of the friction factor versus the Reynolds number for the short test tube, L/D = 400. For purposes of comparison, the theoretical fully developed friction factor

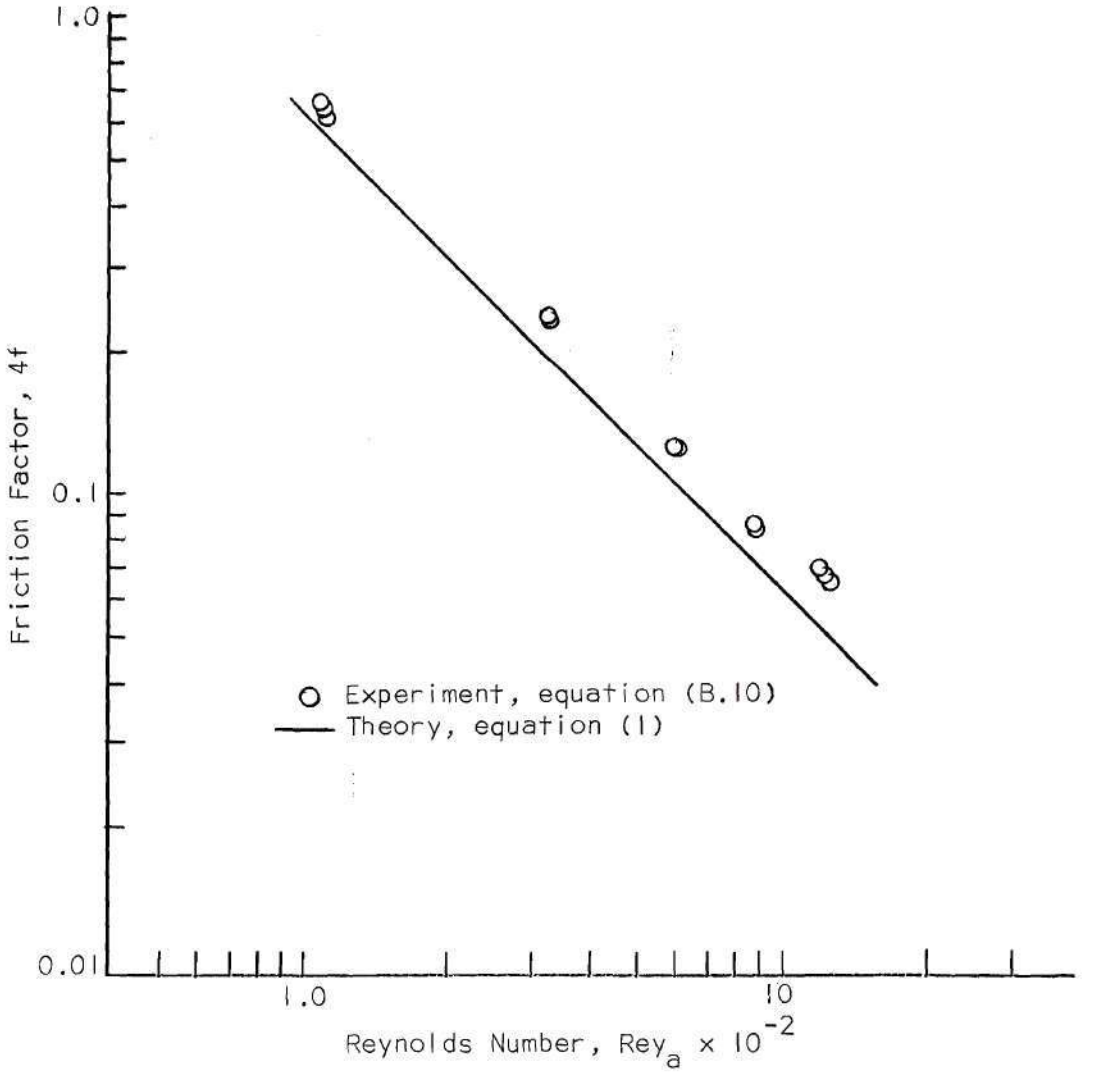

Figure 3. Cold Flow Friction Factors, L/D = 400

$$4f = \frac{64}{Rey_a} \qquad (1)$$

is also shown in the figure. The experimental friction factors are, as expected, higher than the theoretical values corresponding to fully developed flow primarily due to the higher local friction factors in the development region near the entrance of the experimental test tube. Likewise, the experimental values include the pressure drop due to the jump in kinetic energy at the tube inlet and the increase in kinetic energy in the development region. These latter contributions are small in comparison to the contribution due to the development region friction factor, but are not negligible at the higher Reynolds numbers.

The upper limit for the laminar flow Reynolds number in the experimental test tubes was established at approximately 1250. Higher values indicated definite evidence of transition to turbulent flow and accordingly were not included in the scope of the experimental investigation.

It is observed that the cold flow experiments result in data which is sufficiently repeatable. In this respect, the purpose of the cold flow experiments, which was to provide a good indication of the appropriate initial conditions for an unsteady hot flow response study, was considered to have been adequately fulfilled. A systematic representation of the cold flow results is deferred until Chapter VII.

Hot Flow

The hot flow pressure drops and the gas and wall temperatures for the four lengths of test tube are given in Table A-2. For each tube

length five combinations of the Reynolds number, based on ambient temperature, and the inlet temperature were selected to cover the laminar flow range of the tubes and the inlet temperature capability of the furnace. These combinations consisted of runs at an approximate inlet temperature of 600 ^{o}F with Reynolds numbers of approximately 850 and 1200, an inlet temperature of approximately 800 ^{o}F with Reynolds numbers of 850 and 1200, and an inlet temperature of 950 ^{o}F with a Reynolds number of 1200. The calculation of the ambient Reynolds number ($Rey_a = GD_i/\mu_a$), as indicative of the mass flow, was carried out in the same manner as for the cold flow as explained in Appendix B. A hot flow friction factor was not calculated due to the lack of a suitable time invariant reference dynamic pressure as utilized in conventional definitions of the friction factor.

A representative example of the time dependence of the pressure drop for the short test tube is shown in Figure 4 for the five different combinations of Reynolds number and inlet temperature tested. Generally speaking, it is observed that the response of the pressure drop to the increased inlet temperature is a smooth function of time. Some inconsistency of the data for times less than one minute are observable and may be attributed primarily to the combination of manual mass flow control and slow response of the inclined manometer utilized to monitor the mass flow rate. It has been pointed out that the hot flow runs were commenced with a setting of the mass flow control valve slightly below that required for an equilibrium hot flow run at the selected mass flow and inlet temperature. In effect then, for small times the experimental pressure drops may be either above or below the correct values for the

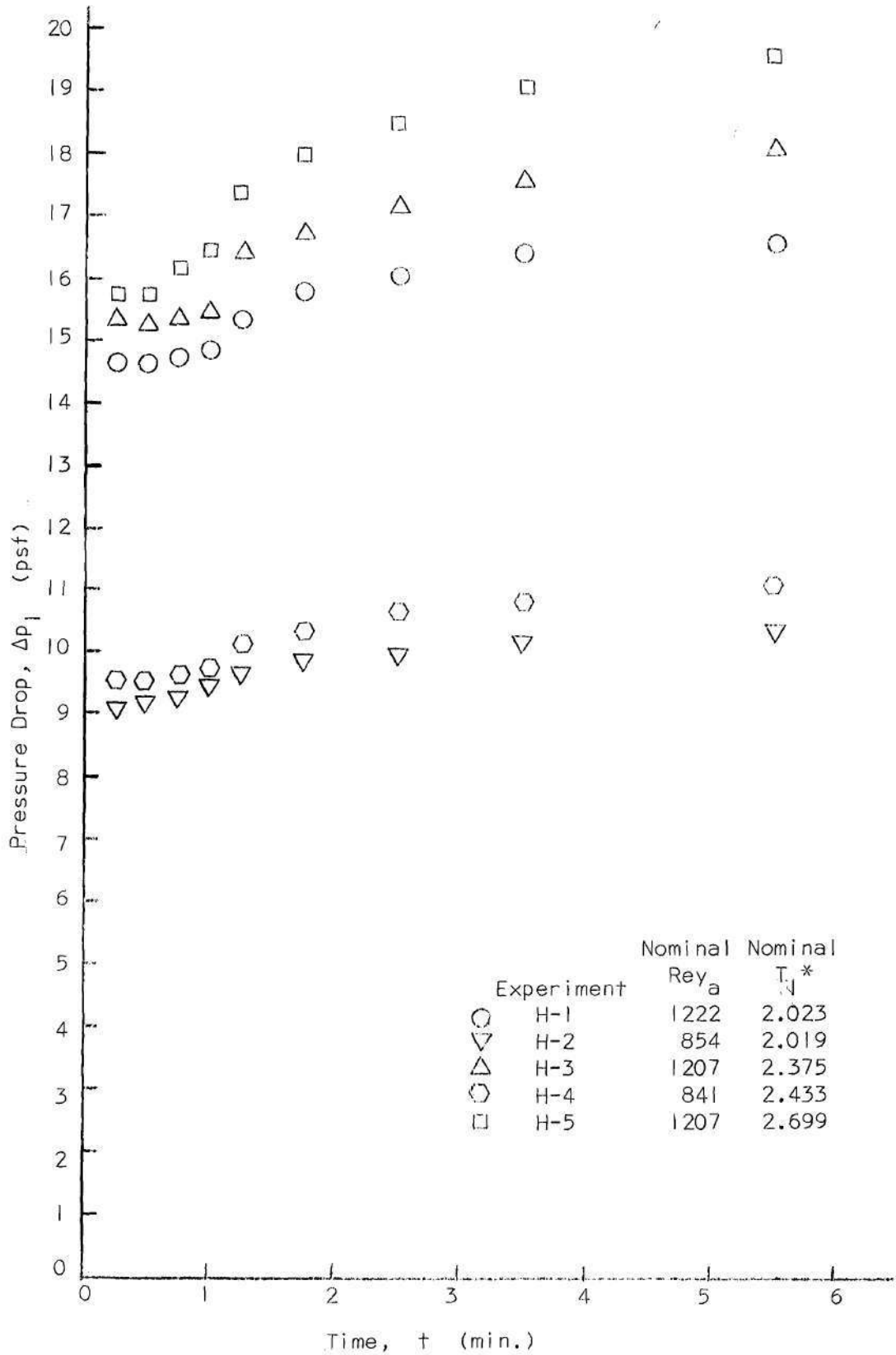

Figure 4. Hot Flow Pressure Drop, L/D = 400

selected mass flow rate due to inaccuracy of the initial setting. For times in the neighborhood of one minute, some scatter should be evident due to efforts to compensate for the changing tube pressure drop and the magnitude of the measured pressure drop should generally be less than or equal the correct value. Finally, due to the preceding, the pressure drops at large times prior to establishment of steady equilibrium hot flow should lag the correct values by some finite time increment. This lag time due to accumulated errors in starting the hot flow runs, while difficult to evaluate, should not exceed approximately 0.25 minutes and consequently the accuracy of the hot flow experiments may generally be estimated to be within a conservative 10 per cent value.

The accuracy of the hot flow runs insofar as repeatability is concerned cannot be demonstrated from the experiments. While each of the hot flow runs were repeated either two or three times for each combination of mass flow and inlet temperature, the results were not comparable in that the flow conditions differed due to the lack of ability to manually control the mass flow and inlet temperature simultaneously to close limits. As a consequence, only one of the attempted repetitive hot flow runs is included in Table A-2 and Figure 4. In each case the included run was selected on the basis of a minimum variation during the run of the Reynolds number based on ambient conditions.

Examples of the measured gas and wall temperatures for an inlet temperature of 801 ^{o}F and a Reynolds number of 1207 are shown in Figures 5 and 6. These results display, as may be expected, large changes in temperature initially near the tube inlet with a relatively fast approach to equilibrium there, whereas changes further down the tube

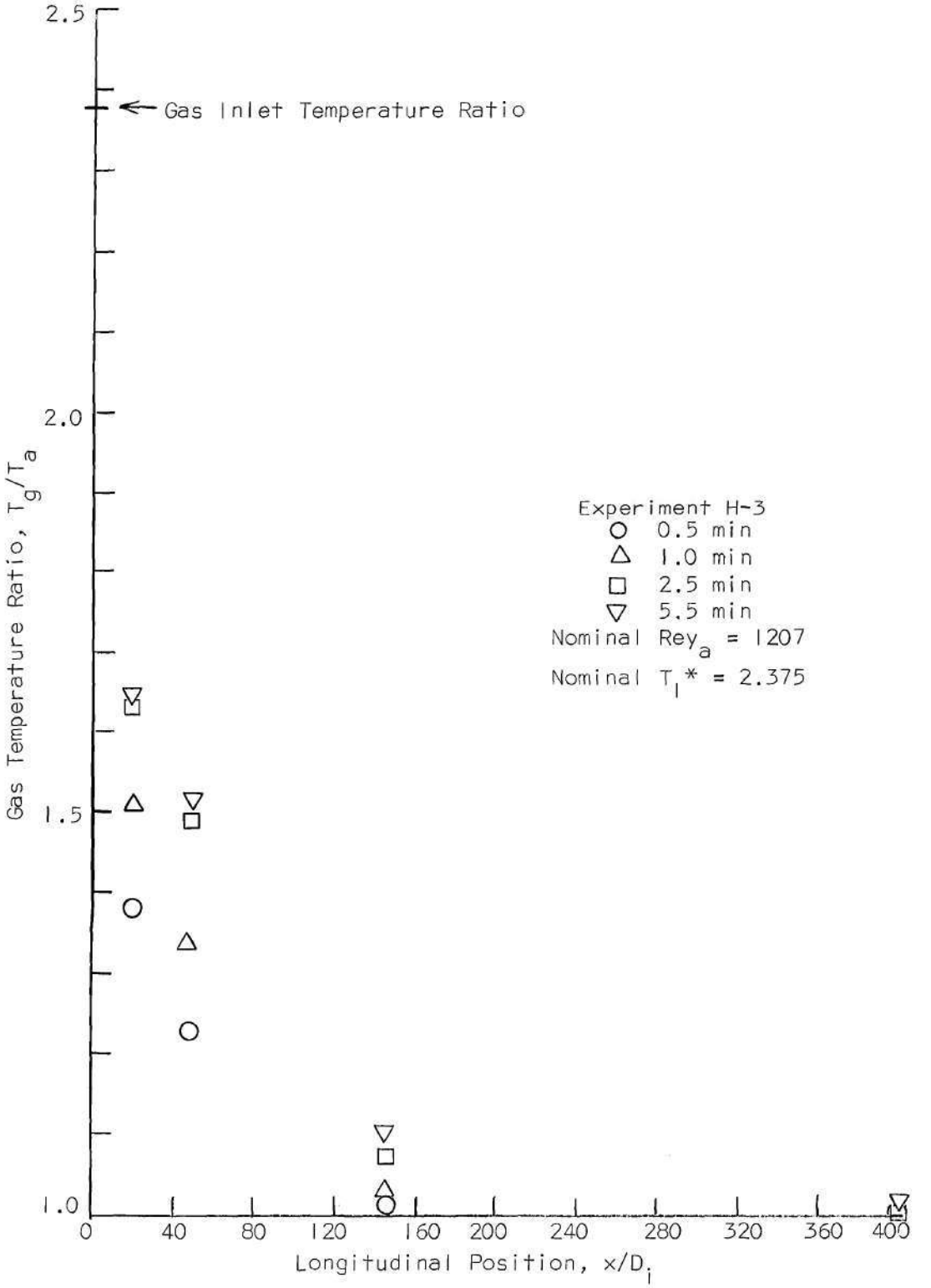

Figure 5. Hot Flow Gas Temperatures, L/D = 400

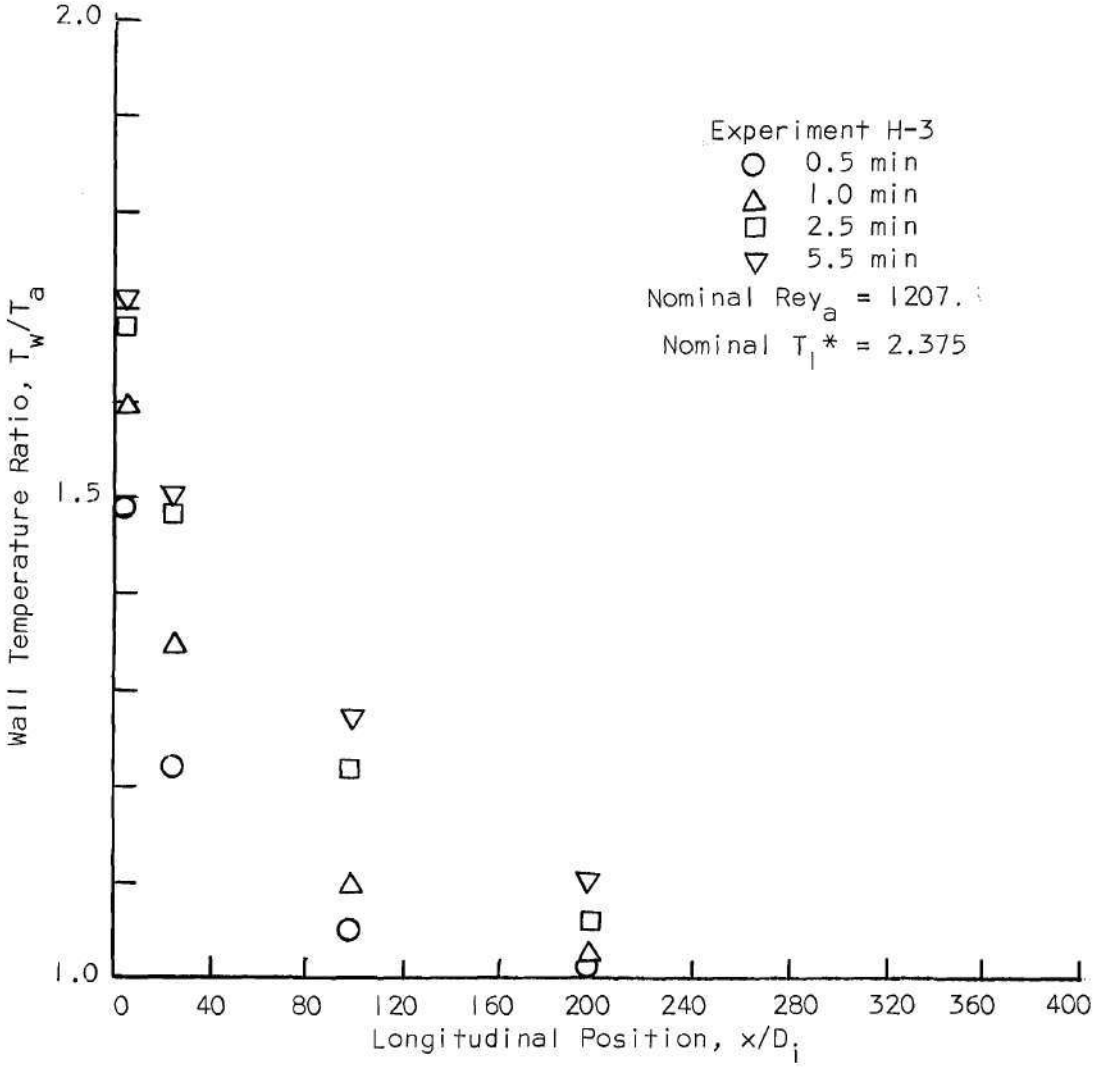

Figure 6. Hot Flow Wall Temperatures, L/D = 400

appear to be delayed somewhat, with a consequent slower approach to equilibrium. One may expect this characteristic of the experimental results from analysis of theory which will be discussed later in Chapter VII.

CHAPTER V

THEORETICAL APPROACH

The theoretical approach utilized to describe the response of an initially cold laminar flow through a long slender tube to a step function increase of the inlet temperature will be formulated in the sections that follow. This formulation entails a description of the equations of continuity, momentum, and energy for the fluid flow, as well as the energy equation for the tube wall, which will be treated as part of the boundary conditions imposed on the flow.

Consistent with the formidable complexity of the unsteady flow problem coupled by heat transfer to a finite tube wall, which in turn experiences natural cooling to its surroundings, the mathematical representation of the problem is restricted first of all to a general one-dimensional formulation. Within this formulation, use is also made of an assumption similar to those employed in boundary layer methods, wherein the flow is assumed to possess predominantly a parallel flow character. In other words, the viscous and heat conduction transport mechanism effects are considered to be significant only in the direction normal to the tube axis, insofar as the fluid is concerned. This assumption, employed in a number of similar problems successfully, is actually based on order of magnitude arguments and results in the implication that the longitudinal transport or forced convection of momentum and energy predominate, at least by two orders of magnitude, over the

comparable longitudinal diffusion processes due to viscosity and conductivity. To the author's knowledge, all significant treatments of the tube gas flow problem available in the literature utilize this assumption of a boundary-layer-like flow. On the other hand, such an assumption is not inherently permissible with regards to the wall energy equation in which longitudinal conduction is a significant, if not predominant, term.

Based upon the preceding concept of the character of the flow the general integral conservation equations for mass, momentum, and energy of the fluid flow may be applied to the simplest choice of a control volume, which is a stationary volume enclosed by two parallel cross-sectional planes, normal to the tube axis, and a surface coincident with the internal surface of the tube wall. A similar simple control volume for the wall energy equation formulation is specified by the two cross-section planes and interior and exterior tube wall surfaces. A brief development of the conservation equations for the fluid, appropriate to the selected control volume, is presented in Appendix C. These equations may be termed the generalized one-dimensional tube flow equations. Inasmuch as the wall energy equation is treated as a part of the imposed boundary conditions on the flow, its formulation will follow in the text of the present chapter at an appropriate time.

In addition to the foregoing assumptions regarding the formulation of the problem as a whole, it is appropriate to mention that specific physical assumptions are also employed. These consist of the usual assumptions of constant pressure over the tube cross-section, neglect of body forces, constant specific heat and Prandtl number of the gas,

and power law representations of the gas viscosity and conductivity dependence on temperature. Also, with reference to the tube itself, it is assumed that all tube properties, such as specific heat, conductivity, and emissivity, are constant. Other assumptions, of all kinds, are more appropriately noted when it becomes convenient or necessary to include them in the development.

Discussion of Solvability of Problem

Subject to the simplifications and approximations mentioned, the governing equations for tube flow in terms of one-dimensional variables are equations (C.24) through (C.27) of Appendix C:

$$\frac{\partial \bar{\rho}}{\partial t} + \frac{\partial}{\partial x} \overline{\rho u} = 0 \tag{2}$$

$$\frac{\partial}{\partial t} \overline{\rho u} + \frac{\partial}{\partial x} \overline{\rho u^2} + \frac{\partial p}{\partial x} + \frac{4}{D_i} \tau_w = 0 \tag{3}$$

$$\frac{\partial}{\partial t} \overline{\rho e} + \frac{\partial}{\partial x} \overline{\rho e u} + p \frac{\partial \bar{u}}{\partial x} + \frac{4}{D_i} q_w = 0 \tag{4}$$

$$p = \overline{\rho T} R \tag{5}$$

In addition the average internal energy per unit volume may be defined for a calorically perfect gas as

$$\overline{\rho e} = (c_p - R) \overline{\rho T} \tag{6}$$

which provides a set of five equations to determine the ten dependent variables: $\bar{u}$, $\bar{\rho}$, $\overline{\rho u}$, $\overline{\rho u^2}$, $\overline{\rho e}$, $\overline{\rho e u}$, p, τ_w, q_w, and $\overline{\rho T}$. In principle

then, solution of the problem in its present form is not possible. This situation has been created obviously by neglecting to consider details of the radial solution, which would provide information pertaining to the coupling between the various cross-section average terms as well as the form of appropriate stress and heat flux quantities. Without resort to the radial solution, any useful progress within a theoretical formulation must proceed by a reduction in the number of unknown variables, which may be accomplished by specification, rather than determination, of the coupling between cross-section average variables. The simplest possible description, which still retains some realism, is obviously that of an idealized one-dimensional flow, whose character and consequences are discussed in the following section.

Idealized One-Dimensional Flow

If the tube flow is assumed to be ideally one-dimensional then all flow properties are assumed to be invariant with radial position, that is, constant over the tube cross-section. Consequently, the bar notation for cross-section average properties is superfluous inasmuch as each individual component in the mean values is, in itself, a mean value; it follows likewise that the mean value of a product of these components is identically equal to the product of the means. Then the notation may be simplified by letting

$$\left.\begin{aligned} \overline{\rho} &= \rho \\ \overline{u} &= U \\ \overline{\rho u} &= \rho U = G \end{aligned}\right\} \quad (7)$$

$$\left.\begin{aligned} \overline{\rho u^2} &= \rho U^2 \\ \overline{\rho e} &= (c_p - R)\,\rho T \\ \overline{\rho e u} &= (c_p - R)\,\rho U T \\ \overline{\rho T} &= \rho T \end{aligned}\right\} \quad (7)$$

so that the resulting governing equations for an idealized one-dimensional flow, equations (2) - (5), become

$$\frac{\partial \rho}{\partial t} + \frac{\partial}{\partial x}\rho U = 0 \quad (8)$$

$$\frac{\partial}{\partial t}\rho U + \frac{\partial}{\partial x}\rho U^2 + \frac{\partial p}{\partial x} + \frac{4}{D_i}\tau_w = 0 \quad (9)$$

$$\frac{\partial}{\partial t}\rho(c_p - R)\,T + \frac{\partial}{\partial x}\rho U\,(c_p - R)\,T + p\,\frac{\partial U}{\partial x} + \frac{4}{D_i}q_w = 0 \quad (10)$$

$$p = \rho R T \quad (11)$$

Due to the assumption of an idealized one-dimensional flow the governing equations of conservation of mass, momentum, and thermal energy and the equation of state, equations (8) - (11), respectively, comprise a system of four equations governing the six variables ρ, U, p, T, τ_w, and q_w. Thus it still remains necessary to eliminate two unknowns. Consistent with the one-dimensional representation of the problem, information pertaining to the shear stress and heat flux vector, which are inherently associated with the actual two-dimensional character of the

flow, is necessarily required. The form of the specification of these variables will be examined further in the following sections after formulating the problem, as it now stands, into a useful system of difference equations and examining the influence of the boundary conditions upon the specification of the problem.

Fluid Flow Difference Equations

The governing equations of the fluid flow, equations (8) - (11), have been restricted to an idealized one-dimensional flow of a perfect gas. In spite of the great simplification afforded by this viewpoint the equations are still too complicated, due to coupling and nonlinearity, to yield closed form analytical solutions. Resort to numerical methods for solution is then acknowledged and the equations are appropriately given in a general finite difference form by introducing the approximations:

$$\frac{\partial(\ )}{\partial t} \approx \frac{\Delta_t(\ )}{\Delta t}$$

$$\frac{\partial(\ )}{\partial x} \approx \frac{\Delta_x(\ )}{\Delta x} \tag{12}$$

Subject to the notation and approximations given by equations (12), the governing conservation equations (8) - (10) become

$$\Delta_t(\rho)\Delta x + U\Delta_x(\rho)\Delta t + \rho\Delta_x(U)\Delta t = 0 \tag{13}$$

$$\rho\Delta_t(U)\Delta x + \rho U\Delta_x(U)\Delta t + \Delta_x(p)\Delta t + \frac{4}{D_i}\tau_w\Delta x\Delta t = 0 \tag{14}$$

$$\rho(c_p-R)\Delta_t(T)\Delta x + \rho U(c_p-R)\Delta_x(T)\Delta t + p\Delta_x(U)\Delta t \tag{15}$$

$$+ \frac{4}{D_i} q_w \Delta t\Delta x = 0$$

Similarly the equation of state in difference form may be written as

$$\Delta_x(p) = RT\Delta_x(\rho) + R\rho\Delta_x(T) \tag{16}$$

It is convenient to introduce at this point the following definitions for the wall friction, heat transfer, and the specific heat ratio

$$\tau_w = f\frac{\rho U^2}{2} \tag{17}$$

$$q_w = h_i(T-T_w) \tag{18}$$

$$\gamma = {c_p}\Big/{(c_p-R)} \tag{19}$$

where f denotes the friction factor and h_i the wall heat transfer film coefficient. The wall heat transfer may be expressed in terms of appropriate dimensionless parameters by introducing the Nusselt, Reynolds, and Prandtl numbers as

$$Nu_i = \frac{h_i D_i}{k} \tag{20}$$

$$Rey = \frac{\rho U D_i}{\mu} \tag{21}$$

$$Pr = \frac{\mu c_p}{k} \tag{22}$$

which allows equation (18) to be rewritten as

$$q_w = \frac{Nu_i}{Rey\ Pr}\,\rho U c_p (T-T_w) \tag{23}$$

The governing equations (13) - (16) involve the spatial dependence of ρ, U, p, and T as well as the time dependence of ρ, U, and T. Regarding the spatial differences as unknowns, these equations may be written in the form of a set of nonhomogeneous linear difference equations by dividing each equation, (13) - (16), by ρU, ρU^2, pU, and p respectively, and collecting the unsteady differences, wall friction, and wall heat transfer terms on the right. This rearrangement, together with the use of the definitions, equations (17), (19), and (23), yields

$$\frac{\Delta_x(\rho)}{\rho} + \frac{\Delta_x(U)}{U} = -\frac{\Delta_t(\rho)}{\rho}\,\frac{1}{U}\,\frac{\Delta x}{\Delta t} \tag{24}$$

$$\frac{\Delta_x(U)}{U} + \frac{\Delta_x(p)}{\rho U^2} = -\frac{\Delta_t(U)}{U}\,\frac{1}{U}\,\frac{\Delta x}{\Delta t} - 4f\,\frac{1}{2}\,\Delta(^x/D_i) \tag{25}$$

$$\frac{\Delta_x(U)}{U} + \frac{1}{\gamma-1}\,\frac{\Delta_x(T)}{T} = -\frac{1}{\gamma-1}\,\frac{\Delta_t(T)}{T}\,\frac{1}{U}\,\frac{\Delta x}{\Delta t} - \frac{\gamma}{\gamma-1}\,4\,\frac{Nu_i}{Rey\ Pr}\,\frac{(T-T_w)}{T}\,\Delta(^x/D_i) \tag{26}$$

$$\frac{\Delta_x(\rho)}{\rho} - \frac{\Delta_x(p)}{p} + \frac{\Delta_x(T)}{T} = 0 \tag{27}$$

The governing equations, (24) through (27), may be solved explicitly for the spatial differences most readily by an elimination procedure. Equations (24) through (26) may be utilized to eliminate $\Delta_x(\rho)/\rho$, $\Delta_x(p)/p$, and $\Delta_x(T)/T$ from the equation of state, equation (27), leaving

it expressed in terms of $\Delta_x(U)/U$, time differences, and the wall heat transfer and stress terms. If, in addition, the definition of the local Mach number

$$M = \frac{U}{\sqrt{\gamma RT}} \tag{28}$$

is introduced, the equation of state by the above elimination procedure yields

$$\frac{\Delta_x(U)}{U} = -\frac{1}{1-M^2}\,4\,\frac{Nu_i}{Rey\ Pr}\,\frac{(T-T_w)}{T}\,\Delta(^x/D_i) \tag{29}$$

$$+\frac{M^2}{1-M^2}\left[4f\,\frac{1}{2}\,\Delta(^x/D_i) - \frac{\Delta_t(p)}{\rho U^2}\,\frac{1}{U}\,\frac{\Delta x}{\Delta t} + \frac{\Delta_t(U)}{U}\,\frac{1}{U}\,\frac{\Delta x}{\Delta t}\right]$$

Briefly then, the equation of state, equation (29), is employed to eliminate the velocity difference $\Delta_x(U)/U$ from the continuity, momentum, and energy equations, (24)-(26), respectively, and to allow the explicit forms for the density, pressure, and temperature differences to be given as:

$$\frac{\Delta_x(\rho)}{\rho} = \frac{1}{1-M^2}\,\frac{4\,Nu_i}{Rey\ Pr}\,\frac{(T-T_w)}{T}\,\Delta(^x/D_i) + \frac{M^2}{1-M^2}\left[-4f\,\frac{1}{2}\,\Delta(^x/D_i)\right. \tag{30}$$

$$\left. - \frac{\Delta_t(U)}{U}\,\frac{1}{U}\,\frac{\Delta x}{\Delta t} + \frac{1}{2}\,\frac{\Delta_t(p)}{\rho U^2}\,\frac{1}{U}\,\frac{\Delta x}{\Delta t}\right] - \frac{\Delta_t(p)}{\rho}\,\frac{1}{U}\,\frac{\Delta x}{\Delta t}$$

$$\frac{\Delta_x(p)}{\rho U^2} = \frac{1}{1-M^2}\left[\frac{4\,Nu_i}{Rey\ Pr}\,\frac{(T-T_w)}{T}\,\Delta(^x/D_i) - 4f\,\frac{1}{2}\,\Delta(^x/D_i)\right. \tag{31}$$

$$- \frac{\Delta_t(U)}{U} \frac{1}{U} \frac{\Delta x}{\Delta t} \Bigg] + \frac{M^2}{1-M^2} \frac{\Delta_t(p)}{\rho U^2} \frac{1}{U} \frac{\Delta x}{\Delta t}$$

$$\frac{\Delta_x(T)}{T} = \left(\frac{\gamma M^2 - 1}{1-M^2} \right) \frac{4\ Nu_i}{Rey\ Pr} \frac{(T-T_w)}{T} \Delta(^x/D_i) - \frac{\Delta_t(T)}{T} \frac{1}{U} \frac{\Delta x}{\Delta t} \tag{32}$$

$$+ \frac{M^2}{1-M^2} (\gamma - 1) \left[- 4f \frac{1}{2} \Delta(^x/D_i) + \frac{\Delta_t(p)}{\rho U^2} \frac{1}{U} \frac{\Delta x}{\Delta t} - \frac{\Delta_t(U)}{U} \frac{1}{U} \frac{\Delta x}{\Delta t} \right]$$

where the pressure unsteadiness

$$\Delta_t(p) = \rho R \Delta_t(T) + RT \Delta_t(\rho) \tag{33}$$

has been introduced for the sake of brevity into the equations.

The explicit form of the governing equations, as provided by equations (29) - (32), incorporates no additional restrictions beyond those already employed in setting forth equations (8) - (11); that is, they pertain to an idealized, one-dimensional, unsteady, compressible flow in a tube. While having retained these general characteristics of the problem, the equations have, however, been set forth with some definite subsequent intentions in mind. It is significant that the degree of influence of wall friction, heat transfer, and unsteadiness on the density, pressure, and temperature differences is affected by the magnitude of the Mach number which appears in the coefficients of these terms. These observations lead systematically to a further simplification of the governing equations consistent with the physics of the problem which is the subject of the present work.

Quasi-Steady Mach Number Zero Flow

The governing equations (29) - (32) in their present form represent a set of four nonhomogeneous first order difference equations in two independent variables. With reference to previous discussion, however, they contain six dependent variables: ρ, U, p, T, f, and Nu_i. The first four of these variables may be readily associated with cross-section average properties whereas the latter two are the dimensionless representations of the wall friction and heat transfer and are intimately associated with details of the two-dimensional character of an actual physical flow by means of the velocity and temperature gradients normal to the tube wall. Consequently, for purposes of a general treatment of the flow dynamics by the one-dimensional approach, it would seem to be the most natural procedure to regard the wall friction factor and Nusselt number as specified or prescribed from other sources of information. This viewpoint, which is adopted in the present work, may entail consideration of experimental results, analytical results of other investigators, or in the absence of these, simply a reasonable estimate of appropriate values. The specification of these variables will be considered in subsequent sections of this thesis.

Regarding the density, velocity, pressure, and temperature as the variables whose solution is sought from equations (29) - (32), one is still faced with a difficult formulation of the difference equations in terms of the two independent variables, x and t. It is possible, however, to simplify the equations in the case of the present problem by invoking two physical approximations which will lead to consideration of a quasi-steady Mach number zero flow.

First, in typical examples of the experimental portion of the present work, the maximum value of the velocity experienced in the tube is approximately 20 fps. The obvious conclusion then is that in all cases considered in the present work the Mach number is small and the flow may consequently be approximated as a Mach number zero flow (26). This logical assumption produces an amazing simplification of the governing equations in that all terms involving M^2 directly in their coefficients are considered negligible. The resulting equations for an unsteady Mach number zero flow then follow from equations (29) - (32) as

$$\frac{\Delta_x(U)}{U} = -4\,\frac{Nu_i}{Rey\ Pr}\,\frac{(T-T_w)}{T}\,\Delta(x/D_i) \tag{34}$$

$$\frac{\Delta_x(\rho)}{\rho} = 4\,\frac{Nu_i}{Rey\ Pr}\,\frac{(T-T_w)}{T}\,\Delta(x/D_i) - \frac{\Delta_t(\rho)}{\rho}\,\frac{1}{U}\,\frac{\Delta x}{\Delta t} \tag{35}$$

$$\frac{\Delta_x(\rho)}{\rho U^2} = 4\,\frac{Nu_i}{Rey\ Pr}\,\frac{(T-T_w)}{T}\,\Delta(x/D_i) - 4f\,\frac{1}{2}\,\Delta(x/D_i) - \frac{\Delta_t(U)}{U}\,\frac{1}{U}\,\frac{\Delta x}{\Delta t} \tag{36}$$

$$\frac{\Delta_x(T)}{T} = -4\,\frac{Nu_i}{Rey\ Pr}\,\frac{(T-T_w)}{T}\,\Delta(x/D_i) - \frac{\Delta_t(T)}{T}\,\frac{1}{U}\,\frac{\Delta x}{\Delta t} \tag{37}$$

As an alternative, the continuity equation (35) could be replaced by an equivalent statement in terms of the mass flux ρU by adding equations (34) and (35) to yield

$$\frac{\Delta_x(\rho U)}{\rho U} = -\frac{\Delta_t(\rho)}{\rho}\,\frac{1}{U}\,\frac{\Delta x}{\Delta t} \tag{38}$$

The governing equations, which are taken as equations (34), (36), (37), and (38) for Mach number zero flow, show the influence of unsteadiness on the pressure, temperature, and mass flow rate in terms of the time differences of the velocity, temperature, and density. Each of these time differences appears as a product of the ratio of the time difference to the local value times a dimensionless quantity $\frac{1}{U}\frac{\Delta x}{\Delta t}$. Accordingly, it may be argued that the ratio of the time difference term to the spatial difference term is small provided

$$U\frac{\partial(\ )}{\partial x} \gg \frac{\partial(\ )}{\partial t} \tag{39}$$

or in terms of the original partial differential equations, (8) - (10), this amounts to the assumption that the time derivatives are negligibly small in comparison to the convective terms. When this is true the flow is termed a quasi-steady flow. In the present problem the time variations of all fluid flow variables are in fact small in comparison to the convective changes except perhaps for an initial transient condition associated with the passage of a thermal contact discontinuity down the tube. This transient condition which will be discussed with the specification of the flow initial conditions is, however, of little consequence.

Accordingly, the differential inequality, equation (39), is assumed to be valid for the present problem and the corresponding quasi-steady implications in the difference representation of the governing equations are given by

$$U\frac{\Delta_x(\ )}{\Delta x} \gg \frac{\Delta_t(\ )}{\Delta t} \tag{40}$$

With the assumption of a quasi-steady flow the governing difference equations for the Mach number zero flow then reduce, with application of equation (40), to

$$\frac{\Delta_x(U)}{U} = -4\,\frac{Nu_i}{Rey\ Pr}\,\frac{(T-T_w)}{T}\,\Delta(^x/D_i) \tag{41}$$

$$\frac{\Delta_x(p)}{\rho U^2} = 4\,\frac{Nu_i}{Rey\ Pr}\,\frac{(T-T_w)}{T}\,\Delta(^x/D_i) - 4f\,\frac{1}{2}\,\Delta(^x/D_i) \tag{42}$$

$$\frac{\Delta_x(T)}{T} = -4\,\frac{Nu_i}{Rey\ Pr}\,\frac{(T-T_w)}{T}\,\Delta(^x/D_i) \tag{43}$$

$$\frac{\Delta_x(\rho U)}{\rho U} = 0 \tag{44}$$

Hence the governing equations, (41) - (44), for quasi-steady Mach number zero flow are ordinary difference equations and may be integrated readily by numerical methods. An attempt at solution of these equations then only requires specification of the proper boundary conditions, as well as the friction factor and Nusselt number, for the present problem. Inasmuch as the time does not appear explicitly in these equations, due to the quasi-steady assumption, the resulting flow will be unsteady only insofar as the boundary conditions dictate unsteadiness. The formulation of the rather complicated boundary conditions for the present problem is discussed in the following sections.

Boundary Conditions

The boundary conditions appropriate to the solution of the governing equations (41) - (44) for the quasi-steady Mach number zero flow

are dictated by the experimental setup and procedure. These conditions are most clearly discussed separately as follows.

Fluid Flow Boundary Conditions

The boundary conditions imposed on the fluid flow in the test tube consist of specification at the tube inlet of the gas temperature and specification at the tube exit of the static pressure and mass flow rate. That is

$$T = T_I \quad \text{at} \quad {}^{x}/_{D_i} = 0$$

$$p = p_E \quad \text{at} \quad {}^{x}/_{D_i} = {}^{L}/_{D_i} \tag{45}$$

$$\rho U = (\rho U)_E = G \quad \text{at} \quad {}^{x}/_{D_i} = {}^{L}/_{D_i}$$

The invariance with time of the inlet temperature and the exit mass flow rate is enforced as part of the experimental procedure which was discussed in Chapter III; the exit pressure is held constant as a consequence of the constant mass flow rate and constant ambient temperature of the gas flow through the Poiseuille tube downstream of the test tube. In consequence of the fact that there are four governing equations, (41) - (44), each of which is first order, it would seem that an additional boundary condition would be required. Such is not the case, inasmuch as the thermodynamic variables must obey the equation of state (11) so that specification of T and p at the inlet and exit, respectively, suffice to implicitly define the density.

Tube Wall Thermal Boundary Condition

The formulation of the approximate governing equations (41) - (44) for the quasi-steady tube flow shows that the heating term is the only significant contributing factor to the temperature and velocity variations, and further, that it contributes a significant influence together with the wall friction to the tube pressure drop. This heating term is, in turn, completely dependent on specification of some condition regarding the wall temperature, wall heat flux, or an energy balance for the tube wall. In the major portion of the problems considered in the literature this heating term is given by specification of the wall temperature or heat flux. In the present problem, however, due to the permissible natural cooling of the wall by radiation and natural convection to the surrounding atmosphere and due to the fact that the wall is a conducting material, the proper form of the wall boundary condition to be applied must evolve from a statement of conservation of thermal energy for the tube wall.

Consistent with the application of the fundamental conservation principles for the fluid flow to a control volume of elemental length dx and tube inside diameter D_i, the statement of conservation of thermal energy for the tube wall is applied to an annular tube control volume with inside diameter D_i, outside diameter D_o, and the same elemental length dx. Likewise consistent with the idealized one-dimensional approach to the fluid flow description, the temperature of the tube wall is assumed independent of radial position or a function only of longitudinal position and time. This assumption is conventional for thin walled tubes.

In terms of the notation of equation (C.8), conservation of thermal energy for the tube wall control volume requires

$$\int_V \frac{\partial}{\partial t} (\rho_w \, c_w \, T_w) \, dV = - \int_A q_j \, n_j \, dA \qquad (46)$$

where V and A refer to the tube wall control volume which is shown in Figure C-1 together with the corresponding tube fluid control volume.

The volume integral in equation (46) may then be written as

$$2\pi \frac{\partial}{\partial t} \int_R^{R_o} \rho_w \, c_w \, T_w \, r \, dr \, dx$$

corresponding to the tube control volume. The negative integral over the volume surface, the right hand side of equation (46), consists of four terms due to forced convection heating from the fluid, longitudinal conduction along the tube wall, natural convection cooling, and radiation, each corresponding to an appropriate portion of the control volume surface. The forced convection heating term is the same as found in the fluid energy equation (C.19), except for sign change, and is given as

$$q_w \, \pi \, D_i \, dx$$

The contribution due to longitudinal conduction along the tube wall is

$$- \frac{\partial}{\partial x} \left[2\pi \int_R^{R_o} - k_w \frac{\partial T_w}{\partial x} \, r \, dr \right] dx$$

In the presence of the surrounding ambient atmosphere at temperature

T_a, the tube outside wall is subject to a heat flux due to natural convection cooling, which is expressed in terms of a convective heat transfer coefficient h_o as

$$- h_o (T_w - T_a) \pi D_o \, dx$$

and a radiation cooling term, which is given as

$$- \varepsilon\sigma (T_w^4 - T_a^4) \pi D_o \, dx$$

with ε, the wall emissivity, and σ, the Stephan-Boltzmann constant.

Collecting these results, together with the assumptions of independence of wall temperatures on radial position and constant wall properties, allows the wall thermal energy equation (46) to be expressed as follows:

$$\rho_w c_w \frac{\partial T_w}{\partial t} = \frac{4 D_i}{D_o^2 - D_i^2} q_w + k_w \frac{\partial^2 T_w}{\partial x^2} \qquad (47)$$

$$- \frac{4 D_o}{D_o^2 - D_i^2} h_o (T_w - T_a) - \frac{4 D_o}{D_o^2 - D_i^2} \varepsilon\sigma (T_w^4 - T_a^4)$$

For purposes of discussion and convenience in the manipulations that follow, equation (47) is expressed in a general difference form as were the fluid flow equations (13) - (16). In the present case, however, there are no arguments for the deletion of the local or time derivatives of the wall internal energy in comparison to the other terms present, as a matter of fact, the time difference of the wall temperature is the

primary source of unsteadiness in the quasi-steady flow problem. Accordingly, equation (47) in difference form is given as

$$\frac{\Delta_t(T_w)}{\Delta t} = \frac{4\,D_i}{D_o^2-D_i^2}\frac{q_w}{\rho_w c_w} + \frac{k_w}{\rho_w c_w}\frac{\Delta x^2(T_w)}{\Delta x^2} \tag{48}$$

$$- \frac{4\,D_o}{D_o^2-D_i^2}\frac{h_o}{\rho_w c_w}(T_w-T_a) - \frac{4\,D_o}{D_o^2-D_i^2}\frac{\varepsilon\sigma}{\rho_w c_w}(T_w^4-T_a^4)$$

In order to write this result in terms of suitable dimensionless parameters reference is made to the work of Rooks (22). In his analysis of the wall boundary condition, Rooks considered the effects of the same terms as represented in equation (48) with the exception of longitudinal conduction in the wall. Thus, although one of the dimensionless parameters he introduced was, in fact, the wall thermal diffusivity α_w, it should be emphasized that the diffusion or longitudinal conduction term was neglected in his analysis. This is made clear if one considers the forced convection heating term in equation (48) which, upon introduction of the definitions of the convective heat transfer and the fluid Nusselt number, equations (18) and (20), respectively, together with the definition of the thermal diffusivity of the wall

$$\alpha_w = \frac{k_w}{\rho_w c_w} \tag{49}$$

and the wall thickness

$$t = \frac{D_o-D_i}{2} \tag{50}$$

may be written as

$$\frac{4\, D_i h_i\, (T-T_w)}{(D_o^2-D_i^2)\rho_w\, c_w} = \frac{{}^{k}/_{k_w}\, Nu_i\, {}^{\alpha_w}/_{D_i^2}}{{}^{+}/_{D_i}\, (1+{}^{+}/_{D_i})}\, (T-T_w) \qquad (51)$$

This result shows that the combination of terms in the numerator of the coefficient is actually representative of the dimensionless quantity $Nu_i(k/\rho_w c_w)$ and not $Nu_i\alpha_w$. On the other hand the coefficient of the diffusion term in equation (48) is, according to the definition, equation (49), simply α_w and is representative of the true effect of thermal diffusion.

The present wall thermal energy equation (48), as expressed in finite difference form, also differs from Rooks' equation in that the difference formulae Rooks used were of a complicated form suggested by Dusinberre (21). The difference formulae to be used in equation (48) need not be specified as yet, but an intuitively more accurate scheme than that suggested by Dusinberre will be utilized. It might also be mentioned that the Dusinberre formulae do not lend themselves readily to treatment of the parabolic equation (48). The different treatment of the differences do not, however, alter the form of the coefficients. In spite of previous objections to Rooks' analysis, his formulation of the coefficients of his wall thermal energy equation is well done and extremely handy, so the present treatment parallels that of Rooks.

The form of the coefficients for the forced convection heating term and the diffusion term have already been given. It remains to define the Nusselt number for the natural convection cooling as

$$Nu_o = \frac{h_o D_o}{k_o} \tag{52}$$

where k_o denotes the conductivity of the mean ambient air surrounding the tube, that is, a conductivity based on the mean temperature

$$T_o = \frac{T_w + T_a}{2} \tag{53}$$

Utilizing equations (52) and (49), the remaining coefficients of the thermal energy equation are easily formulated and the equation is given in final form as

$$\frac{\Delta_+(T_w)}{\Delta t} = \frac{k/k_w \; Nu_i \; \alpha_w/D_i^2}{t/D_i \; (1+t/D_i)} (T-T_w) + \alpha_w \frac{\Delta_x^2(T_w)}{\Delta x^2} \tag{54}$$

$$- \frac{k_o/k_w \; Nu_o \; \alpha_w/D_i^2}{t/D_i \; (1+t/D_i)} (T_w-T_a) - \frac{\frac{\varepsilon\sigma \; D_o}{k_w} \alpha_w/D_i^2}{t/D_i \; (1+t/D_i)} (T_w^4-T_a^4)$$

In addition to specification of physical and geometrical constants, equation (54) requires knowledge of how the fluid thermal conductivity depends on temperature and knowledge of the free convection Nusselt number. Inasmuch as the Prandtl number has been assumed constant, the thermal conductivity follows the same equation for variation with temperature as does the coefficient of viscosity, which is given by a power law representation

$$\mu/\mu_a = (T/T_a)^{0.68} \tag{55}$$

so that the conductivity is expressed as

$$k/k_a = (T/T_a)^{0.68} \tag{56}$$

For the special cases dealing with k_o and μ_o, the temperature T in equations (55) and (56) refer to the mean film temperature T_o.

The free convection Nusselt number, Nu_o, has been extensively investigated for long horizontal cylinders with longitudinally uniform temperature distribution. In the present analysis it is assumed that the local value of Nu_o corresponds to that experienced by such a cylinder if it were subjected uniformly to the local value of the wall temperature T_w. This assumption explicitly ignores the effect of the deviation of the wall temperature from a uniform value; however, this assumption should not be in serious error inasmuch as the slope of the wall temperature distribution is not large in the present case except possibly near the entrance end of the tube.

Typical correlation results for long cylinders subject to uniform temperature distributions are given in reference (27). These results correlate the free convection Nusselt number Nu_o in terms of the product of the Grashof number

$$Gr_o = \left(\frac{D_o^3 \, g \, \beta}{\nu^2} \right)_o (T_w - T_a) \tag{56}$$

and the Prandtl number, where the fluid properties are evaluated at the mean film temperature, equation (53). In the present case, the tube wall temperatures observed experimentally are such that one expects

$$Gr_o Pr < 10^4 \tag{57}$$

As a consequence, experimental results are sufficiently well represented by the equation, due to Rooks (22),

$$Nu_o = 0.95 \, (Gr_o Pr)^{0.2} \tag{58}$$

It follows then from the definition, equation (56), the viscosity relation, equation (55), and use of a constant pressure relation for the variation of density with temperature in the ambient surroundings that equation (58) may be written as

$$Nu_o = 0.95 \left[\frac{D_o^3 \, g \, Pr}{\left(\mu_a / \rho_a \right)^2} \right]^{0.2} \left[\left(\frac{T_w}{T_a} - 1 \right) \left(\frac{2}{\frac{T_w}{T_a} + 1} \right)^{4.36} \right]^{0.2} \tag{59}$$

Finally, the thermal energy equation (54) may be rewritten subject to the definitions and values of its various coefficient variables and parameters pertinent to the present problem. This step is deferred, however, to the next chapter, wherein the formulation of the entire problem is assembled together and the procedure for execution of a solution is discussed in some detail.

Initial Conditions

Description of the tube flow initial conditions consists of prescribing an initial steady cold flow which is consistent with the one-dimensional representation of the flow as already given. The thermodynamic initial conditions appropriate to the present problem are

given as

$$T = T_a \quad \text{at} \quad t = 0$$

$$T_w = T_a \quad \text{at} \quad t = 0 \tag{60}$$

corresponding to a cold flow. The fluid dynamics are specified by the constant mass flux

$$\rho U = G \quad \text{for} \quad t \geq 0 \tag{61}$$

together with specification of the initial pressure distribution along the tube and the equation of state. Actually, since the fluid flow equations, (41) - (44), as set forth for quasi-steady Mach number zero flow, do not contain the time explicitly as a dependent variable and since the mass flux, equation (61), is time invariant, no initial pressure distribution is formally required as an initial condition. The existence of a cold flow, however, implies an initial pressure distribution which is equivalent to saying that the friction factor must be specified for any flow, whether hot or cold. Likewise, in order to proceed with a solution the Nusselt number must also be known.

Specification of Friction Factor and Nusselt Number

These two specifications which were mentioned earlier as being required for solution of the idealized one-dimensional flow are treated separately in the following paragraphs.

Friction Factor

The specification of a friction factor applicable to the tube flow follows from details of the flow dependence on both the radial and longitudinal coordinates in the case of a developing flow. A convenient reference for this purpose is the analytical work of Langhaar (8), who by means of a linearizing approximation to the Navier-Stokes equations for incompressible flow, has obtained a solution for the steady flow in the development length of a straight tube. The velocity profiles, defined in terms of Bessel functions, allow calculation of a dimensionless pressure function P by means of mechanical energy considerations. In terms of the present notation, the pressure drop measured from an assumed stagnation condition ahead of the tube entrance to a position x in the tube is given by

$$\Delta p = \frac{1}{2} \rho U^2 + (p_1 - p) \tag{62}$$

The dimensionless pressure function of Langhaar is then

$$P = \frac{\Delta p}{\frac{1}{2} \rho U^2} \tag{63}$$

where P is a function of the dimensionless variable

$$\sigma = \frac{4\ x/D_i}{Rey} \tag{64}$$

The tabulated results of Langhaar are shown in Figure 7 as a plot of P vs. σ. In this figure it may be noted that for large values of σ,

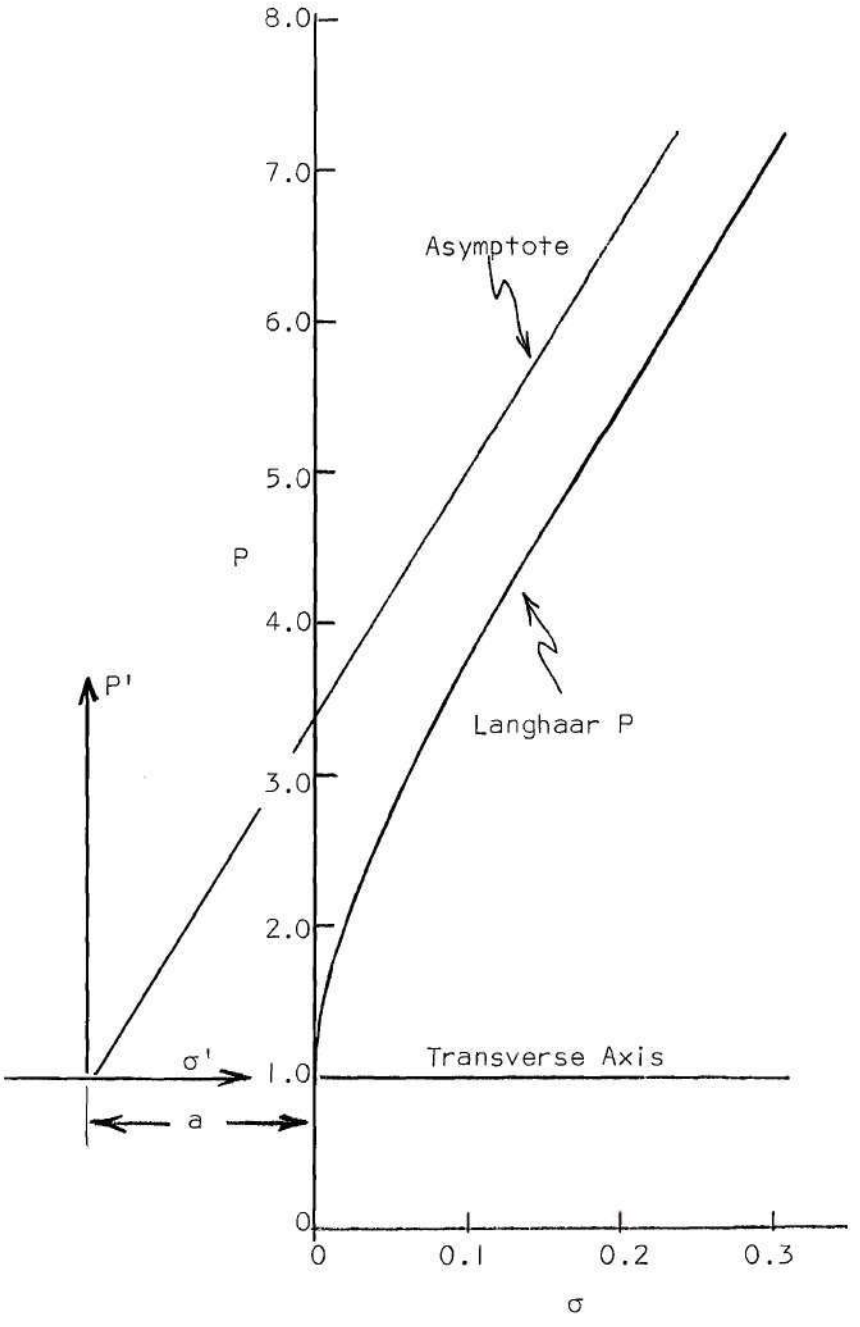

Figure 7. Langhaar Pressure Function

that is far from the tube entrance, the slope $dP/d\sigma$ approaches a value of 16 which corresponds to the friction factor

$$f = \frac{16}{Rey} \tag{65}$$

for fully developed flow.

In the present analysis the cold tube flow may be prescribed approximately in terms of an isothermal flow with a pressure distribution given by representing the Langhaar pressure function, P, in terms of a hyperbola. Such a hyperbola may be conveniently defined by introducing new coordinates P' and σ' whose origin is at the center of the hyperbola or that point where the asymptotes of the hyperbola cross its transverse axis as shown in Figure 7. The equation of the matching hyperbola is then given by

$$\frac{\sigma'^2}{a^2} - \frac{P'^2}{b^2} = 1 \tag{66}$$

and the corresponding equation for its asymptote is

$$P' = \frac{b}{a}\sigma' \tag{67}$$

The slope b/a of the asymptote, in order to agree with the friction factor for fully developed flow, must be 16. As a consequence, the equation for the hyperbola, equation (66), may be expressed as

$$P'^2 = 256\ (\sigma'^2 - a^2)$$

or, inasmuch as

$$\sigma' = \sigma + a$$

the pressure function P' is given by

$$P' = 16\ (\sigma^2 + 2\sigma a)^{\frac{1}{2}} \tag{68}$$

and obviously, since P = 1 is the transverse axis of the hyperbola,

$$P = P' + 1$$

or

$$P = 1 + 16\ (\sigma^2 + 2\sigma a)^{\frac{1}{2}} \tag{70}$$

The result, equation (70), of matching a hyperbola to Langhaar's pressure function leaves one parameter, a, to be determined experimentally. This parameter is specified by matching the pressure function P of equation (70) to the experimental results for the cold flow in each test tube, where the experimental value of P corresponds to the total length of the test tube or a length parameter of

$$\sigma_E = \frac{4\ L/D_i}{Rey} \tag{71}$$

As a consequence, a value for the parameter, a, is found for each test tube specified by its particular L/D_i. The results of this evaluation are given in the discussion of the cold flow in the section on theoretical results.

The pressure distribution for the initial cold flow is then given by equations (62) and (63) as

$$p = p_I + \frac{1}{2} \rho U^2 (1 - P)$$

The inlet pressure p_I is expressible, by this result applied at the exit, in terms of p_E and P_E so that it is more convenient to write

$$p = p_E + \frac{1}{2} \rho U^2 (P_E - P) \tag{72}$$

where according to equation (45), p_E is known and the dynamic pressure $1/2\ \rho U^2$ is given as $G^2/2\rho$. The pressure functions P and P_E are given by equation (70) for appropriate values of σ defined by equation (64). The Reynolds number expressed in terms of the mass flux is

$$Rey = \frac{GD_i}{\mu} \tag{73}$$

with the coefficient of viscosity, μ, taken to be equal to its local value which would be μ_a in the case of a cold flow.

The complete prescription of the initial steady cold flow corresponding to a mass flux G, an ambient temperature T_a, and an exit pressure p_E is then given in terms of the pressure distribution by equation (72), a constant temperature corresponding to ambient conditions, and a density distribution satisfying the equation of state. Inasmuch as the maximum pressure drops across the tube are of the order of 0.01 atmospheres, the corresponding density variations along the tube are for all practical purposes negligible for the case of a cold flow. Corresponding to the pressure function P, equation (70), and the momentum equation (42) applied to the cold flow, the local friction factor may be specified as

$$4f = \frac{64}{Rey} \frac{(\sigma + a)}{(\sigma^2 + 2\sigma a)^{\frac{1}{2}}} \tag{74}$$

In the case of a hot flow, it is assumed that the local friction factor is likewise given by equation (74) subject to calculations based on the local values of the Reynolds number which in the case of quasi-steady flow will be entirely temperature dependent.

Nusselt Number

Due to the lack of both analytical and experimental information pertaining to hot flows with arbitrary temperature distribution, the specification of a correct representation of the forced convection heat transfer or the fluid Nusselt number remains, at best, a rather crude semi-empirical guess. Kays (14), as a result of numerical solutions for idealized boundary conditions such as constant wall temperature, constant heat flux, or constant temperature difference between gas and wall, gives empirical correlation equations for the local Nusselt number in terms of the parameter $(x/D_i)/Rey\ Pr$. Rooks (22) utilized Kays' constant heat flux equation for his analysis of the present problem; there is, however, no evidence to suggest that it is the proper specification.

In view of the essential difficulty in specifying the Nusselt number, the viewpoint taken in the present work is that the Nusselt number will be regarded as a semi-empirical parameter which must be specified in such a way that the theoretical predictions for the tube pressure drop agree with the experiments. The conclusion of this specification will be discussed later in the section on theoretical results.

CHAPTER VI

THEORETICAL PROCEDURE

The purpose of a discussion of the theoretical procedure employed in the present work is to explain the mechanical details of the execution of a solution of the unsteady tube flow problem as described in the preceding chapter.

A complete mathematical description of the problem is provided by the governing difference equations for the fluid, equations (41) - (44), the difference equation for the wall thermal energy, equation (54), the fluid flow boundary conditions (45), the fluid and wall initial conditions, equations (60) and (61), specification of the friction factor by equation (74), and knowledge of the Nusselt number as an empirical parameter.

Fluid Flow

Actually, due to the assumption of a quasi-steady flow and the constant mass flow specification at the tube exit, the mathematical description may be expressed in somewhat simpler terms. The constant mass flux G at the tube exit, equation (45), together with the continuity equation (44) dictates that the mass flux is invariant with both position and time. Also the equation of state may be employed in its original form so that for calculation purposes the flow problem may be summarily represented as follows:

$$U = {}^{G}/\rho \tag{75}$$

$$\Delta_x(p) = \frac{G^2 R}{p}\left[\frac{4\ Nu_i}{Rey\ Pr}\ (T^*-T_w^*)\Delta({}^{x}/D_i) - T_a T^*\ 4f\ \frac{1}{2}\ \Delta({}^{x}/D_i)\right] \tag{76}$$

$$\Delta_x(T^*) = -\frac{4\ Nu_i}{Rey\ Pr}\ (T^*-T_w^*)\Delta({}^{x}/D_i) \tag{77}$$

$$\rho = {}^{p}/RT^*T_a \tag{78}$$

with the boundary conditions

$$\begin{aligned} T^* &= T_i^* \quad \text{at } {}^{x}/D_i = 0 \\ p &= p_E \quad \text{at } {}^{x}/D_i = {}^{L}/D_i \end{aligned} \tag{79}$$

where the gas and wall temperatures have been nondimensionalized, as indicated by the ( )* superscript, with reference to the ambient temperature. In order to execute a solution for that portion of the problem pertaining to the fluid flow it is necessary to perform an integration of equations (76) and (77). Due to the nature of the equations and the boundary conditions, this integration is readily performed by a standard Runge-Kutta process (28) by first integrating the energy equation (77) down the tube from entrance to exit to obtain the gas temperature distribution. Then the momentum equation (76) may be integrated back up the tube from exit to entrance determining the pressure distribution while simultaneously employing equations (78) and (75) to calculate the local density and velocity. The pressure drop may then be determined as

the sum of the integrated pressure change in the tube plus the kinetic energy jump at the tube inlet based on the hot flow density and velocity in the tube entrance. For calculation purposes it was found sufficiently accurate (within one per cent) to utilize a spatial step size of $\Delta(^{x}/D_i)$ = 1; this fine a step size actually being required only due to the large temperature gradients near the tube inlet.

The above procedure is carried out as a quasi-steady calculation inasmuch as the only dependence on time is reflected in the wall temperatures. The wall temperature time history is thus fundamental to the unsteadiness or response of the fluid flow to a step function increase of the inlet temperature. In fact, if the wall temperatures vary rapidly, corresponding to a very thin tube walls of small heat capacity, then the quasi-steady representation of the fluid flow may be invalid. On the other hand, as mentioned previously, one would expect that in response to a step function increase of the gas temperature at the inlet, there will ensue a transient flow corresponding to the passage down the tube of a thermal contact discontinuity. Whereas this transient flow represents an unsteadiness that could not be termed quasi-steady, there are other physical considerations which allow this transient to be entirely ignored in the present problem. Not only would the thermal contact discontinuity be smeared out with time due to the thermal diffusivity of the gas (which is not accounted for in the present problem), but the magnitude of the temperature rise across the discontinuity would decay rapidly with passage down the tube due to the heat transfer to a wall of large heat capacity. Further, the elapsed time required for the discontinuity to traverse even the entire length of tube is of the order

of a fraction of a second with velocities of the order of 20 fps. Consequently, in this short period of time no appreciable change in the wall temperature occurs due to its relatively high heat capacity and bulk.

In view of the preceding arguments, it is assumed for purposes of calculating the flow response in the present work that the proper initial specifications for the flow consist of a constant wall temperature at ambient value and a gas temperature distribution which is readily calculated by equation (77), corresponding to this constant wall temperature. Subsequent response of the fluid flow is then quasi-steady and is dictated by the wall temperature changes with time as governed by the wall thermal energy equation.

Wall Temperatures

The wall thermal energy equation (54) may be given in a more compact form by nondimensionalization of the temperatures with reference to the ambient value and use of equations (56) and (59) to yield

$$\frac{\Delta_t(T_w^*)}{\Delta t} = K_1\, Nu_i\, (T^*)^{0.68}\, (T^*-T_w^*) + K_2 \frac{\Delta_x^2(T_w^*)}{\Delta(x/D_i)^2} \qquad (80)$$

$$- K_3\, (T_w^*-1)^{1.2}\, (T_w^*+1)^{-0.192} - K_4\, (T_w^{*4}-1)$$

with

$$K_1 = \frac{k_{r/k_w}\, \alpha_{w/D_i}\, 2 \left(T_{a/T_r}\right)^{0.68}}{t/D_i\, (1+t/D_i)} \qquad (81a)$$

$$K_2 = {}^{\alpha_w}/_{D_i}{}^2 \tag{81b}$$

$$K_3 = \frac{{}^{k_r}/_{k_w}\ {}^{\alpha_w}/_{D_i}{}^2 \left({}^{T_a}/_{2T_r}\right)^{0.68}}{{}^{\dagger}/_{D_i}\ (1+{}^{\dagger}/_{D_i})}\ (0.95)\left[\frac{D_o{}^3 g\ Pr}{\left({}^{\mu_a}/_{\rho_a}\right)^2}\right]^{0.2}(2)^{0.872} \tag{81c}$$

$$K_4 = \frac{\frac{\varepsilon\sigma\ D_o}{k_w}\ {}^{\alpha_w}/_{D_i}{}^2\ T_a{}^3}{{}^{\dagger}/_{D_i}\ (1+{}^{\dagger}/_{D_i})} \tag{81d}$$

where T_r denotes a gas reference temperature for evaluation of the gas conductivity k_r.

The difference equation (80) may be solved numerically by application of methods appropriate to parabolic equations. Utilizing superscripts to denote time and subscripts for position, the time difference is represented as a forward difference

$$\Delta_{\dagger}(T_w{}^*) = T_w{}^{*\,n+1}_j - T_w{}^{*\,n}_j \tag{82}$$

and the second order spatial difference corresponding to longitudinal conduction in the wall may be replaced by a general time weighted centered spatial difference

$$\Delta_x{}^2(T_w{}^*) = \theta\left(T_w{}^{*\,n+1}_{j+1} - 2T_w{}^{*\,n+1}_j + T_w{}^{*\,n+1}_{j-1}\right) \tag{83}$$

$$+\ (1-\theta)\left(T_w{}^{*\,n}_{j+1} - 2T_w{}^{*\,n}_j + T_w{}^{*\,n}_{j-1}\right)$$

where θ is a positive constant. Various values of θ give either

explicit or implicit schemes; $\theta = 0$ gives a four-point explicit scheme with forward time difference, $\theta = 1$ gives a four-point implicit scheme with backward time difference, and the value of θ employed in the present work, $\theta = \frac{1}{2}$, gives a six point scheme with centered time difference. The primary reasons for this choice of $\theta = \frac{1}{2}$ are the intuitively simple representation of the centered time difference and the avoidance of stability problems such as are encountered in the simpler explicit representation.

Consistent with the representation of the second order spatial difference by equation (83), all functions of the gas or wall temperature on the right hand side of equation (80) are also represented in terms of the general time weighted scheme with $\theta = \frac{1}{2}$. For example, the last term is represented as

$$(T_w{}^{*4}-1) = \theta\ (T_w{}^{*4}-1)_j^{n+1} + (1-\theta)(T_w{}^{*4}-1)_j^{n} \tag{84}$$

and similarly for the other terms. Substitution of the representations given by equations (82) and (83) together with treatment of all the terms on the right hand side of equation (80), as in equation (84), and rearrangement allows equation (80) to be written as

$$- K_2 \frac{\Delta t}{\Delta(x/D_i)^2}\,\theta\ T_w{}^{*n+1}_{j+1} + T_w{}^{*n+1}_{j} \tag{85}$$

$$+ K_1\ \Delta t\ \theta\ Nu_i\ (T^{*n+1}_j)^{0.68}\ (T_w{}^{*n+1}_j) + 2K_2 \frac{\Delta t}{\Delta(x/D_i)^2}\,\theta\ T_w{}^{*n+1}_j$$

$$+ K_3 \Delta t\, \theta \left[(T_w^*-1)^{1.2} (T_w^*+1)^{-0.192} \right]_j^{n+1} + K_4 \Delta t\, \theta \left[T_w^{*4} \right]_j^{n+1}$$

$$- K_2 \frac{\Delta t}{\Delta (x/D_i)^2} \theta\, T_{w\,j-1}^{*\,n+1}$$

$$- K_1 \Delta t\, \theta\, Nu_i \left(T_j^{*\,n+1} \right)^{0.68} \left(T_{w\,j}^{*\,n+1} \right) - K_4 \Delta t\, \theta$$

$$= T_{w\,j}^{*\,n} + K_1 \Delta t\, (1-\theta) \left[Nu_i\, (T^*)^{0.68} (T^*-T_w^*) \right]_j^n$$

$$+ K_2 \frac{\Delta t}{\Delta (x/D_i)^2} (1-\theta) \left[T_{w\,j+1}^{*\,n} - 2T_{w\,j}^{*\,n} + T_{w\,j-1}^{*\,n} \right]$$

$$- K_3 \Delta t\, (1-\theta) \left[(T_w^*-1)^{1.2} (T_w^*+1)^{-0.192} \right]_j^n$$

$$- K_4 \Delta t\, (1-\theta) \left[T_w^{*4}-1 \right]_j^n$$

The presence of the nonlinear bracketed terms in T_w^* at time n+1 is not desirable and may be eliminated by linearizing these terms as follows. Letting

$$\left[(T_w^*-1)^{1.2} (T_w^*+1)^{-0.192} \right]_j^{n+1} = f\, (T_w^*)_j^{n+1} \tag{86}$$

then by a Taylor series expansion

$$f\, (T_w^*)_j^{n+1} \approx f\, (T_w^*)_j^n + f'\, (T_w^*)_j^n \left(T_{w\,j}^{*\,n+1} - T_{w\,j}^{*\,n} \right) \tag{87}$$

and evaluating the derivative $f'(T_w^*)^n$ yields

$$f'(T_w^*)_j^n = \left[(T_w^*+1)^{-0.192}\ (1.2)(T_w^*-1)^{0.2}\right. \tag{88}$$

$$\left. -\ (0.192)(T_w^*+1)^{-1.192}\ (T_w^*-1)^{1.2}\right]_j^n$$

Similarly

$$\left[T_w^{*4}\right]_j^{n+1} = (T_w^{*4})_j^n + 4\ (T_w^{*3})_j^n\ (T_w^*)_j^{n+1} \tag{89}$$

$$-\ 4\ (T_w^{*3})_j^n\ (T_w^*)_j^n$$

Use of the linearization procedure for these two terms then allows equation (85) to be rewritten after considerable rearrangement in the form

$$-\ A_j\ T_w^*{}_{j+1}^{n+1} + B_j\ T_w^*{}_j^{n+1} - C_j\ T_w^*{}_{j-1}^{n+1} = D_j \tag{90}$$

with

$$A_j = K_2\ \frac{\Delta\tau}{\Delta(x/D_i)^2}\ \theta \tag{91}$$

$$B_j = 1 + K_1\ \Delta\tau\ \theta\ Nu_i\ (T^{*0.68})_j^{n+1} + 2A_j \tag{92}$$

$$+\ K_3\ \Delta\tau\ \theta\left[1.2\ (T_w^*{}_j^n+1)^{-0.192}\ (T_w^*{}_j^n-1)^{0.2}\right.$$

$$- 0.192\ (T_w{}^{*n}_{j}+1)^{-1.192}\ (T_w{}^{*n}_{j}-1)^{1.2}\Big]$$

$$+ 4K_4\ \Delta t\ \theta\ (T_w{}^{*n}_{j})^{3}$$

$$C_j = A_j \tag{93}$$

$$D_j = T_w{}^{*n}_{j} + K_1\ \Delta t\ \Big[(1-\theta)Nu_i\ (T^{*n}_{j})^{0.68}\ (T^{*n}_{j}-T_w{}^{*n}_{j}) \tag{94}$$

$$+ \theta\ Nu_i\ (T^{*n+1}_{j})^{0.68}\ T^{*n+1}_{j}\Big] + A_j\ \frac{(1-\theta)}{\theta}\ \Big[T_w{}^{*n}_{j+1} - 2T_w{}^{*n}_{j} + T_w{}^{*n}_{j-1}\Big]$$

$$- K_3\ \Delta t\ (T_w{}^{*n}_{j+1})^{-0.192}\ (T_w{}^{*n}_{j}-1)^{1.2}$$

$$+ K_3\ \Delta t\ \theta\ \Big[1.2\ (T_w{}^{*n}_{j}+1)^{-0.192}\ (T_w{}^{*n}_{j}-1)^{0.2}$$

$$- 0.192\ (T_w{}^{*n}_{j}+1)^{-1.192}\ (T_w{}^{*n}_{j}-1)^{1.2}\Big]\ T_w{}^{*n}_{j} - K_4\ \Delta t\ \Big[(T_w{}^{*n}_{j})^{4}\ (1-4\theta) - 1\Big]$$

The difference equation (90) together with the coefficients, equations (91) - (94), thus represents the wall thermal energy equation in terms of a six-point difference scheme in space and time. The coefficients are regarded as known, which upon inspection requires that the temperatures of the wall $T_w{}^{*n}_{j}$ and the gas T^{*n}_{j} be known at time n for all positions j. In addition, it is required that the gas temperatures

T^{*n+1}_j be known corresponding to the time n+1. Letting n = 0 correspond to the time t = 0, the gas and wall temperatures are prescribed by the initial conditions, equations (60). Then, neglecting the initial transients that occur for small times while a thermal contact discontinuity is swept through the tube, it is assumed that the gas temperatures T^{*1}_j reach an initial equilibrium distribution corresponding to a solution of equation (77) with a cold wall, $T_w{}^{*0}_j = 1$, during the first time increment. The staggered computing scheme is continued by solving equation (90) for the new wall temperatures at time n = 1, and repeated use of first equation (77) and then equation (90) to find the gas and wall temperatures following each new time increment.

A solution to equation (90) may be effected subject to specification of two boundary conditions on the wall temperatures and the fact that the equation must possess a one-parameter family of solutions (29). The exact wall temperature boundary conditions appropriate to the tube experiments of the present work are not known. It is assumed, however, that due to the small exposed cross-sectional area of the tube ends in comparison to the exposed internal surface area, the overall effect of any heat transfer at the tube ends must be small in comparison to the internal or convective heat transfer to the tube interior surface. Consequently, it may be assumed that the tube ends are insulated to longitudinal heat conduction. If j = 1 and j = M respectively represent the entrance and exit positions in the tube, the boundary conditions appropriate to the insulated ends may be given as

$$T_w{}^{*n}_0 = T_w{}^{*n}_1 \tag{95}$$

$$T_w{}^{*n}_{M+1} = T_w{}^{*n}_{M} \tag{96}$$

A one-parameter solution of equation (90) may be represented in the form

$$T_w{}^{*n+1}_{j} = E_j \, T_w{}^{*n+1}_{j+1} + F_j; \quad j = M, M-1, \ldots, 1 \tag{97}$$

and due to the boundary condition at the tube inlet, equation (95), it must follow that

$$E_o = 1 \quad , \quad F_o = 0 \tag{98}$$

The solution given by equation (97) may be assured to represent the desired solution from equation (90) by substituting

$$T_w{}^{*n+1}_{j-1} = E_{j-1} \, T_w{}^{*n+1}_{j} + F_{j-1}$$

from equation (97) into equation (90). The equivalence of these two equations thus demands that

$$E_j = \frac{A_j}{B_j - C_j E_{j-1}} \tag{99}$$

$$F_j = \frac{D_j + C_j F_{j-1}}{B_j - C_j E_{j-1}} \tag{100}$$

With the aid of equations (99) and (100), the inlet boundary condition in the form of equations (98), and knowledge of the coefficients A_j, B_j,

C_j, and D_j, it is then possible to calculate the E_j and F_j for all positions down the tube. At the tube exit, however, equation (96) demands from equation (97) that

$$T_{w_M}^{*n+1} = \frac{F_M}{1 - E_M} \tag{101}$$

and inasmuch as F_M and E_M are known from equations (99) and (100), the exit wall temperature is determined. Finally then, equation (97) allows determination of the wall temperatures proceeding backwards down the tube from $j = M-1$ to $j = 1$.

The aforegoing treatment of the wall energy equation coupled with the fluid flow analysis for a quasi-steady Mach number zero flow allows a solution of the physical problem of the present investigation to be obtained. The only additional specifications required at this point are the appropriate gas physical constants and reference values together with the tube wall constants already given in Table I. The gas constants are accordingly given as follows:

$R = 1718$ ft-lb/slug $^{\circ}F$

$Pr = 0.72$

$k_r = 0.01516$ Btu/hr ft $^{\circ}F$ at 80 $^{\circ}F$

CHAPTER VII

PRESENTATION AND DISCUSSION OF RESULTS

Introduction

The results of the present investigation consist of experimental and theoretical descriptions of tube pressure drops, gas temperatures, and wall temperatures for various tube lengths (L/D = 400, 600, 800, 1000) at selected mass flow rates (as represented by Rey_a) and inlet gas temperature ratios (T_I^*). Thus the primary variables of interest, the pressure drop and temperatures, may be defined as functions of position, time, and the other variables that were investigated. It is to be noted that whereas the pressure drop, by definition, depends on the overall length of the tube, the temperatures inherently depend only on position as measured from the tube inlet, a result that is consistent with the Mach number zero assumption. For clarity, the primary variables may be expressed in terms of functional relations pertinent to the present work as follows

$$\Delta p = fcn(t, L/D_i, Rey_a, T_I^*)$$

$$T_w^*,\ T_g^* = fcns(t, x/D_i, Rey_a, T_I^*) \qquad (102)$$

In the general case the primary variables are of course dependent upon a number of additional variables such as wall material properties, wall thickness to diameter ratio, etc., which were not investigated.

The number of variables involved in the present investigation, as given by equations (102), is sufficiently large to dictate an unreasonable amount of experimentation in order to describe completely the effects of just these variables. Thus the experimental results obtained do not encompass such a description and reliance must be placed on theory to fair in the results for a complete description. On the other hand, the theory as it has been presented, is incomplete in that it must rely on some experimental observations for the determination of a satisfactory friction factor and Nusselt number in order that it can give reasonable predictions. For these reasons it is deemed appropriate to present the experimental and theoretical results together.

The order of presentation to follow will involve the following considerations: first, the use of experiment to determine an appropriate friction factor parameter and Nusselt number for the theory, second, theoretical predictions of the pressure drop dependence on the various variables given by equation (102), third, comparisons of theory and experiment with regard to pressure drops, fourth, comparisons for the gas and wall temperatures, and finally, theoretical predictions for the tube pressure distribution and the effect of various wall thickness ratios on the tube pressure drop.

Semi-Empirical Experimental Results

The experimentally measured pressure drops for each test tube were employed together with predictions of the theory to allow a choice of friction factor parameter, a, and Nusselt number, Nu_i, appropriate for use in the theory.

Friction Factor Parameter

The friction factor parameter, as required by equation (74), was determined from the cold flow experimental results for each test tube; these results which encompass the range of Reynolds numbers from approximately 100 to 1250 are shown in Figure 8. Pertinent to each of the test tubes the theoretical pressure drop may be calculated using the definition of equation (63), equation (70), and equation (71) in the form

$$\Delta p = \frac{G^2}{2\rho}\left\{1 + 16\left[\left(\frac{4L/D}{Rey}\right)^2 + 2\left(\frac{4L/D}{Rey}\right)a\right]^{\frac{1}{2}}\right\} \qquad (103)$$

for different values of the friction factor parameter, a, until a suitable value is found which matches the experimental results. Accordingly, values of a = 0.300, 0.375, 0.425, and 0.4613 were selected corresponding to values of L/D = 400, 600, 800, and 1000, respectively. The theoretical pressure drops using these values are also shown in Figure 8 for comparison and a good representation of the cold flow pressure drop by the theory must be acknowledged.

An interesting comparison with the results of Langhaar (8) for the friction factor in the development region of the tube may be made by utilizing equation (103) together with Langhaar's results for the pressure function P, given by equation (63). For a small value of σ, corresponding to a position in the flow development region near the tube inlet, a value of the friction parameter, a, may be calculated. As an example, for $4\frac{L}{D}/Rey = 0.0715$, Langhaar's tabulated results together with equation (103) yield for the friction factor parameter, a = 0.0952. The values of the friction factor parameter, and consequently also the

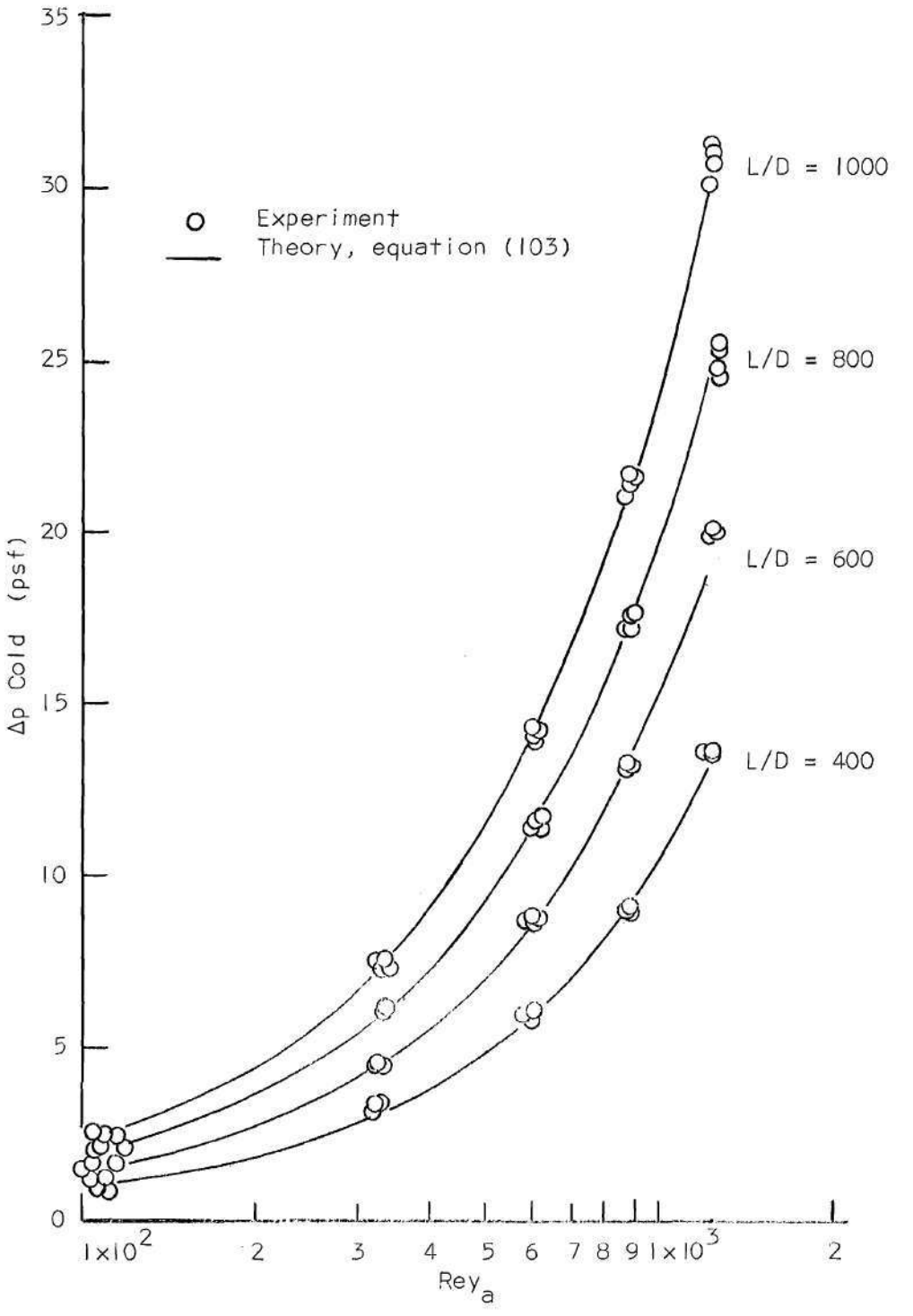

Figure 8. Cold Flow Theory and Experiment

friction factor, as determined from the cold flow experiments of the present work are larger than those predicted from Langhaar's analysis throughout the development region. This result is physically logical inasmuch as Langhaar's analysis pertains to an ideal, smoothly rounded tube inlet whereas the tubes of the present work are cut straight across perpendicular to the tube axis with no attempt at smoothing the inlet. Consequently the pressure drop and friction factors associated with these tubes should be significantly higher than those of tubes with smooth inlets.

The flow development length, as given by Boussinesq (5),

$$\left(\frac{x}{D_i}\right)_{\text{development}} = 0.065\ Re_y \tag{104}$$

is less than the overall length of any one of the four test tubes employed in the present work. Accordingly, in the analysis of the experimental results and their theoretical representation in terms of the friction factor, equation (74), and the pressure drop, equation (103), two significant facts should be examined. First, for tube lengths greater than the development length, the effect of additional length, such as the addition of 200 diameter increments to the short (L/D = 400) test tube, should be evidenced by equal increments of pressure drop corresponding to fully developed flow in that additional length. This result is verified by the experimental results shown in Figure 8 and the theory is matched to these results with the different values for the friction factor parameter for each test tube.

The second fact to be examined is the requirement that the local friction factor in the development region be independent of the added length or the total L/D. The friction factor as given by equation (74), does not satisfy this latter statement unless the friction factor parameter, a, is independent of the tube length. In summary, the present theory satisfies the first requirement if it agrees with the experimental total tube pressure drop, an agreement which is obtained by using different values of a, but it does not satisfy the second requirement by virtue of this choice of different values for a.

The explanation of the preceding apparent contradiction is obviously the fact that the friction factor equation, equation (74), is not an exact representation of the actual friction factor, which is not readily described in terms of such a simple expression. That this choice of representation for the friction factor does not satisfy the second requirement exactly is not a serious objection inasmuch as the range of values chosen for the friction factor parameter, $0.300 \leq a \leq 0.4613$, causes a significant variation in the local friction factor only for very small values of σ. Thus, inasmuch as the present work is concerned primarily with the tube overall pressure drop and must rely on experimental measurements of this quantity, rather than the tube pressure distribution, to represent implicitly a local friction factor, the different selected values for the friction factor parameter for each tube are used together with the definition of the friction factor based on the local Reynolds number in all subsequent theoretical predictions.

Nusselt Number

The Nusselt number appropriate to the hot flow theory of the

present investigation is not known and cannot be accurately predicted from any experimental or theoretical analysis known to the author. Due to the complicated wall boundary conditions imposed on the heat transfer, this problem is not readily amendable to theoretical analysis and would pose a difficult experiment due to the large number of parameters involved.

It is acknowledged that the proper Nusselt number, in all likelihood, would pose an even more complicated functional relation than those of the primary variables of the present problem, as given by equations (102). An attempt was made to formulate a three parameter Nusselt number of the form

$$Nu_i = 3.66 + \frac{1}{C_1\left(\frac{x/D_i}{Rey\ Pr}\right)^{C_2} + C_3} \qquad (105)$$

similar to the correlation formulae of Kays (17). The value 3.66 corresponds to the fully developed Graetz solution for constant wall temperature with parabolic velocity distribution and the other term of the formula represents an attempt to assign the proper distribution of Nu_i in the development region. For various choices of C_1, C_2, and C_3 the theory was applied to the series of hot flows in the short tube, L/D = 400, and comparisons of the pressure drop, gas temperatures, and wall temperatures were made with their corresponding experimental values. These attempts did not meet with success, primarily due to the relatively large number of parameters and variables involved in the problem and lack of knowledge of the nature of the influence of the significant parameters.

As an alternative to the above efforts it was found that by specification of a constant Nusselt number of appropriate magnitude, the theoretical predictions of the tube overall pressure drop, as a function of time, could be made to describe the experimental results for the short test tube (L/D = 400) with very good accuracy. A comparison of these results for the theory and experiment is shown in Figure 9 for a theoretical Nusselt number of 11. This value was chosen to allow the theory to duplicate the experimental pressure drop at 5.5 minutes for the short tube runs with inlet temperature ratios of approximately 2.4. Inasmuch as the temperature distribution, as given by equation (43), should not be dependent on the tube length, this value of the Nusselt number is specified and employed for all of the hot flow runs in all four test tubes. Thus for purposes of the theory the Nusselt number is chosen semi-empirically as

$$Nu_i = 11 \tag{106}$$

It is acknowledged that the preceding treatment of the Nusselt number is not exact since the analysis is based on details of the tube pressure drop rather than consideration of the temperature distributions. With regard to the pressure distribution, as determined from equation (42), the primary Nusselt number effects are restricted to the region near the tube inlet where the temperature difference $T - T_w$ is significant and the temperature T is high. Consequently, a good first approximation of the Nusselt number effect need only specify an average Nusselt number appropriate to the tube inlet region. The value given by equation (106) while large in comparison to the fully developed value of

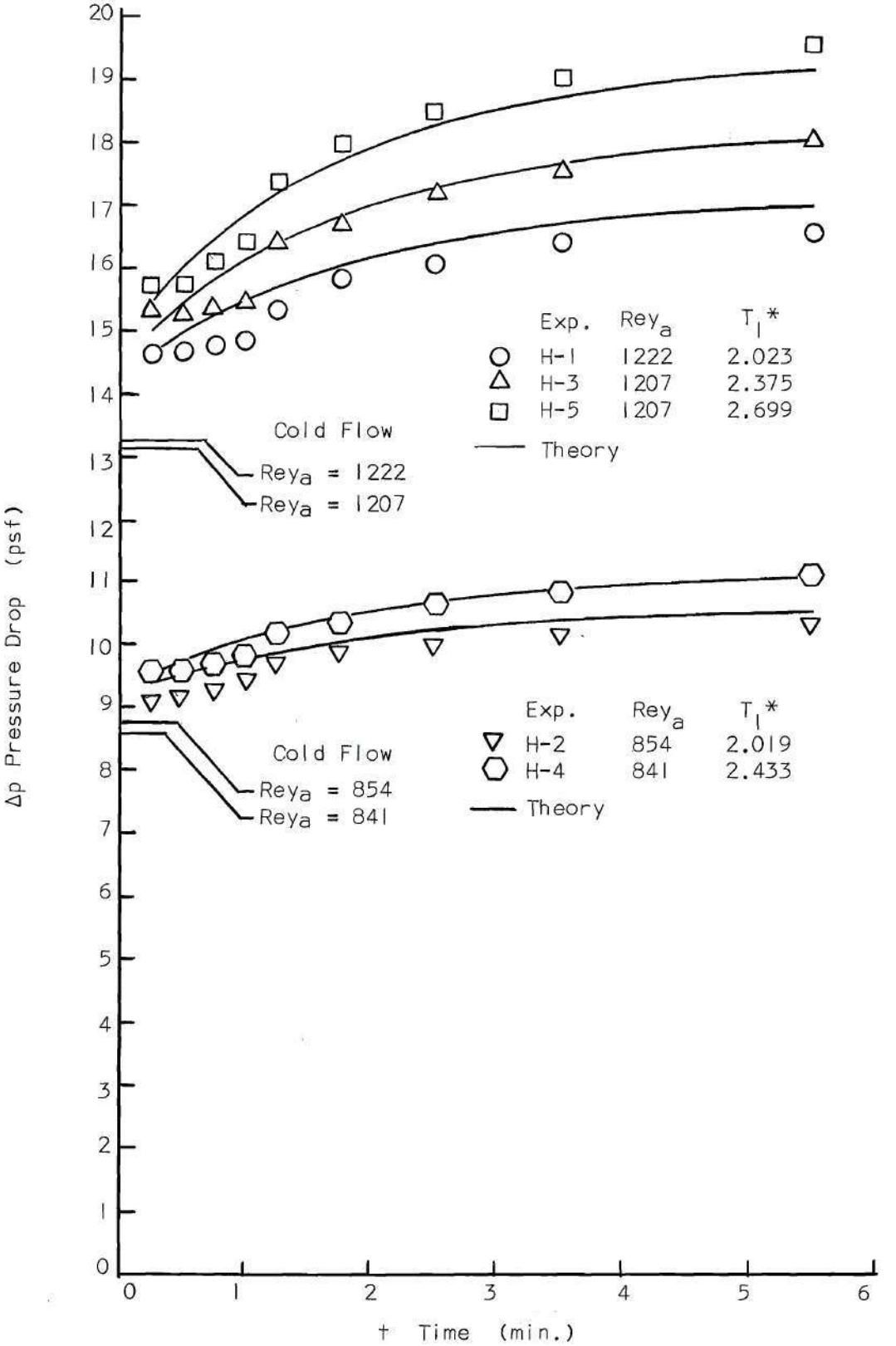

Figure 9. Hot Flow Pressure Drop, L/D = 400

the Graetz solution (3.66), is of comparable magnitude to the values given by Kays (14) for the inlet region.

Theoretical Pressure Drop

The agreement of the theoretical and experimental pressure drops for the short test tube (L/D = 400), as shown in Figure 9, is within approximately 5 per cent. Assuming that this agreement should also be representative of the longer tube experiments, an attempt is now made to fair in the limited experimental results by means of the theory, and to predict the dependence of the pressure drop on the variables and parameters given in equation (102).

The dependence of the tube pressure drop on time has been depicted according to the theory and experiment for the short tube hot flow in Figure 9. It is noted that the trend of the theory, with regard to this time dependence, agrees well with the experiment if one discounts the experimental results for small times, as was explained earlier, due to inadequate control of the experimental system. Consequently, for purposes of presenting and discussing the theoretically predicted pressure drops with brevity, only the results at a time corresponding to 5.5 minutes of elapsed time (approximately the time for the tube wall to reach thermal equilibrium) following the inlet temperature jump will be given. The dependence of the theoretical pressure drop on the remaining parameters of equation (102) will be presented in the order of the following sections.

Reynolds Number Dependence

The theoretical results for the pressure drop after 5.5 minutes

of hot flow are depicted as a function of Reynolds number in Figure 10 for the short test tube (L/D = 400). The figure is given in the form of the ratio of the hot flow pressure drop to the corresponding cold flow pressure drop which was presented in Figure 8.

It is observed that the higher inlet temperatures exert their greatest influence at the higher Reynolds numbers, a trend which is consistent with the larger magnitude of convected heat and longer flow development region for high Reynolds number flow. Correspondingly, for low Reynolds numbers the development region with its high friction factors is so short that the pressure drop tends to become less sensitive to Reynolds number.

Inlet Temperature Dependence

The theoretical pressure drop ratios at 5.5 minutes, given in Figure 10, are shown in Figure 11 as a function of the gas inlet temperature ratio. These results clearly demonstrate that according to the theory the pressure drop is essentially a linear function of the inlet temperature ratio for any given mass flow rate in the laminar flow range. In view of the complicated dependence of the pressure drop and temperature distribution on a wall thermal energy balance, this result is somewhat surprising.

Likewise, due to these complications, the essential character of the problem which produces this result is not discernible by simple analytical means. This conclusion is evident if one attempts to derive a hot flow pressure drop formula comparable to the cold flow formula, equation (103). Such a derivation proceeds by recourse to the governing equations for quasi-steady Mach number zero flow, equations (41) through

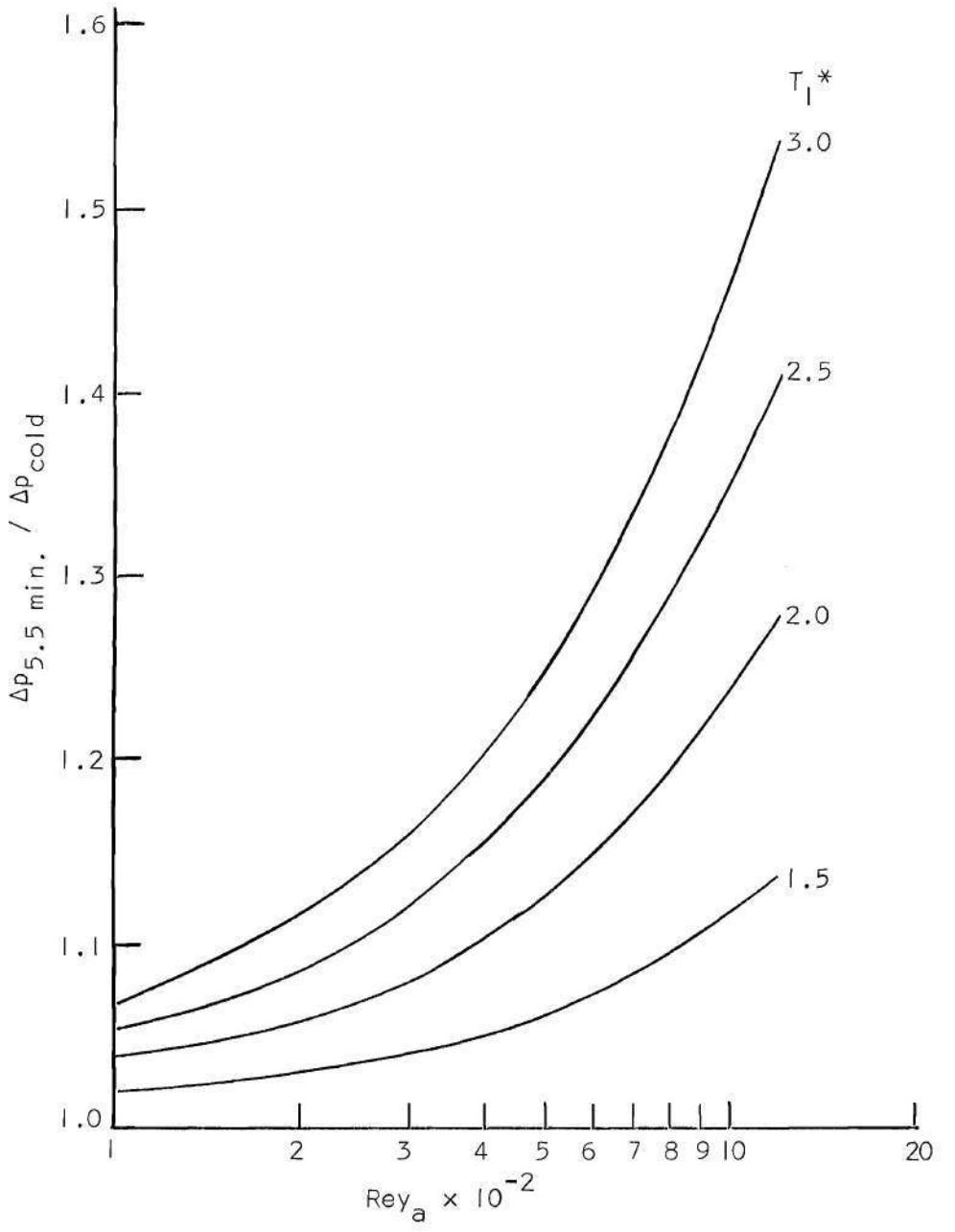

Figure 10. Effect of Reynolds Number on Theoretical Pressure Drop, L/D = 400

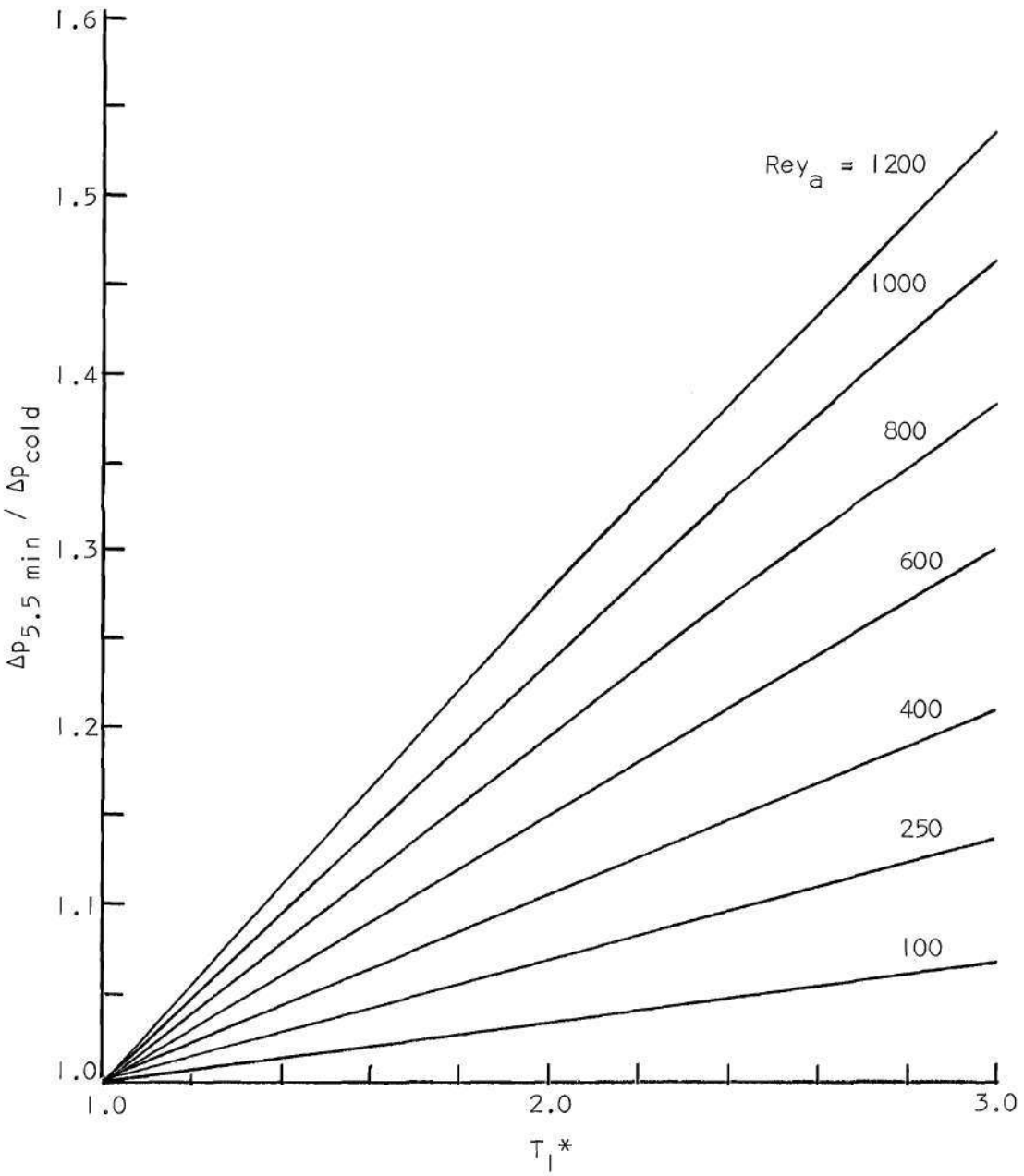

Figure 11. Effect of Temperature Ratio on Theoretical Pressure Drop, L/D = 400

(44). Using equations (41) and (44), the momentum equation (42) may be expressed as

$$\Delta_x(p) = -\Delta_x(\rho U^2) - 4\frac{\rho U^2}{2} f\Delta(^x/D_i) \tag{107}$$

and integration from the tube entrance to exit, together with the addition of the kinetic energy jump at the tube inlet yields the overall tube pressure drop

$$\Delta p = q_1 + 2(q_E - q_1) + \int_1^E 4qfd(^x/D_i) \tag{108}$$

If the dynamic pressure terms are rearranged in the form $q_E + (q_E - q_1)$ then equation (108) shows that the additional pressure drop for a hot flow due to the higher dynamic pressure at the tube inlet is compensated for by the loss in kinetic energy as the gas cools in passing to the tube exit. Then if the weak dependence of the dynamic pressure on the local pressure, as indicated by equation (78) for the local density, is neglected, the dynamic pressure terms in equation (108) are seen to be essentially linear functions of temperature. This result follows from the equality of the right hand sides of equations (41) and (43) and the boundary condition, equation (45), imposed on the mass flow.

On the other hand, the integral term in equation (108) may be explicitly defined in terms of equation (74) for the friction factor. Utilizing the exit dynamic pressure as a reference, equation (108) then is given as

$$\frac{\Delta p}{q_E} = 1 + \left(1 - \frac{T_1}{T_E}\right) + \int_1^E 4\frac{T}{T_E}\frac{64}{Rey}\frac{(\sigma + a)}{(\sigma^2 + 2\sigma a)^{\frac{1}{2}}} d(^x/D_i) \tag{109}$$

where

$$\sigma = \frac{4\ {}^{x}/D_i}{Rey} \tag{110}$$

and the Reynolds number depends upon the local temperature by virtue of the dependence of the viscosity on temperature. In the case of the cold flow, the integral term in equation (109) may be evaluated and inasmuch as the dynamic pressure is constant, the cold flow pressure drop is given by

$$\frac{\Delta p}{q_E} = 1 + \frac{64}{Rey}\frac{L}{D}\left[1 + 2\left(\frac{Rey}{4\ {}^{L}/D}\right)a\right]^{\frac{1}{2}} \tag{111}$$

For the hot flow, however, the integral must be evaluated numerically and its linear character cannot be demonstrated analytically. Likewise, slight departures from this essentially linear character, which may be observed in Figure 11 for the higher Reynolds numbers and temperature ratios, cannot be readily attributed to any specific cause analytically.

Length to Diameter Ratio Dependence

The dependence of the hot flow pressure drop at 5.5 minutes on the tube length to diameter ratio is given in Figure 12. Results of the theory for two inlet temperature ratios of 1.0 and 3.0, corresponding to a cold flow and a hot flow, are given for the entire range of Reynolds number investigated.

Comparison of the cold flow and hot flow results for a given Reynolds number shows that the increase in the pressure drop due to elevated inlet temperature is practically independent of the tube length. Figure 12 shows, however, that for hot flows in tubes shorter than approximately

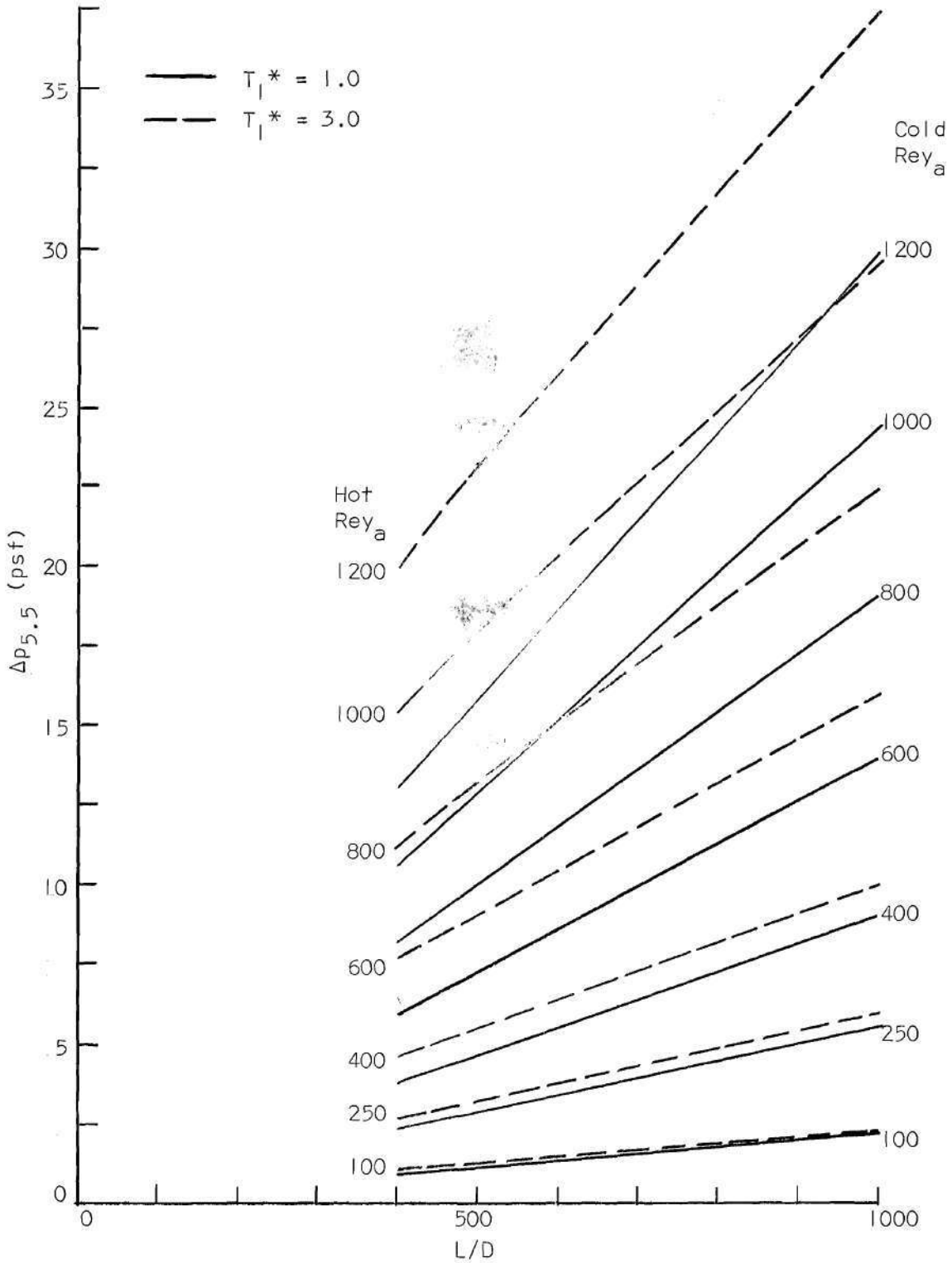

Figure 12. Effect of L/D on Theoretical Pressure Drop

600 diameters at the higher Reynolds numbers a slight downward trend of the pressure drop occurs with decreasing L/D. This nonlinearity, as mentioned previously, was not attributable analytically to a specific cause. However, inasmuch as the nonlinearity is not evident for the longer tubes in Figure 12, some physical reasoning applied to the pressure drop equation (109) indicates a probable explanation. First, in the integral term of equation (109) the local gas temperatures and frictional effects in the development region should be essentially independent of L/D. Thus if the shortest test tube (L/D = 400) is longer than the thermodynamic development length required for the gas temperature to be cooled to an ambient value, it should follow that longer tube lengths are equivalent to the addition of lengths of cold fully developed flow at the tube exit. Hence the dependence of the pressure drop on L/D for these longer tubes should be linear. Inasmuch as the short tube (L/D = 400) is, in fact, longer than the thermodynamic development length, the only plausible explanation for the existing nonlinearity in the theory is attributable to the choice of the different friction factor parameters for the various tubes so that the nonlinearity is a peculiarity of the inexactness of the theory.

Comparison of Experimental and Theoretical Pressure Drops

Based upon a choice of friction factor parameters and Nusselt number, theoretical predictions of the dependence of the tube pressure drop on Reynolds number, inlet gas temperature ratio, and tube length to diameter ratio have been given for the entire ranges of these parameters that were experimentally investigated. With this knowledge in

mind, a more complete comparison of the theoretical and experimental pressure drops is now given. Figure 9 gives such a comparison for the short test tube, L/D = 400, and similar comparisons for the longer tubes are presented in Figures 13, 14, and 15. It is immediately apparent from these latter figures that the comparison between experiment and theory is not as good for the longer tubes as was the case for the shorter tube. In some cases the theory and experiment agree well while in other cases the theory may be either above or below the experiment in its predictions. In any case, however, the discrepancy between the two is at most only about 10 per cent for the longer tubes as compared to 5 per cent for the short tube.

In view of the good agreement obtained for the short tube, Figure 9, and the realization that the tube length for the longer tubes should not significantly influence the change in the pressure drop from a cold to a hot flow, some suspicion may be placed on the experimental results. This is emphasized by close examination of Figures 13 through 15. The fact that the theory very accurately describes the trend of the experimental results with time may be demonstrated by comparing the experiment and theory with reference to the pressure drop at 5.5 minutes. The results of this comparison for the different test tubes are shown in Figures 16, 17, 18, and 19 in terms of the ratio of $\Delta p/\Delta p_{5.5\ min.}$ versus time. Considering the magnification utilized in the ordinates of these plots it is seen that the maximum discrepancy is only of the order of four per cent. Thus the trend of the theoretical predictions is acknowledged to be excellent.

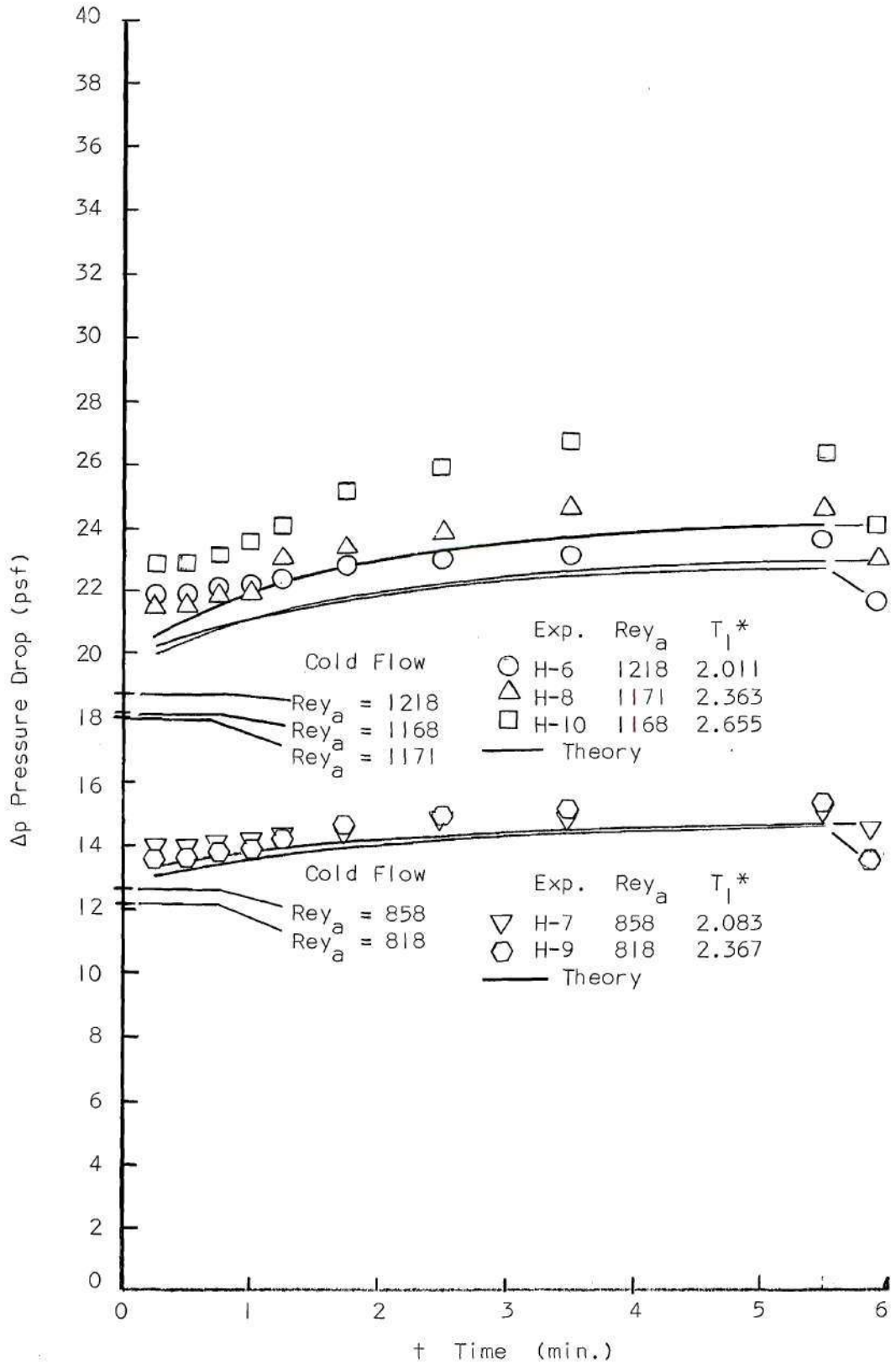

Figure 13. Hot Flow Pressure Drop, L/D = 600

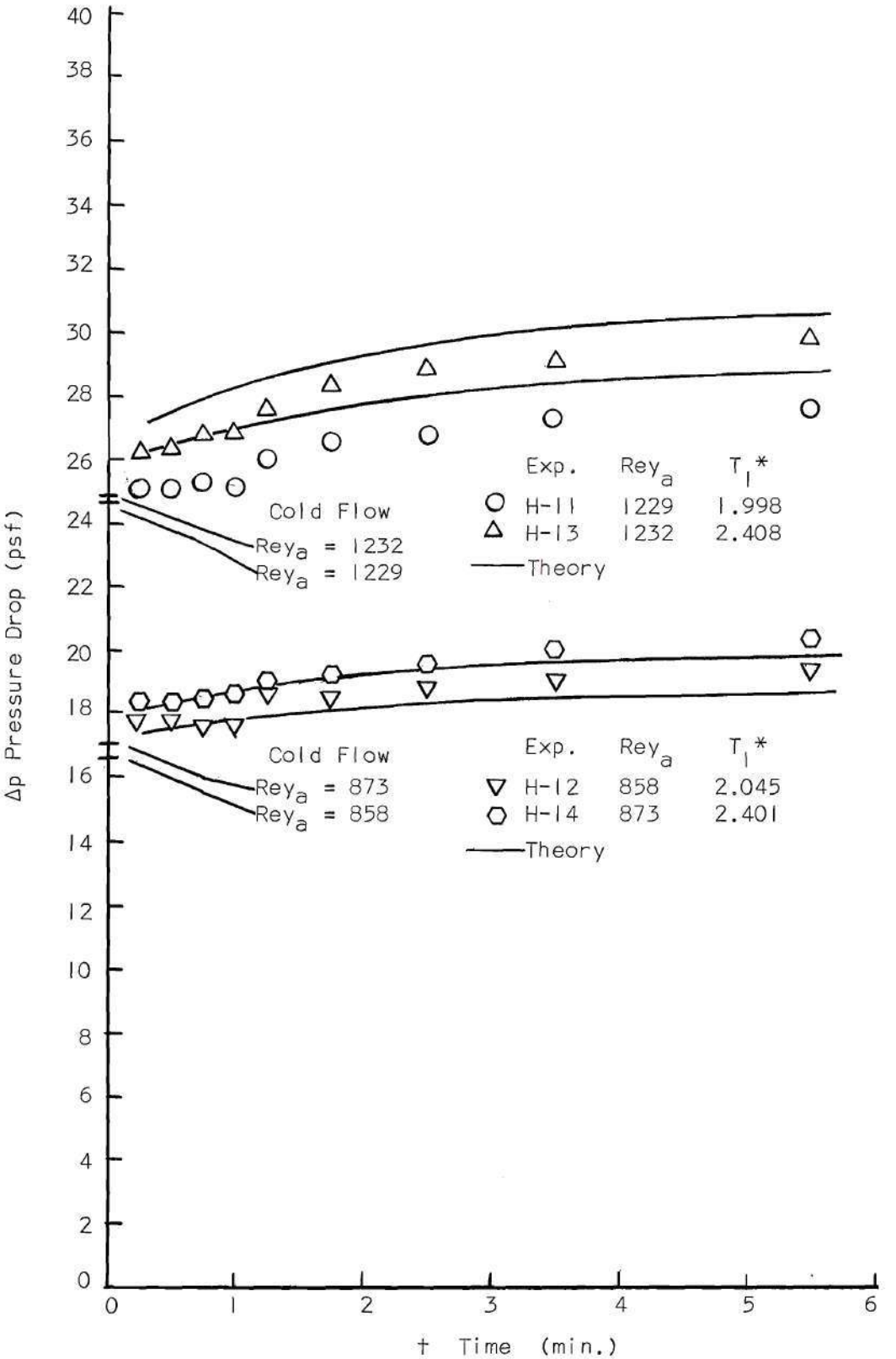

Figure 14. Hot Flow Pressure Drop, L/D = 800

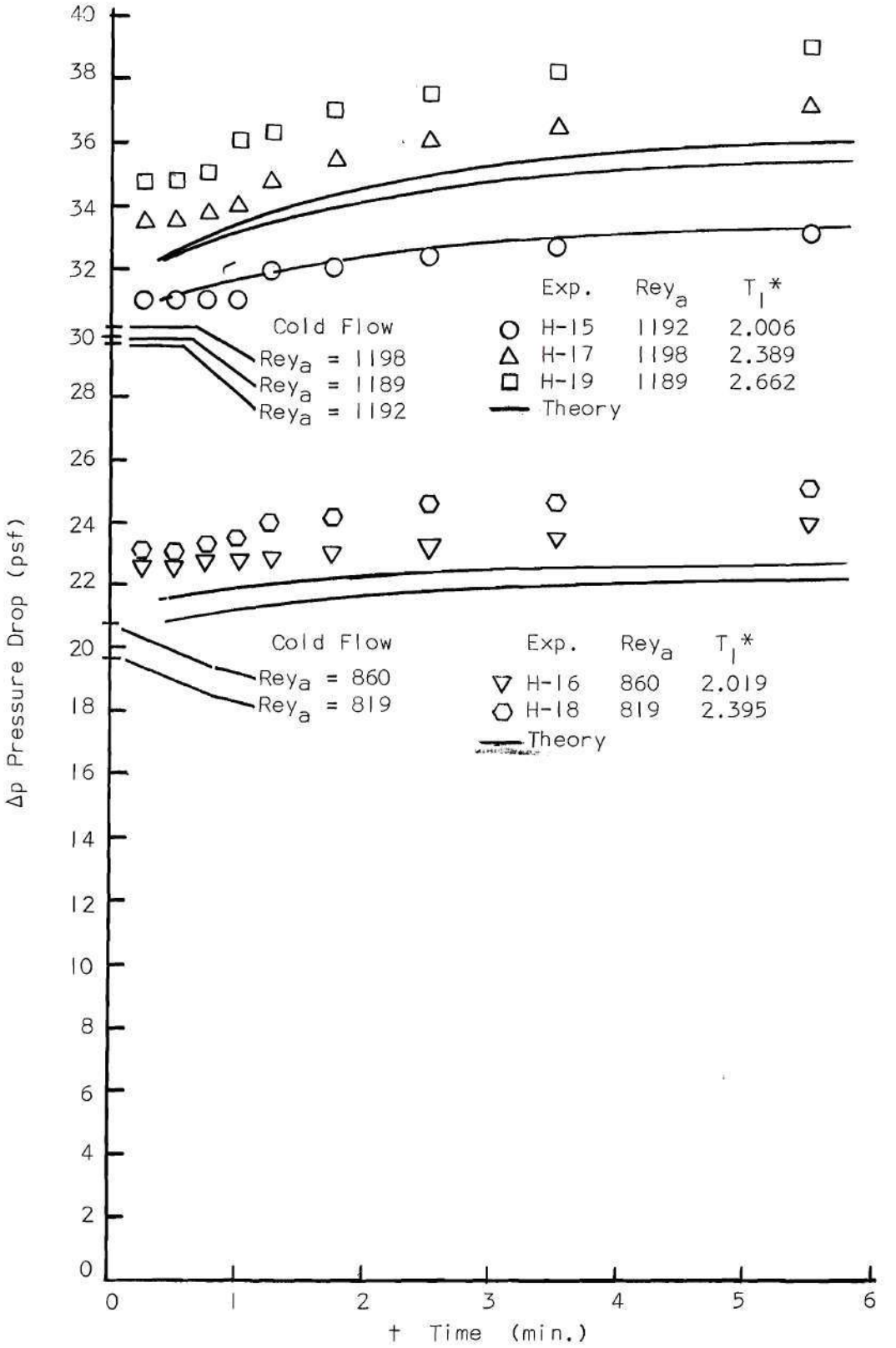

Figure 15. Hot Flow Pressure Drop, L/D = 1000

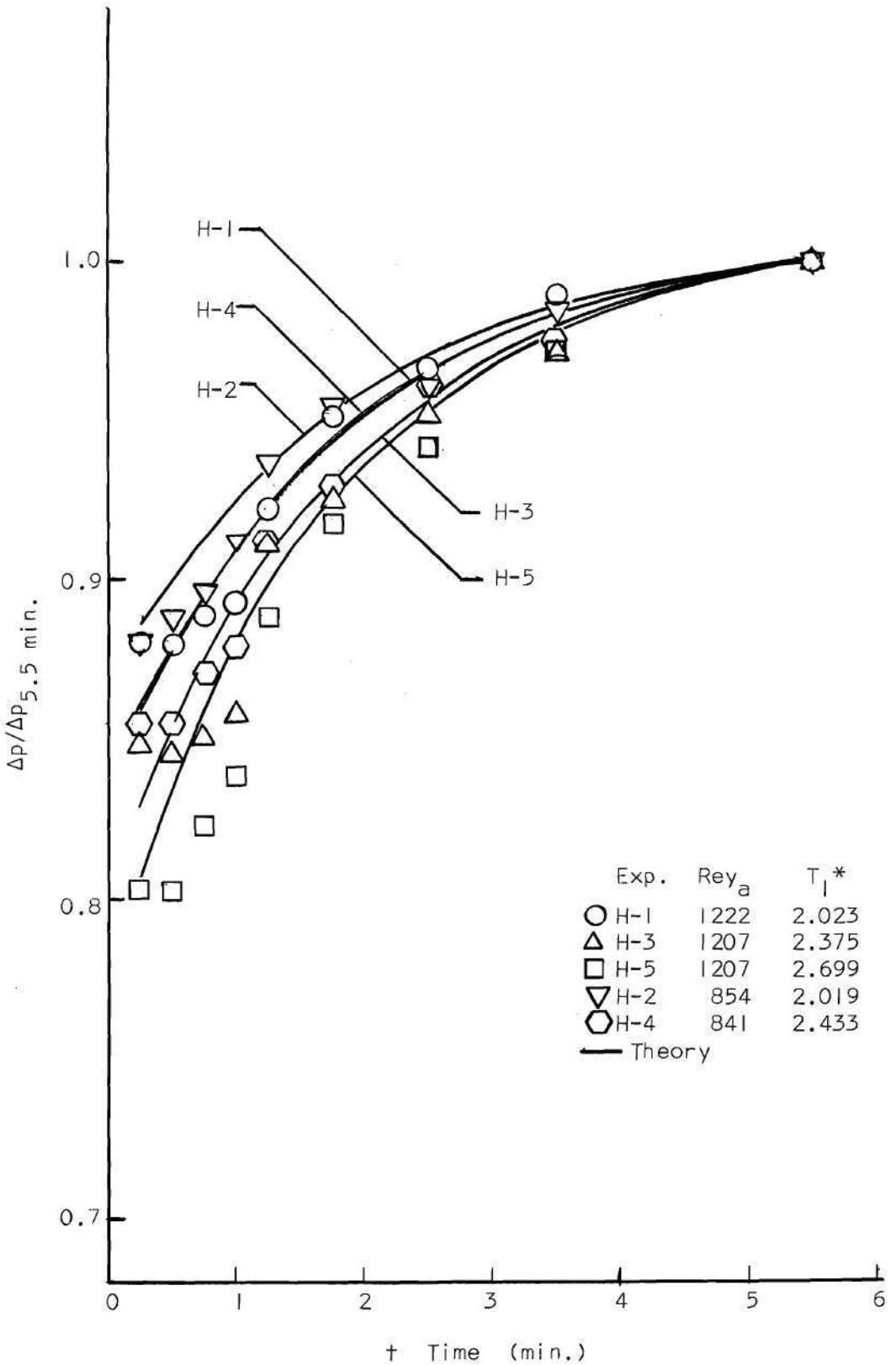

Figure 16. Hot Flow Pressure Drop Ratio, L/D = 400

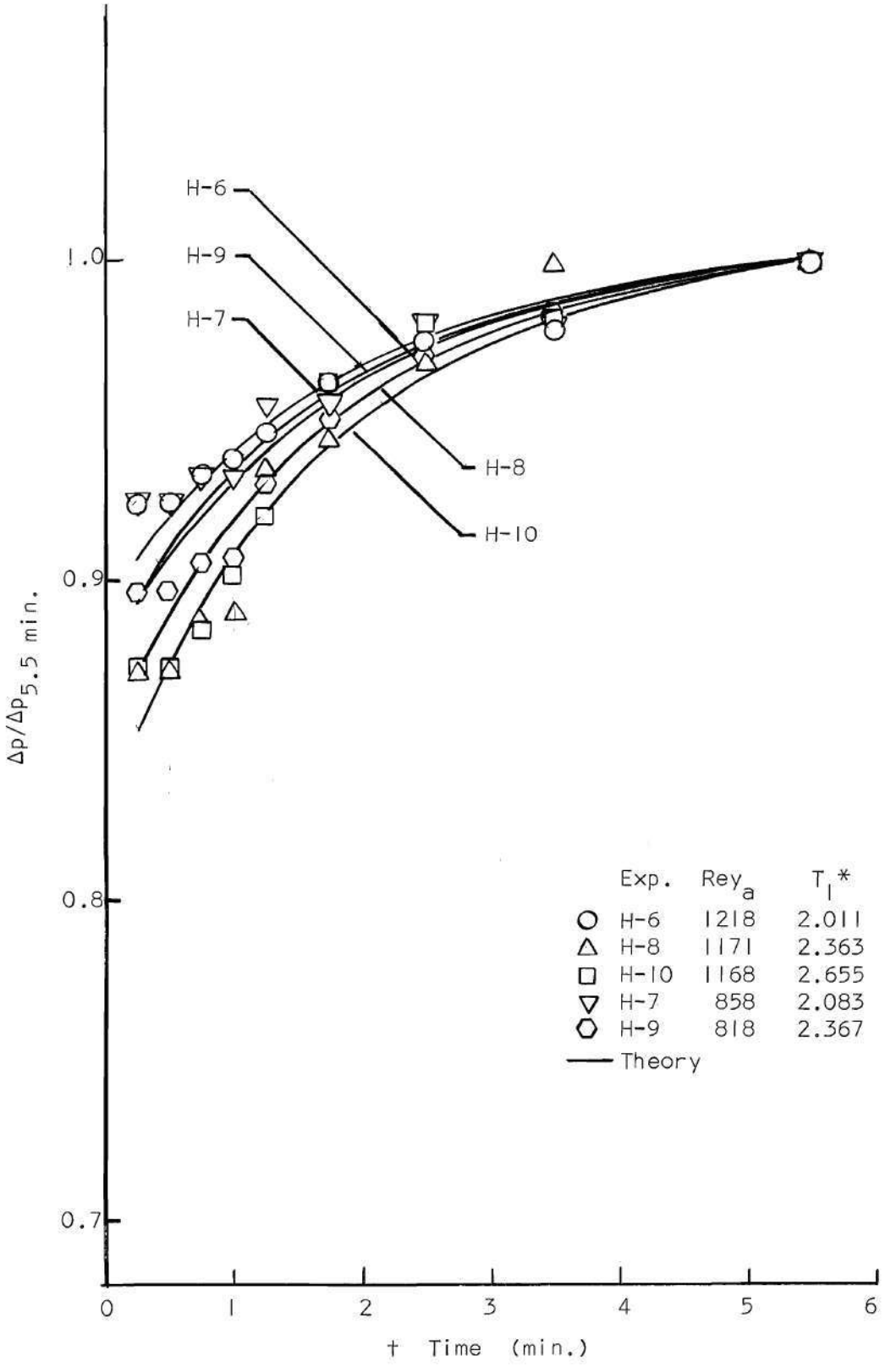

Figure 17. Hot Flow Pressure Drop Ratio, L/D = 600

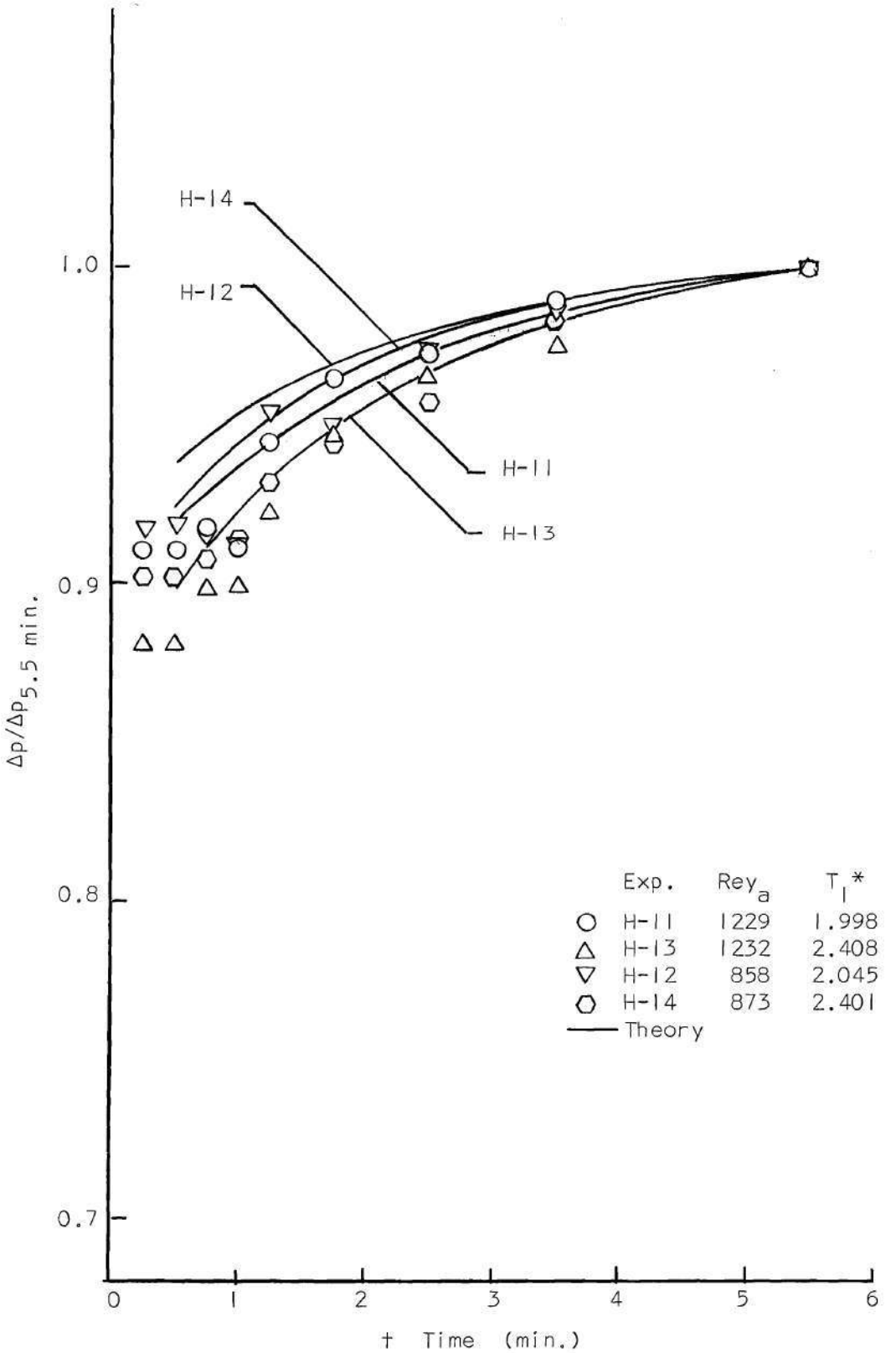

Figure 18. Hot Flow Pressure Drop Ratio, L/D = 800

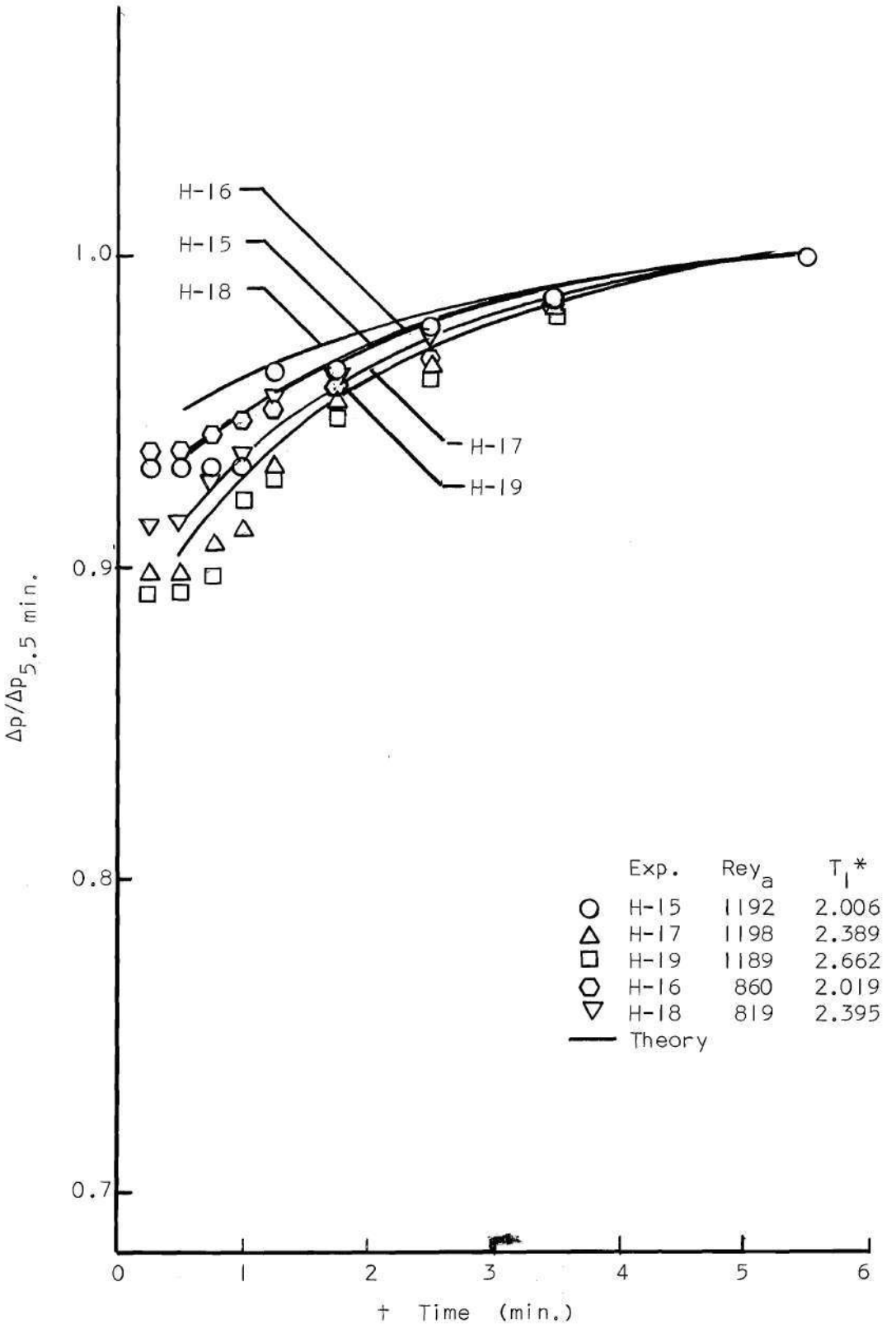

Figure 19. Hot Flow Pressure Drop Ratio, L/D = 1000

The additional 5 per cent discrepancy between the theory and experiment for the longer tubes as compared to the results for the short test tube may be accounted for satisfactorily in terms of several considerations pertinent to the experiments. First, the short tube was utilized as a model in the perfection of the experimental setup and the final runs for this tube were conducted carefully. In the case of the runs for the longer tubes, care was exercised but these experiments were completed somewhat more quickly than those for the short tube. As a consequence, the long tube results, as given in Table A-2, show generally more variation in the Reynolds number and inlet temperature ratio during a run than is the case for the short tube. These variations are, however, not large and at most should not effect discrepancies of more than two per cent judging by the percentage variation of the Reynolds number during a run. On the other hand, the presence of this type of variation in the experiment makes it difficult to choose the correct nominal value for the Reynolds number, in particular, for use in the theory. Thus uncertainty in the correct theoretical input to check the experimental results may contribute an additional error of several per cent depending upon the magnitudes of the variations in the Reynolds number and inlet temperature ratio.

Comparison of Experimental and Theoretical Gas and Wall Temperatures

The theory and experiments pertaining to the short tube, L/D = 400, are compared in Figures 20-24 and Figures 25-29 corresponding to the gas temperatures and wall temperatures, respectively. In each figure

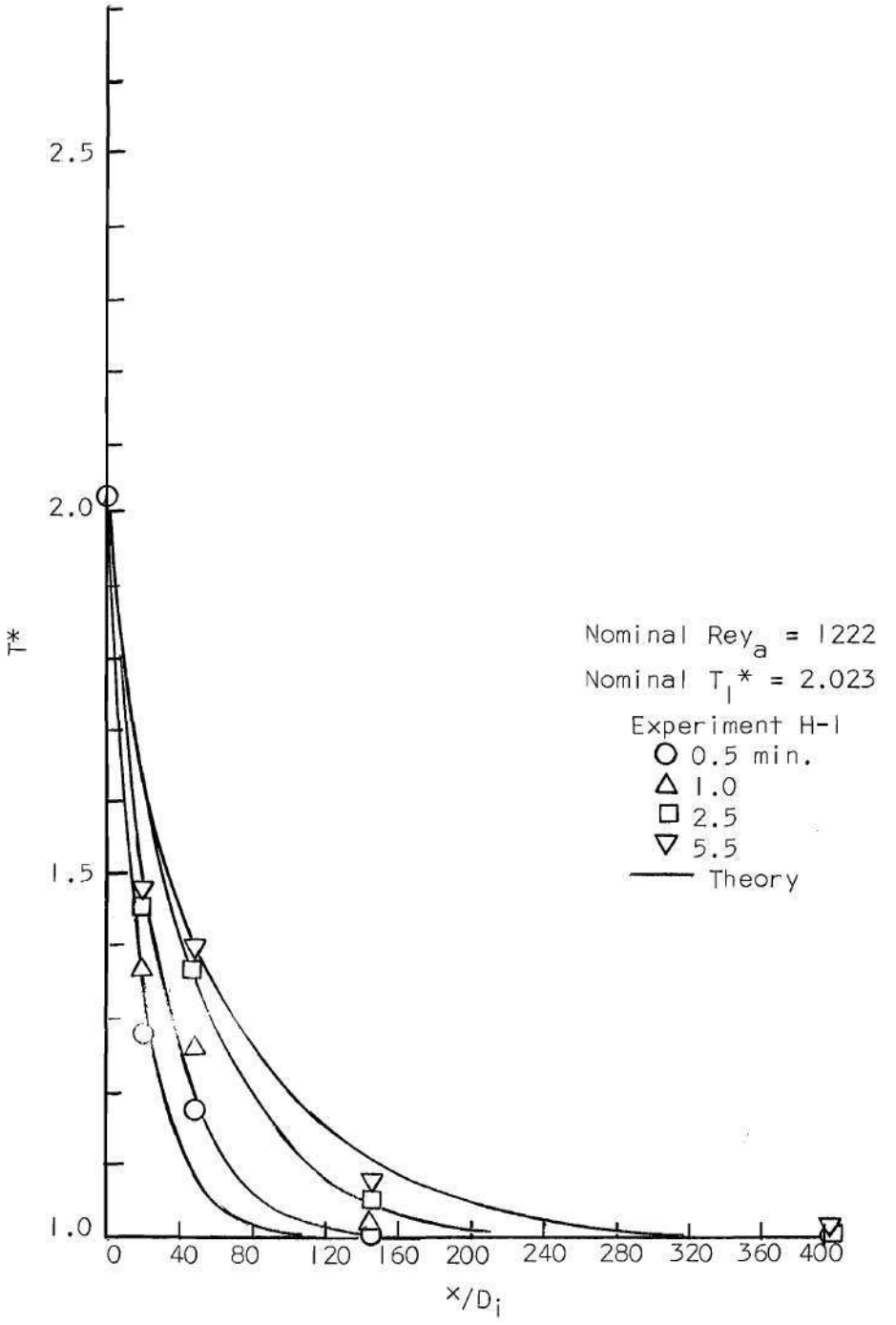

Figure 20. Gas Temperature Distribution, L/D = 400

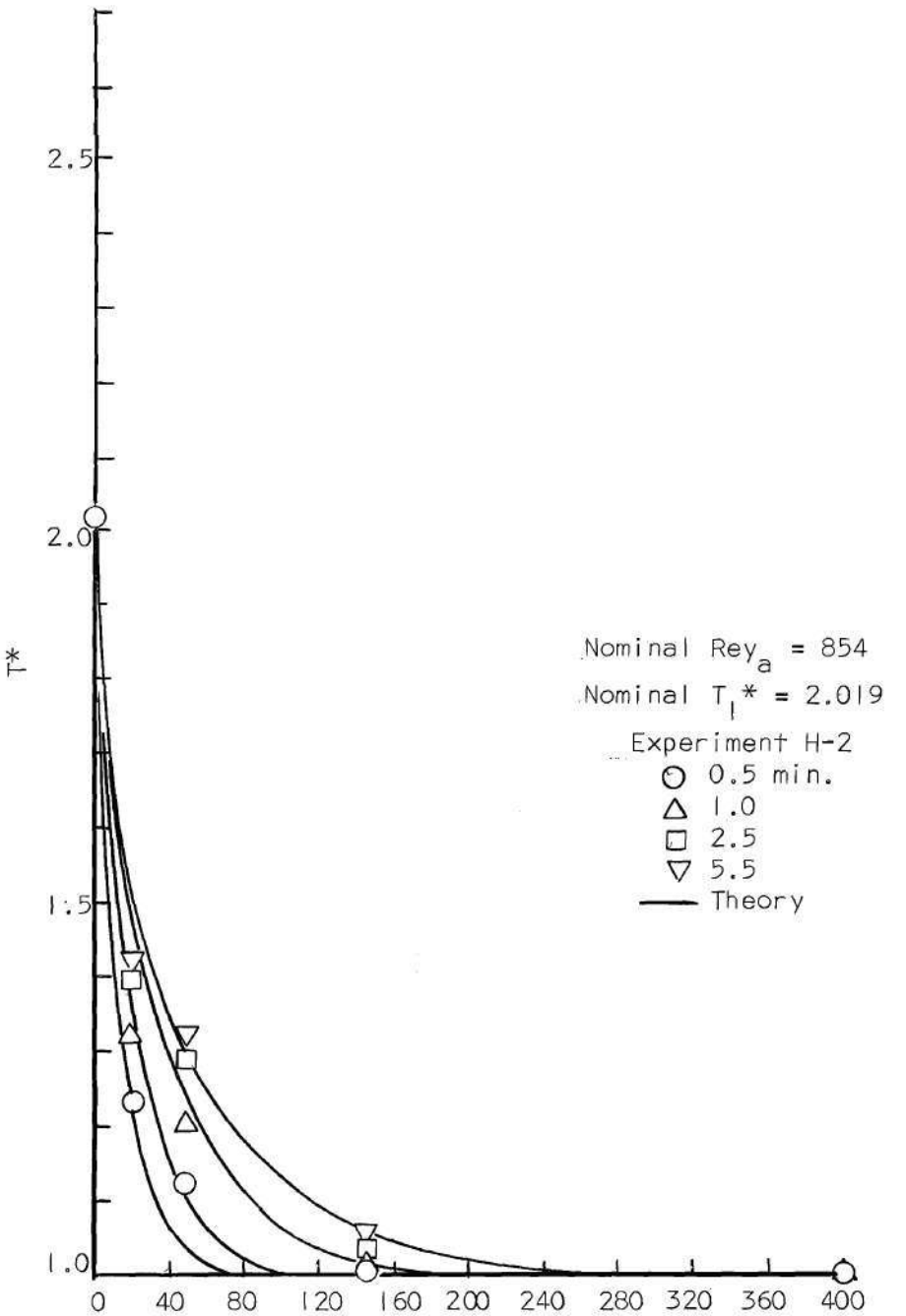

Figure 21. Gas Temperature Distribution, L/D = 400

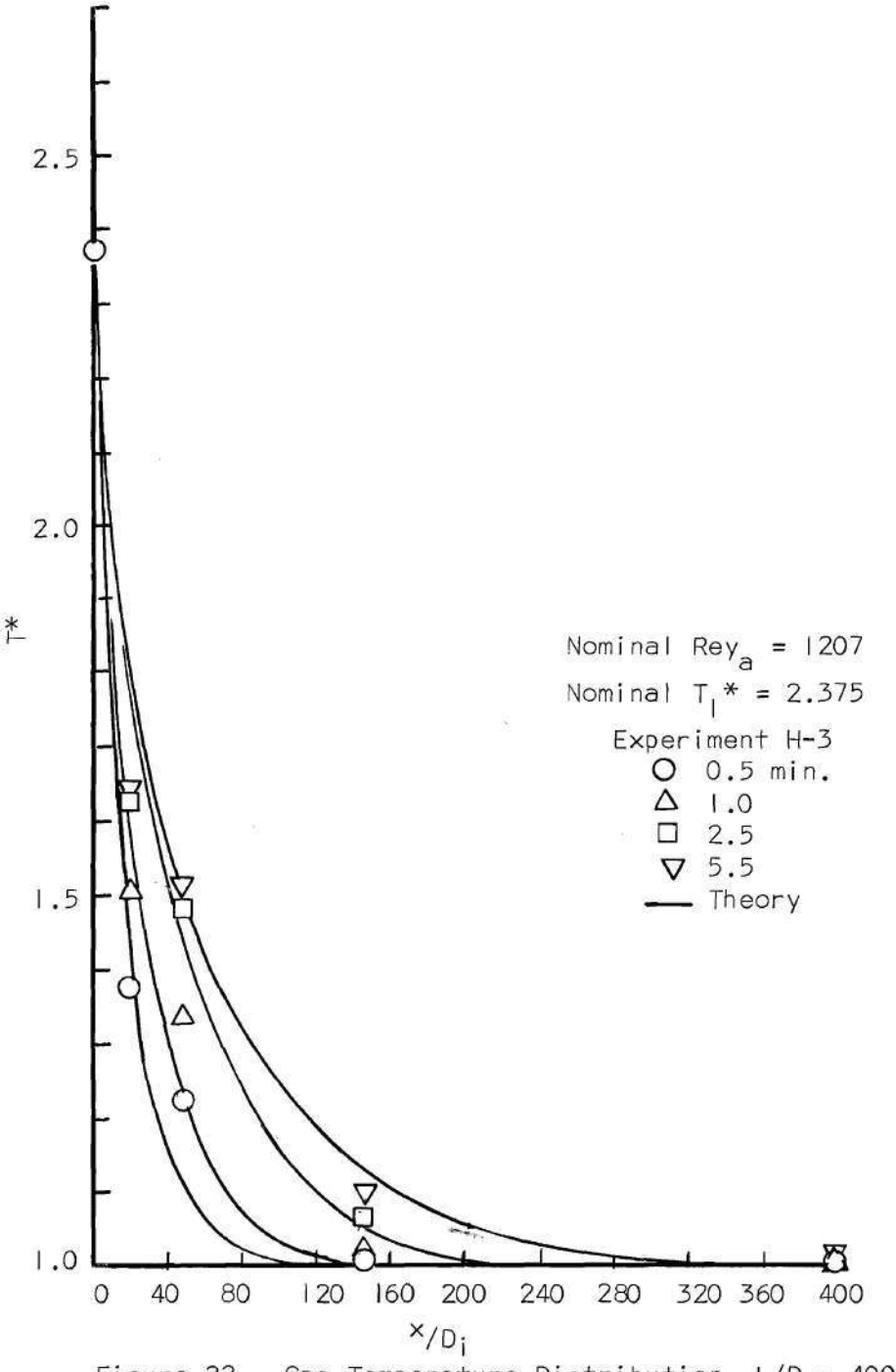

Figure 22. Gas Temperature Distribution, L/D = 400

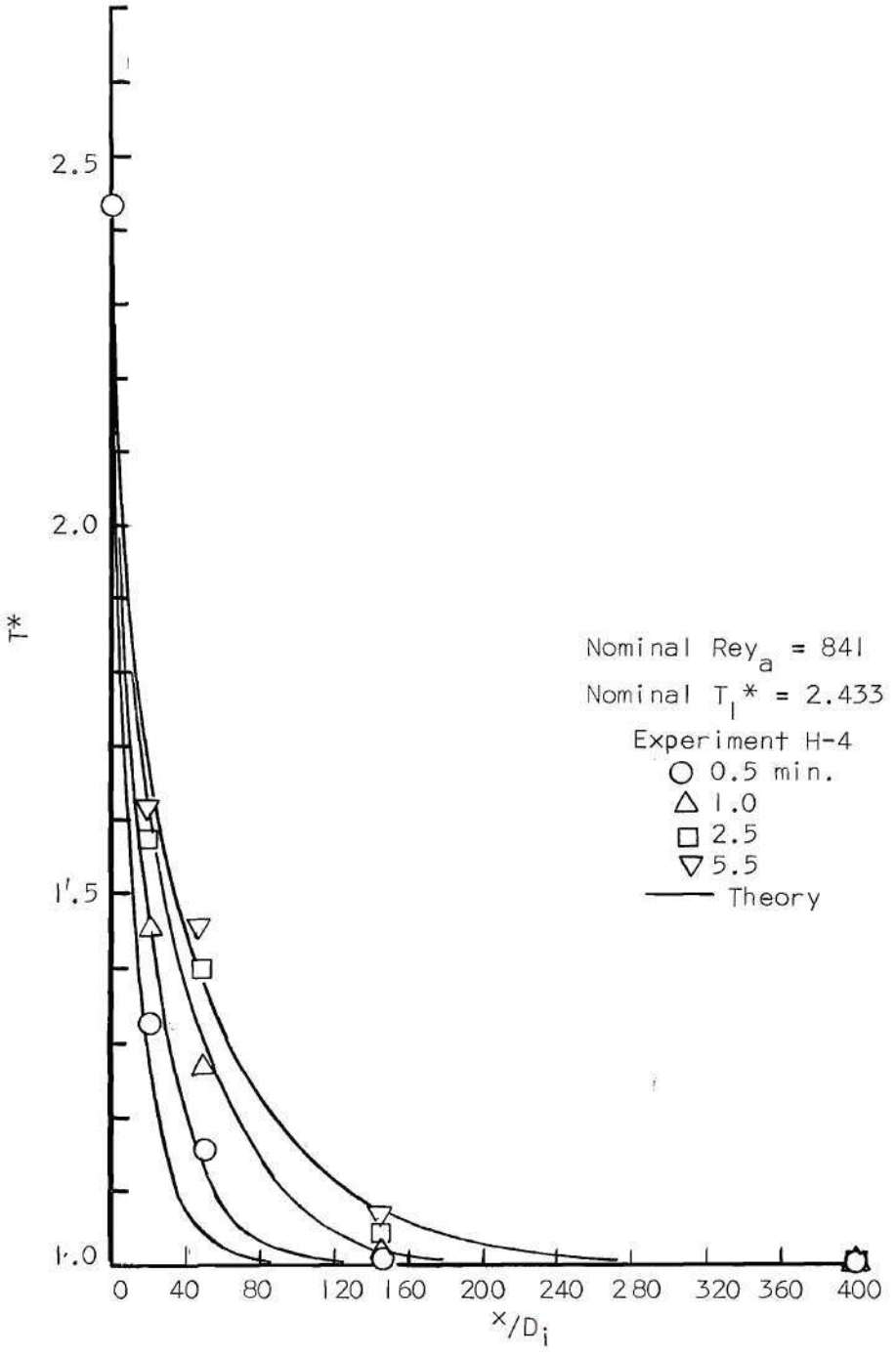

Figure 23. Gas Temperature Distribution, L/D = 400

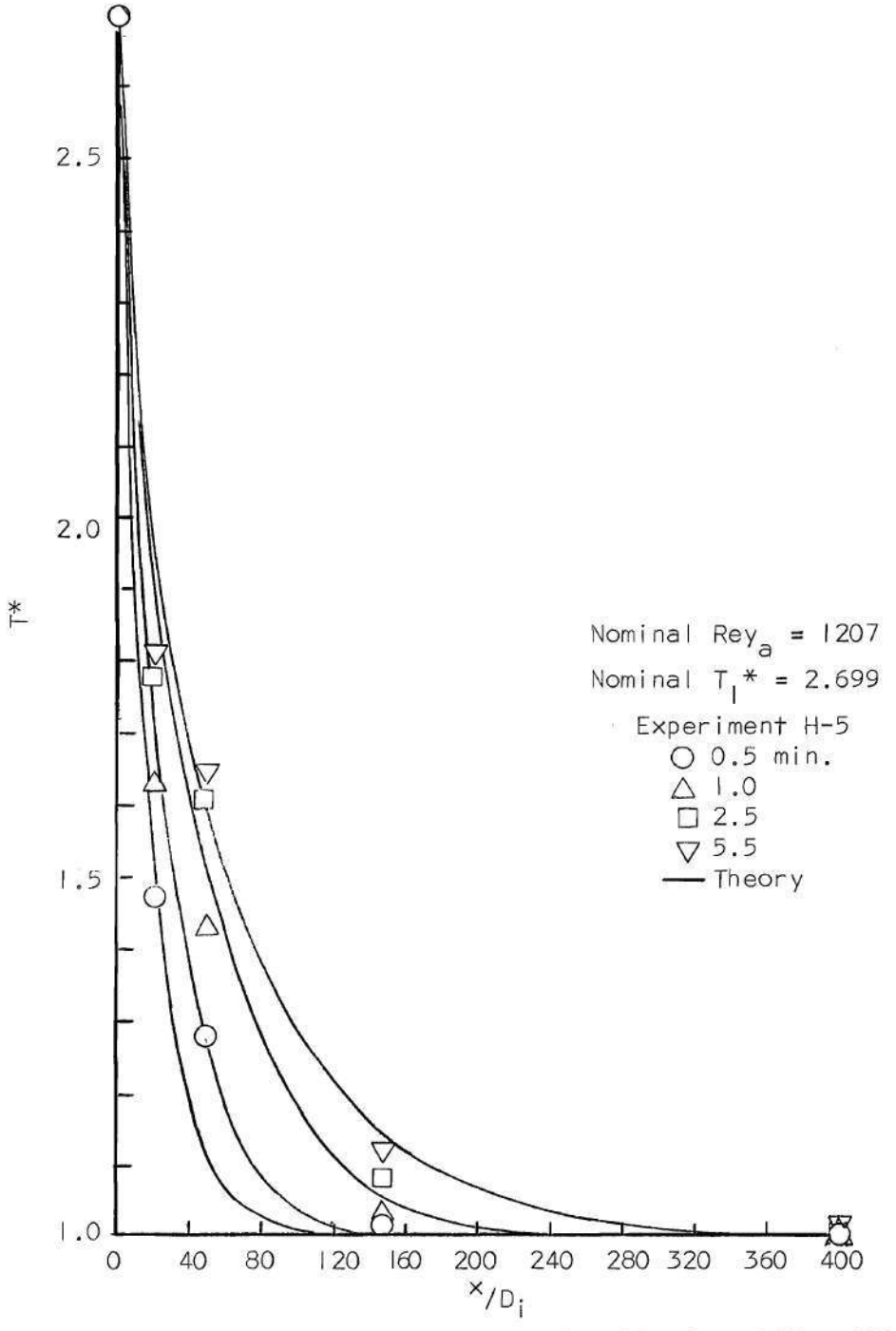

Figure 24. Gas Temperature Distribution, L/D = 400

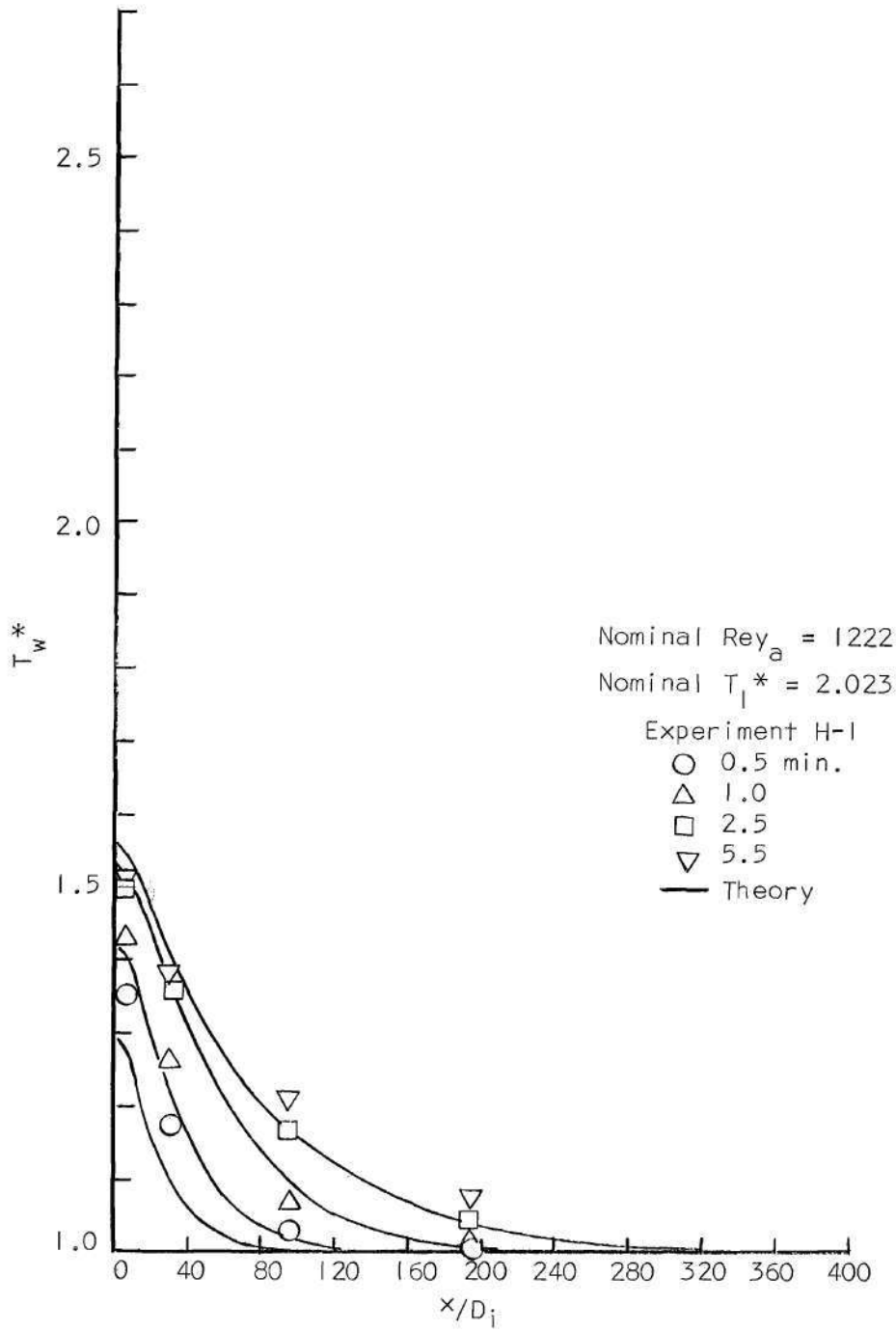

Figure 25. Wall Temperature Distribution, L/D = 400

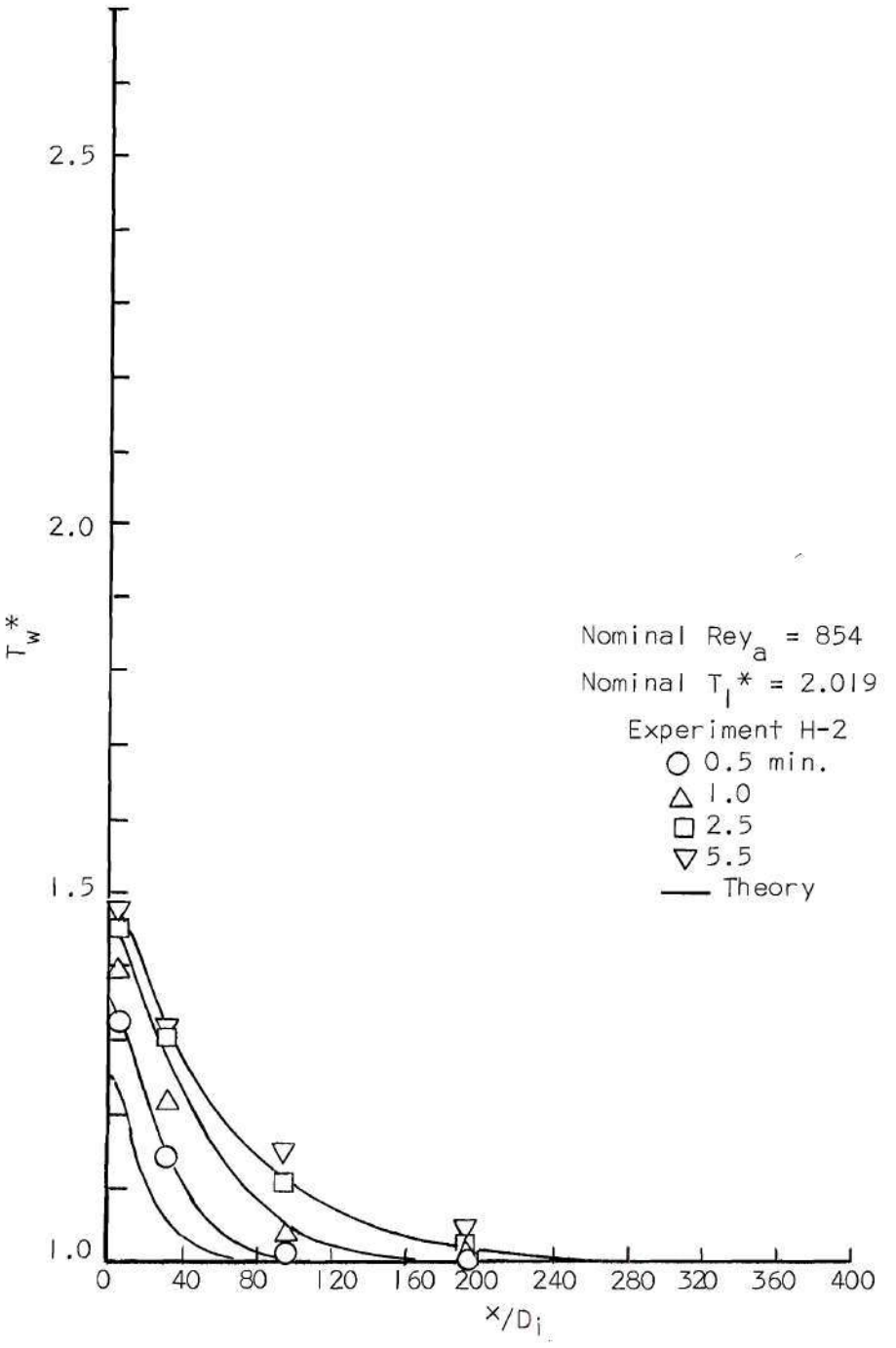

Figure 26. Wall Temperature Distribution, L/D = 400

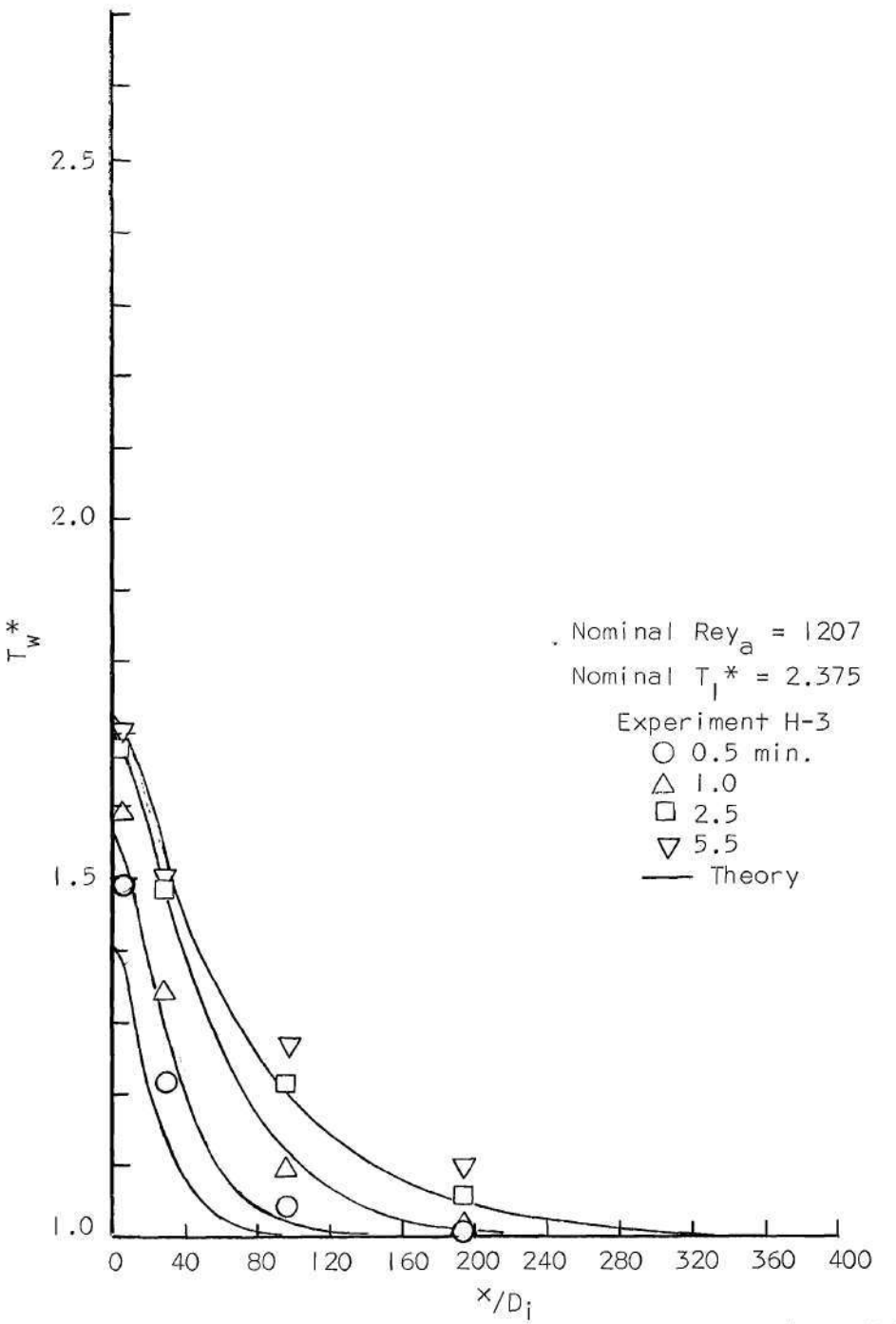

Figure 27. Wall Temperature Distribution, L/D = 400

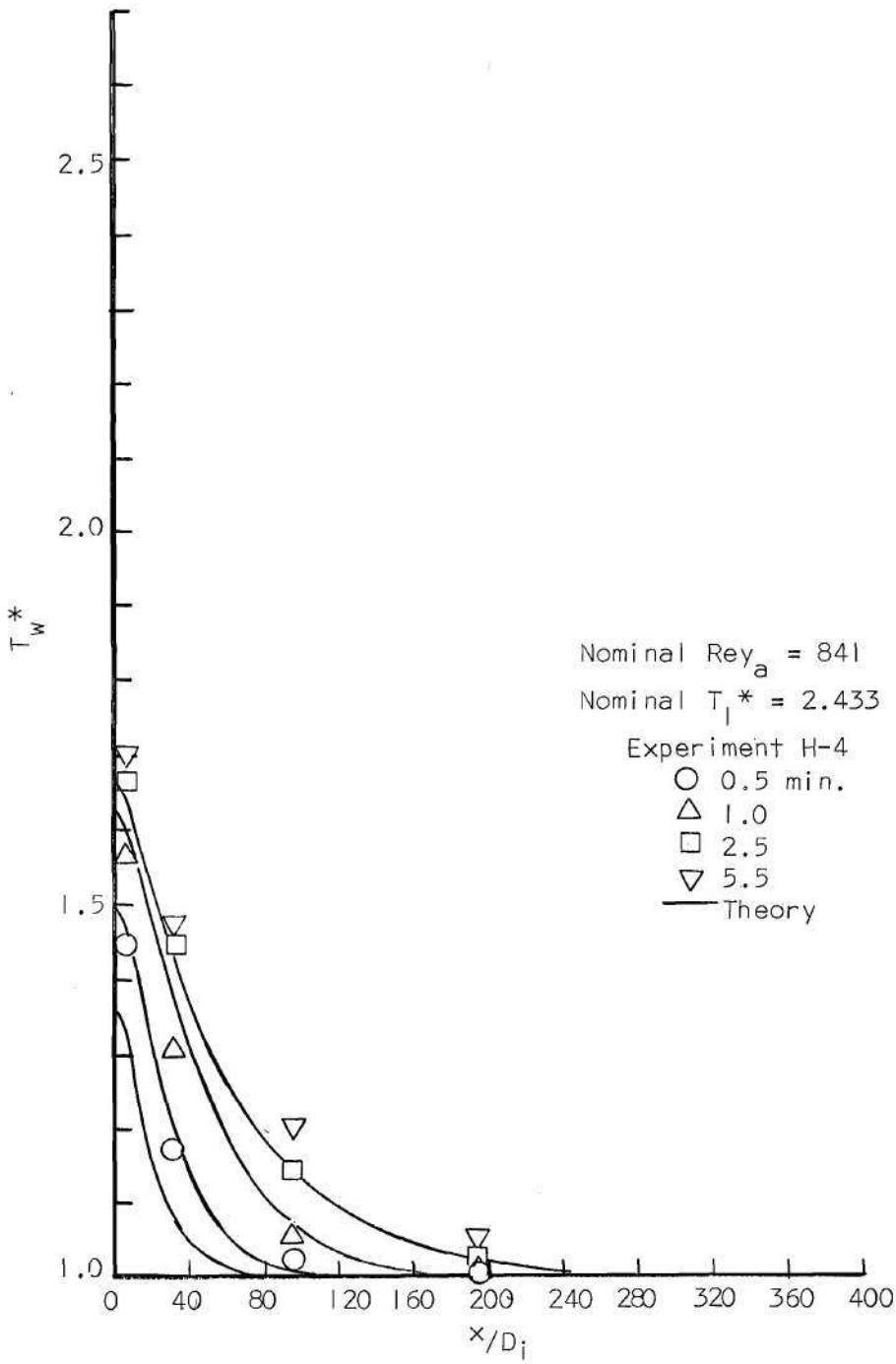

Figure 28. Wall Temperature Distribution, L/D = 400

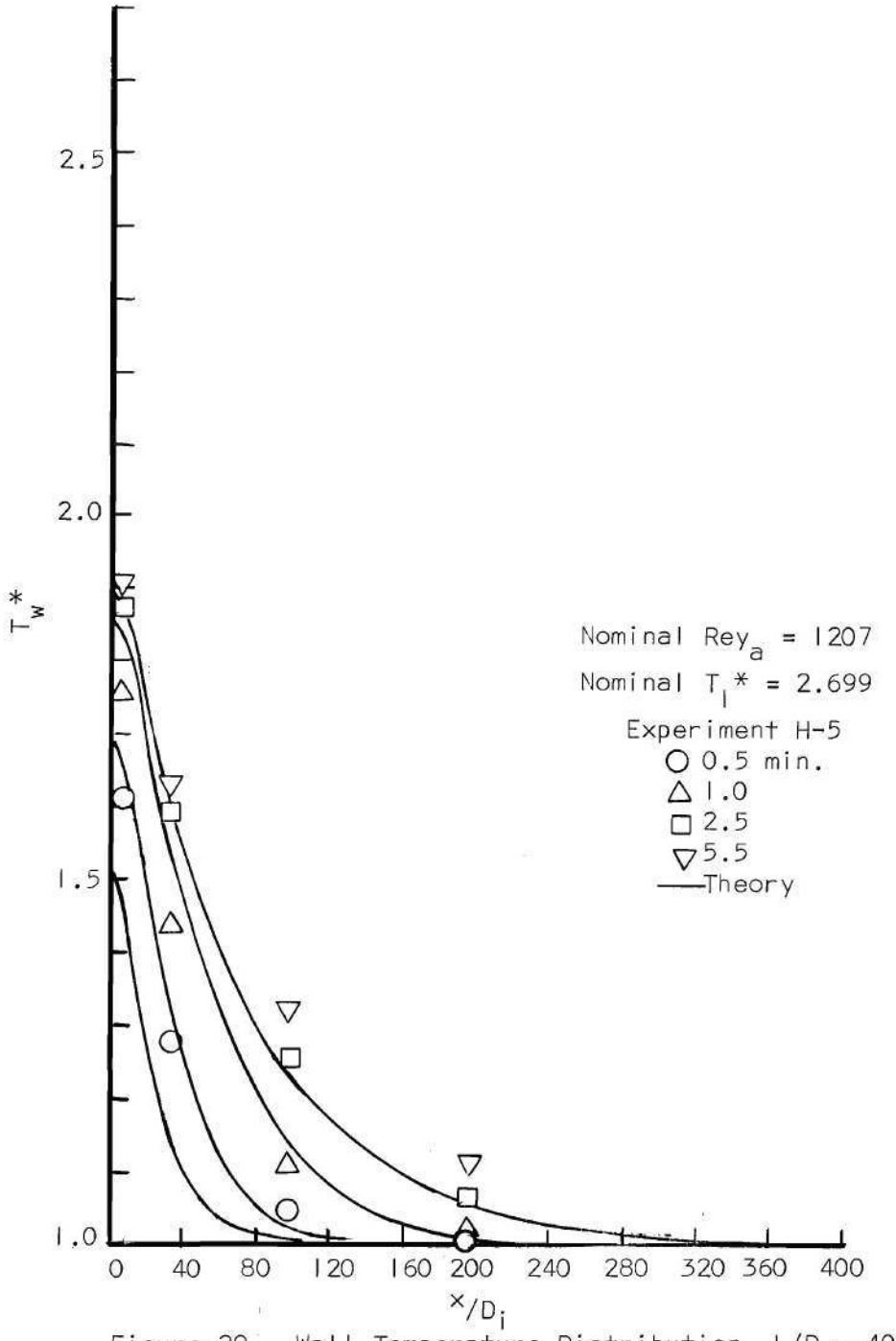

Figure 29. Wall Temperature Distribution, L/D = 400

results are shown in the form of temperature ratios versus position for times corresponding to 0.5, 1.0, 2.5, and 5.5 minutes of elapsed time from initiation of the hot flow run. Practically the same results are obtained for the temperature distributions of the longer tubes, so these results are not illustrated graphically. For reference purposes, however, all experimental results are given in Appendix A.

Due to the large number of variables and parameters, as well as the assumptions, utilized in the present investigation, it is difficult to make a definite and concise criticism of the comparisons of the temperature distributions. Based upon both analytical and experimental experience with the problem, however, it is generally observed that the comparisons are good.

Specific observations as they pertain to, first, the gas temperatures and then the wall temperatures, are given as follows.

Gas Temperatures

The gas temperature ratio distributions shown in Figures 20-24 demonstrate general tendencies for the theory to overpredict results near the tube inlet for large times and to underpredict results further down the tube for small times. In view of the complications of coupling with the wall, it is difficult to explain why this happens; however, it should be pointed out that the experimental results corresponding to gas temperatures at about $x/D_i = 20$ are low in comparison to those obtained with the longer tubes. Also it may be noted that for large times the results for the first three gas temperatures at $x/D_i = 20$, 50, and 150 lie on either a straight line or a curve with negative curvature, which is not to be expected. This result may be attributable to an amplifier

nonlinearity, inasmuch as several of the DC amplifiers experienced this difficulty, and attempts were made to remedy this situation in the tests for the longer tubes. If allowance is made, in the comparison, for this inaccuracy, better comparison should be expected near the tube inlet.

The trend of the gas temperatures along the test tube according to both theory and experiment shows that with time the temperatures near the tube inlet increase rapidly for small times with a relatively early approach to their equilibrium value. The gas temperatures further down the tube, on the other hand, change slowly at small times and appear to undergo the significant part of their change after the temperatures near the tube inlet have already approximately reached equilibrium.

Wall Temperatures

The wall temperature distributions, Figures 25-29, illustrate that the theory underpredicts all wall temperatures for small times and those further down the tube for larger times. Attempts were made to analyze these results and alter them by use of a Nusselt number distribution, as discussed previously, with some small improvement in the wall temperature distributions near the tube inlet, poorer agreement further down the tube, and a sacrifice of gas temperature agreement near the inlet. Rather than attempt to improve on these results by what may be referred to as computer experimentation, efforts at improvement must involve some accurate physical knowledge of the Nusselt numbers for the forced convection and also for the free convection external to the tube in the presence of a varying wall temperature.

In general the wall temperatures show a time and spatial dependence similar to the gas temperatures, evidence suggesting that the role

played by longitudinal conduction in the tube wall is secondary to the forced convection heating interior to the tube. At the tube inlet, the influence of the boundary condition corresponding to an insulated end is observed only over a very small length of the tube and it is concluded that this influence is for practical purposes insignificant.

Tube Pressure Distribution

From the preceding examination of the tube gas and wall temperatures some observations regarding the contributing factors to the tube pressure drop and pressure distribution may be made. The contribution to the increase in the tube pressure drop, for hot flow, due to the kinetic energy jump at the tube inlet has already been examined and was found to be directly proportional to the inlet temperature for all practical purposes. Likewise, it was pointed out that this contribution was compensated for by the gas cooling as it passed through the tube. This cooling term is given in terms of the gas and wall temperatures and the Nusselt number in the equation for the pressure difference, equation (42). Inasmuch as the local dynamic pressure varies directly with the temperature, the cooling contribution alleviates the pressure difference, $\Delta_x(p)$, in proportion to the quantity $Nu_i(T - T_w)/Rey$. Examination of the tube gas and wall temperatures, Figures 20 through 29, shows that the temperature difference is large only very near the tube inlet and consequently the relatively large magnitude of the Nusselt number is appropriate to this term, as mentioned previously. Likewise the gas temperatures are large near the inlet, so that a significant portion of the contribution of the cooling term should come from the inlet region.

Further down the tube the temperature difference and the gas temperature are smaller and a significant contribution from this portion of the tube is accounted for as an accumulation of smaller values.

In opposition to the cooling contribution, the frictional term in equation (42) increases the local pressure gradient throughout the region of elevated temperatures. Again, however, the major contribution of the friction term to the increase in the tube pressure drop due to hot flow comes from the development region where the higher friction factors are magnified by the high temperatures. Likewise, further down the tube the accumulated contributions due to essentially fully developed flow at elevated temperatures are significant.

The net result of these effects may be observed in Figure 30, which presents a sample pressure distribution for various times for the short test tube at high Reynolds number and inlet temperature ratio. The development length, according to Boussinesq (5), is shown in the figure and good agreement with the cold flow theory development length is evidenced by the slope of the pressure distribution for $t = 0$. As a consequence, it is observed that for small times all of the increase in the pressure drop is due to the altered pressure distribution in the development region and for large times the major portion (approximately 5/6) of the increase is also due to development region effects.

Dependence of Pressure Drop on Wall Thickness Ratio

Besides the parameters already discussed, the only other parameter which may be easily investigated by means of the theory is the tube wall thickness to internal diameter ratio. The results of a series

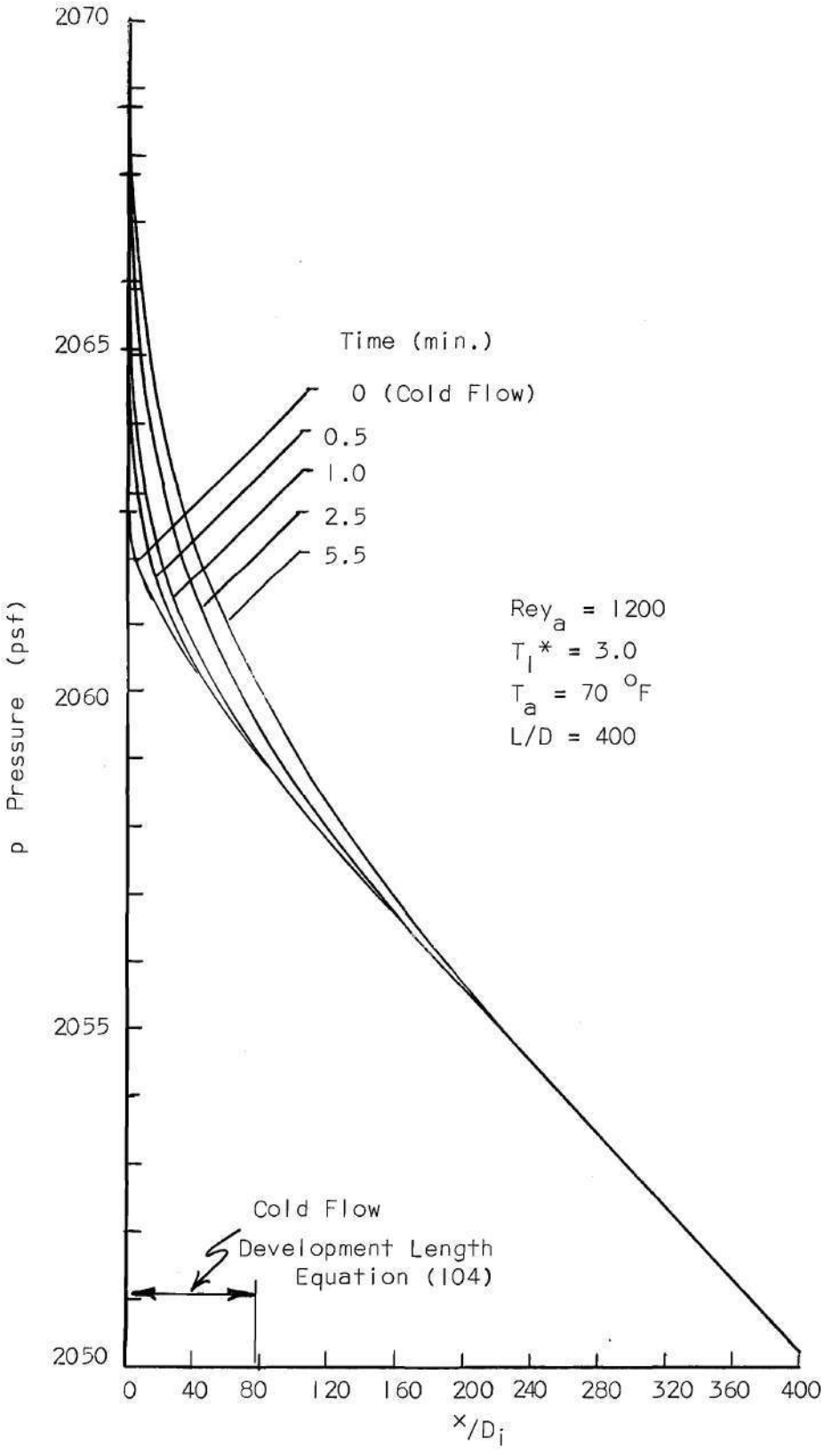

Figure 30. Hot Flow Pressure Distribution

of computer runs for the short tube, L/D = 400, with a mass flow rate corresponding to Rey_a = 1200 and inlet temperature ratio of T_1^* = 3.0 are presented in Figure 31 for thickness ratios from 0.05 to 0.90. These values, corresponding to a range from very thin to thick walled tubes, bracket the experiments of the present investigation in which t/D_i = 0.3.

As would be expected the very thin walled tubes demonstrate a much faster response to an elevated inlet temperature with consequent shorter time to approach equilibrium and higher pressure drops due to the higher gas temperatures that would result due to the decreased heat capacity of the wall. Just the opposite performance would occur for the thick walled tubes.

An interesting observation is made for the very thin walled tubes at small times. The results of Figure 31 show very high rates of change of the pressure drop and consequently the pressures with time and thus indicate that the quasi-steady assumption applied to the gas flow would decrease in its validity for thin walled tubes. On the other hand, as the wall thickness is increased without limit, the theory is likewise invalid due to the assumption of a finite control volume and constant wall temperature radially. The theory would predict incorrectly in this case no change in wall temperature and no change in pressure drop after the initial transients of the flow.

Inasmuch as no experimental verification of these results were sought in the present work, the dependence on the wall thickness ratio in the neighborhood of t/D_i = 0.3 should be utilized with care.

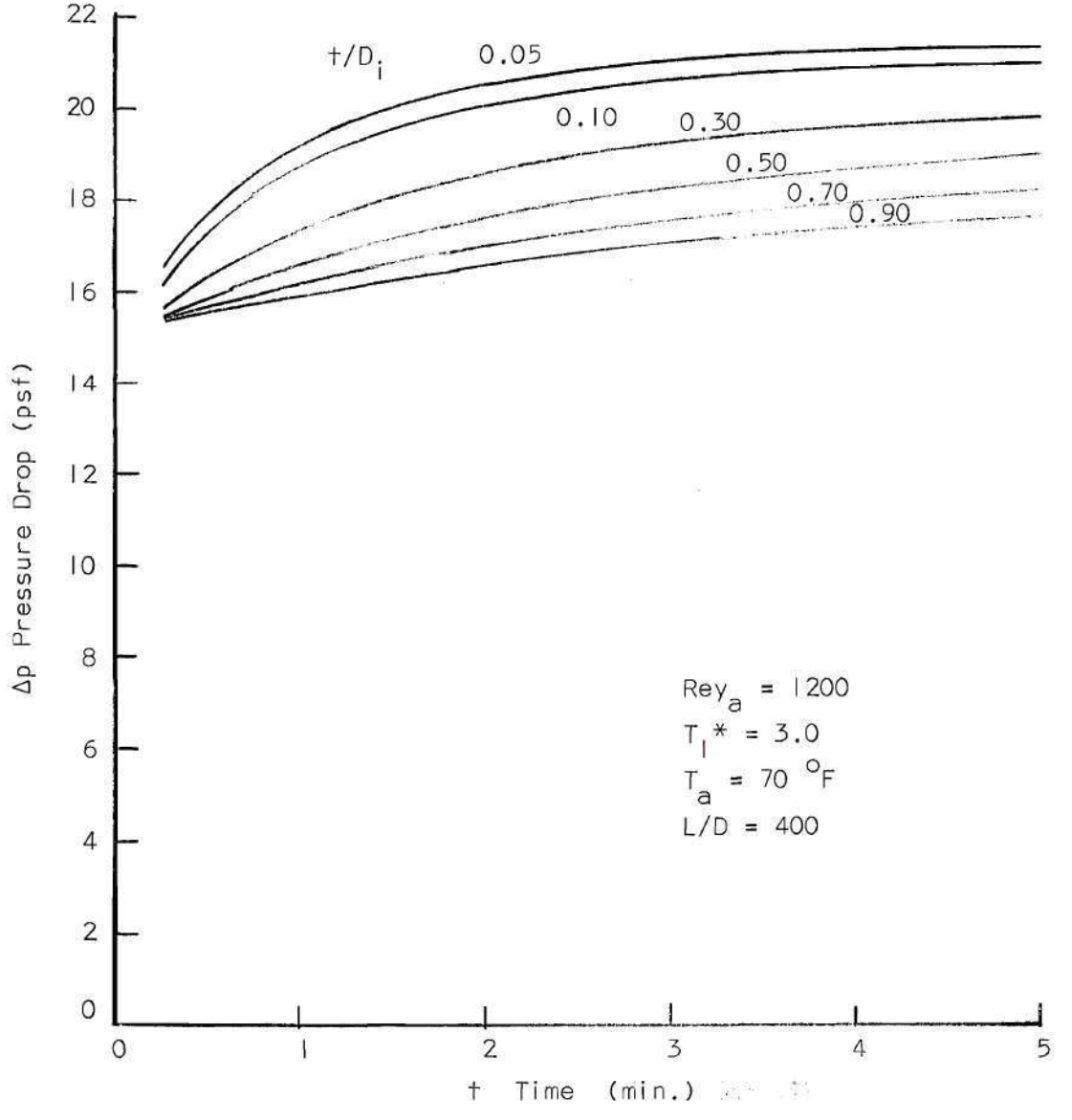

Figure 31. Effect of Wall Thickness Ratio on Theoretical Pressure Drop

CHAPTER VIII

CONCLUSIONS AND RECOMMENDATIONS

The time dependent flow of air in long slender tubes subjected to a step function increase in gas inlet temperature with natural cooling of the wall to the surrounding atmosphere has been investigated analytically and experimentally. The results of this study lead to the following conclusions:

1. The assumption of an idealized one-dimensional quasi-steady Mach number zero flow allows the governing equations for a compressible gas to be simplified to a finite difference form which is very amenable to calculation and which is of such a magnitude as to be readily handled on a large digital computer.

2. With regard to the theory, the complications of natural cooling of a conducting tube wall to its surroundings pose no essential difficulty to the formulation of the overall problem.

3. A comparison of the theory with experiment shows good overall accuracy in the ability of the theory to predict tube pressure drop and gas and wall temperature distributions for the range of parameters investigated.

4. Based on the correlation of the experiment and the theory, the tube wall, in terms of a thermal energy balance, provides the entire mechanism for unsteadiness in the presence of steady boundary conditions after an initial transient flow of short duration, subject to the

limitation that the wall thickness to diameter ratio or wall heat capacity is not small.

5. The change in the pressure drop for a hot flow initiated by a step function increase in the gas inlet temperature depends on time in a manner typical of solutions to parabolic equations and is for all practical purposes a linear function of the gas inlet temperature ratio for the range of parameters investigated in this thesis.

6. Engineering predictions of pressure drop and gas and wall temperature distributions are not demanding of accurate information pertaining to the Nusselt number distribution but require only good estimates appropriate to the flow development region inasmuch as the major portion of the elevated temperature effects derive from this region.

The difficulties encountered in the present work lead to the following recommendations:

1. Experimental and analytical work dealing with the determination of the forced convection Nusselt number distribution corresponding to an arbitrary wall temperature distribution in the flow development region should be carried out.

2. Experimental and theoretical results pertaining to free convection heat transfer from long cylinders with arbitrary temperature distribution are desired from the standpoint of the proper formulation of the boundary conditions for any problem dealing with hot flow in tubes subjected to natural cooling.

3. As a matter of interest the problems dealing with the fast unsteady flow in very thin walled tubes and the quasi-steady flow in very thick walled tubes should be considered inasmuch as these limit cases are not far removed from the present problem.

APPENDIX A

EXPERIMENTAL RESULTS

Table A-1. Experimental Cold Flow Pressure Drops and Friction Factors

L/D = 400

Experiment $C\text{-}1_a$			Experiment $C\text{-}1_b$		
Rey_a	Δp_l	4f	Rey_a	Δp_l	4f
108.25	1.047	0.6610	110.34	1.056	0.6421
320.70	3.256	0.2344	320.70	3.239	0.2332
605.48	6.077	0.1228	605.48	6.060	0.1225
890.48	9.023	0.0844	881.30	9.006	0.0860
1203.45	13.541	0.0695	1249.41	13.622	0.0648
Experiment $C\text{-}1_c$			Experiment $C\text{-}1_d$		
Rey_a	Δp_l	4f	Rey_a	Δp_l	4f
112.42	1.061	0.6214	112.42	1.051	0.6157
320.70	3.270	0.2354	329.03	3.314	0.2266
596.30	5.932	0.1236	595.45	5.949	0.1243
881.30	8.976	0.0857	889.63	8.993	0.0843
1249.41	13.592	0.0647	1239.37	13.511	0.0653

L/D = 600

Experiment $C\text{-}2_a$			Experiment $C\text{-}2_b$		
Rey_a	Δp_l	4f	Rey_a	Δp_l	4f
115.10	1.532	0.5790	102.07	1.162	0.5585
332.38	4.411	0.2001	323.69	4.490	0.2148
600.19	8.523	0.1187	591.50	8.705	0.1248
886.67	13.046	0.0834	887.21	13.228	0.0844
1247.46	19.934	0.0645	1248.00	20.013	0.0647
Experiment $C\text{-}2_c$			Experiment $C\text{-}2_d$		
Rey_a	Δp_l	4f	Rey_a	Δp_l	4f
99.90	1.479	0.7421	104.24	1.664	0.7667
321.52	4.543	0.2202	325.86	4.516	0.2132
598.55	8.758	0.1227	612.13	8.731	0.1169
885.04	13.384	0.0858	889.38	13.254	0.0842
1236.58	19.963	0.0657	1240.94	20.039	0.0655

Table A-1. Continued

L/D = 800

Experiment $C\text{-}3_a$			Experiment $C\text{-}3_b$		
Rey_a	Δp_l	4f	Rey_a	Δp_l	4f
119.41	2.036	0.5364	108.36	2.087	0.6677
338.45	6.052	0.1987	329.60	6.103	0.2113
621.24	11.442	0.1117	631.23	11.705	0.1106
904.25	17.044	0.0786	914.24	17.517	0.0791
1272.53	24.575	0.0574	1282.53	25.551	0.0587
Experiment $C\text{-}3_c$			Experiment $C\text{-}3_d$		
Rey_a	Δp_l	4f	Rey_a	Δp_l	4f
106.15	1.909	0.6364	108.36	2.010	0.6433
334.03	6.030	0.2033	331.81	6.027	0.2058
616.81	11.632	0.1152	605.18	11.417	0.1174
899.82	17.234	0.0803	888.18	17.124	0.0819
1277.53	24.765	0.0574	1275.32	25.409	0.0591

L/D = 1000

Experiment $C\text{-}4_a$			Experiment $C\text{-}4_b$		
Rey_a	Δp_l	4f	Rey_a	Δp_l	4f
109.76	2.367	0.5839	114.16	2.341	0.5340
329.40	7.334	0.2012	333.79	7.203	0.1924
603.71	13.993	0.1145	617.24	13.967	0.1093
869.09	20.968	0.0829	891.78	21.365	0.0803
1226.33	30.044	0.0598	1249.03	30.693	0.0589
Experiment $C\text{-}4_c$			Experiment $C\text{-}4_d$		
Rey_a	Δp_l	4f	Rey_a	Δp_l	4f
107.57	2.443	0.6276	105.37	2.621	0.7017
331.60	7.516	0.2034	329.40	7.483	0.2053
615.05	14.280	0.1126	603.71	14.353	0.1174
907.86	21.679	0.0786	887.38	21.751	0.0825
1246.83	31.006	0.0597	1244.63	31.331	0.0606

Table A-2. Experimental Hot Flow Pressure Drop and Temperatures

Experiment No. H-1 p_a = 735.0 mm Hg

L/D = 400 T_a = 70 °F

Nominal Rey_a = 1222.4 Nominal T_1 = 612 °F

Time (min)	Δp_1 (psi)	Rey_a	T_1	T_{g_1}	T_{g_2}	T_{g_3}	T_{g_4}	T_{w_1}	T_{w_2}	T_{w_3}	T_{w_4}	T_{w_5} °F
0.25	14.63	1231.6	612	168	135	72	71	216	119	-	78	71
0.50	14.63	1231.6	-	218	163	74	71	259	162	-	88	72
0.75	14.73	1222.4	612	247	189	77	72	283	187	-	97	74
1.00	14.82	1213.2	-	263	207	79	72	296	208	-	108	76
1.25	15.32	1222.4	612	280	224	83	72	310	230	-	120	79
1.75	15.81	1231.6	612	300	246	89	72	327	245	-	139	83
2.50	16.00	1222.4	612	312	266	98	73	334	261	-	160	93
3.50	16.40	1231.6	612	317	275	107	75	337	263	-	176	103
5.50	16.59	1231.6	612	325	284	113	77	341	273	-	184	112

Experiment No. H-2 p_a = 735.0 mm Hg

L/D = 400 T_a = 70 °F

Nominal Rey_a = 854.3 Nominal T_1 = 610 °F

Time (min)	Δp_1 (psi)	Rey_a	T_1	T_{g_1}	T_{g_2}	T_{g_3}	T_{g_4}	T_{w_1}	T_{w_2}	T_{w_3}	T_{w_4}	T_{w_5} °F
0.25	9.03	854.3	607	149	115	72	71	199	106	-	73	70
0.50	9.13	854.3	-	192	135	73	70	242	145	-	79	72
0.75	9.23	845.1	607	220	157	74	70	266	168	-	85	72
1.00	9.43	845.1	-	239	176	76	71	279	185	-	92	73
1.25	9.62	854.3	609	254	189	77	70	293	204	-	99	73
1.75	9.82	854.3	609	268	209	80	71	306	220	-	113	77
2.50	9.92	854.3	609	280	222	86	71	310	230	-	128	81
3.50	10.12	854.3	611	290	237	92	71	324	243	-	143	86
5.50	10.31	854.3	615	293	242	98	72	324	239	-	152	95

Table A-2. Continued

Experiment No. H-3 p_a = 735.0 mm Hg

L/D = 400 T_a = 71 °F

Nominal Rey_a = 1207.3 Nominal T_1 = 801 °F

Time (min)	Δp_1 (psi)	Rey_a	T_1	T_{g_1}	T_{g_2}	T_{g_3}	T_{g_4}	T_{w_1}	T_{w_2}	T_{w_3}	T_{w_4}	T_{w_5} °F
0.25	15.32	1216.4	799	200	151	73	72	267	133	-	84	73
0.50	15.22	1216.4	-	272	190	77	72	331	188	-	95	77
0.75	15.32	1198.1	799	316	225	82	72	336	227	-	108	79
1.00	15.42	1189.0	-	341	251	84	72	386	253	-	121	81
1.25	16.40	1216.4	801	365	279	91	73	403	280	-	133	84
1.75	16.70	1207.3	801	385	306	97	74	423	303	-	158	92
2.50	17.19	1207.3	801	405	329	108	75	430	327	-	185	102
3.50	17.58	1207.3	802	409	338	117	77	440	327	-	201	114
5.50	18.07	1216.4	802	414	347	124	79	447	337	-	214	125

Experiment No. H-4 p_a = 735.0 mm Hg

L/D = 400 T_a = 71 °F

Nominal Rey_a = 841.0 Nominal T_1 = 832 °F

Time (min)	Δp_1 (psi)	Rey_a	T_1	T_{g_1}	T_{g_2}	T_{g_3}	T_{g_4}	T_{w_1}	T_{w_2}	T_{w_3}	T_{w_4}	T_{w_5} °F
0.25	9.53	850.1	827	176	124	73	72	243	117	-	78	68
0.50	9.53	841.0	-	243	155	75	72	307	166	-	84	72
0.75	9.62	841.0	827	281	186	75	72	345	201	-	92	73
1.00	9.72	831.8	-	311	212	80	72	369	233	-	100	74
1.25	10.12	841.0	829	281	229	69	72	386	253	-	111	76
1.75	10.31	841.0	831	350	256	84	72	403	283	-	128	79
2.50	10.61	841.0	832	375	283	93	72	423	307	-	148	85
3.50	10.80	831.8	832	385	292	100	73	423	313	-	166	92
5.50	11.10	841.0	835	400	315	108	74	444	324	-	182	100

Table A-2. Continued

Experiment No. H-5 p_a = 735.0 mm Hg

L/D = 400 T_a = 71 °F

Nominal Rey_a = 1207.3 Nominal T_1 = 973 °F

Time (min)	Δp_1 (psi)	Rey_a	T_1	T_{g_1}	T_{g_2}	T_{g_3}	T_{g_4}	T_{w_1}	T_{w_2}	T_{w_3}	T_{w_4}	T_{w_5} °F
0.25	15.71	1207.3	967	233	173	75	72	315	150	-	83	72
0.50	15.71	1207.3	-	321	221	80	72	397	217	-	96	76
0.75	16.11	1198.1	967	375	265	82	72	443	271	-	112	79
1.00	16.40	1189.0	-	405	297	86	72	473	301	-	127	82
1.25	17.38	1216.4	970	434	329	93	73	493	332	-	147	83
1.75	17.97	1207.3	971	458	361	102	74	513	362	-	175	91
2.50	18.46	1207.3	971	482	392	115	72	533	387	-	209	105
3.50	19.05	1207.3	973	492	401	126	77	538	392	-	230	115
5.50	19.54	1207.3	975	502	415	137	80	533	407	-	242	132

Experiment No. H-6 p_a = 740.4 mm Hg

L/D = 600 T_a = 69 °F

Nominal Rey_a = 1218.9 Nominal T_1 = 604 °F

Time (min)	Δp_1 (psi)	Rey_a	T_1	T_{g_1}	T_{g_2}	T_{g_3}	T_{g_4}	T_{w_1}	T_{w_2}	T_{w_3}	T_{w_4}	T_{w_5} °F
0.25	21.89	1228.1	603	174	127	73	70	208	124	-	75	72
0.50	21.89	1228.1	-	227	158	78	70	257	167	-	85	74
0.75	22.10	1228.1	603	255	184	82	70	283	201	-	93	74
1.00	22.20	1218.9	-	280	206	87	70	303	225	-	104	77
1.25	22.41	1218.9	602	294	223	93	70	319	240	-	114	78
1.75	22.82	1218.9	602	309	241	102	70	324	255	-	129	83
2.50	23.03	1218.9	604	324	259	115	71	339	269	-	148	91
3.50	23.13	1209.6	602	329	272	126	71	344	279	-	160	98
5.50	23.64	1218.9	604	334	277	137	71	349	289	-	173	109

Table A-2. Continued

Experiment No. H-7 p_a = 740.4 mm Hg

L/D = 600 T_a = 69 °F

Nominal Rey_a = 858.7 Nominal T_1 = 642 °F

Time (min)	Δp_1 (psi)	Rey_a	T_1	T_{g_1}	T_{g_2}	T_{g_3}	T_{g_4}	T_{w_1}	T_{w_2}	T_{w_3}	T_{w_4}	T_{w_5} °F
0.25	13.98	858.7	638	156	109	73	70	198	109	83	73	71
0.50	13.98	858.7	-	203	136	76	70	242	148	99	79	74
0.75	14.08	858.7	638	231	158	78	70	268	177	116	83	71
1.00	14.08	858.7	-	250	171	82	70	288	201	132	91	75
1.25	14.29	858.7	638	265	188	85	70	303	215	148	99	75
1.75	14.39	858.7	638	285	210	91	70	319	240	168	110	78
2.50	14.80	858.7	641	294	223	98	70	324	249	188	124	83
3.50	14.80	849.5	642	304	237	107	70	339	264	204	135	88
5.50	15.11	858.7	647	319	245	117	71	344	269	207	145	92

Experiment No. H-8 p_a = 740.4 mm Hg

L/D = 600 T_a = 71 °F

Nominal Rey_a = 1171.1 Nominal T_1 = 795 °F

Time (min)	Δp_1 (psi)	Rey_a	T_1	T_{g_1}	T_{g_2}	T_{g_3}	T_{g_4}	T_{w_1}	T_{w_2}	T_{w_3}	T_{w_4}	T_{w_5} °F
0.25	21.59	1171.1	790	223	146	75	72	267	143	99	79	72
0.50	21.59	1171.1	-	286	190	80	72	328	204	132	90	76
0.75	21.90	1171.1	790	331	221	86	72	369	250	163	103	77
1.00	22.00	1171.1	-	360	251	90	72	393	286	188	115	80
1.25	23.13	1171.1	791	380	274	100	72	410	303	211	128	82
1.75	23.44	1171.1	792	405	306	113	72	430	330	246	152	88
2.50	23.95	1171.1	793	424	324	128	72	444	350	268	176	96
3.50	24.67	1180.2	795	434	338	141	72	457	367	282	193	104
5.50	24.77	1171.1	796	439	342	158	73	461	364	286	202	120

Table A-2. Continued

Experiment No. H-9 p_a = 740.4 mm Hg

L/D = 600 T_a = 72 °F

Nominal Rey_a = 818.9 Nominal T_1 = 799 °F

Time (min)	Δp_1 (psi)	Rey_a	T_1	T_{g_1}	T_{g_2}	T_{g_3}	T_{g_4}	T_{w_1}	T_{w_2}	T_{w_3}	T_{w_4}	T_{w_5} °F
0.25	13.77	818.9	795	191	121	74	72	237	131	90	79	74
0.50	13.77	818.9	-	248	151	78	72	298	179	111	84	75
0.75	13.88	809.8	795	287	178	81	72	329	218	135	91	76
1.00	13.98	809.8	-	317	200	83	72	349	244	154	100	77
1.25	14.39	818.9	796	337	221	87	72	370	264	176	111	79
1.75	14.60	809.8	796	356	248	96	73	394	287	201	123	82
2.50	14.91	809.8	799	376	270	105	73	407	311	226	142	86
3.50	15.11	809.8	801	391	288	116	73	418	328	244	157	92
5.50	15.32	818.9	806	396	297	129	73	431	338	255	172	100

Experiment No. H-10 p_a = 740.4 mm Hg

L/D = 600 T_a = 73 °F

Nominal Rey_a = 1168.8 Nominal T_1 = 955 °F

Time (min)	Δp_1 (psi)	Rey_a	T_1	T_{g_1}	T_{g_2}	T_{g_3}	T_{g_4}	T_{w_1}	T_{w_2}	T_{w_3}	T_{w_4}	T_{w_5} °F
0.25	22.92	1168.8	947	259	-	80	74	317	176	110	83	75
0.50	22.92	1168.8	-	343	-	86	74	394	253	149	95	76
0.75	23.23	1159.7	947	392	-	91	74	445	309	192	112	79
1.00	23.64	1150.6	-	427	-	100	74	475	354	224	129	82
1.25	24.16	1186.9	951	456	-	111	74	500	379	250	143	84
1.75	25.29	1168.7	950	480	-	124	74	515	414	291	172	93
2.50	26.01	1168.7	951	499	-	143	74	525	434	321	202	104
3.50	26.83	1177.8	955	514	-	162	75	550	454	348	227	119
5.50	26.52	1168.7	959	518	-	180	76	555	459	348	238	134

Table A-2. Continued

Experiment No. H-11 p_a = 737.4 mm Hg

L/D = 800 T_a = 69 °F

Nominal Rey_a = 1229.4 Nominal T_1 = 597 °F

Time (min)	Δp_1 (psi)	Rey_a	T_1	T_{g_1}	T_{g_2}	T_{g_3}	T_{g_4}	T_{w_1}	T_{w_2}	T_{w_3}	T_{w_4}	T_{w_5} °F
0.25	25.10	1229.4	590	189	118	77	70	198	111	85	75	71
0.50	25.10	1229.4	-	231	149	81	70	238	146	105	82	72
0.75	25.36	1210.6	590	260	171	85	70	265	173	124	90	73
1.00	25.10	1191.8	-	280	193	90	70	282	192	144	99	75
1.25	26.11	1229.4	593	299	212	96	70	295	207	159	109	76
1.75	26.61	1229.4	594	316	237	106	70	309	225	181	126	80
2.50	26.86	1229.4	596	331	254	119	70	323	237	200	146	87
3.50	27.36	1229.4	597	339	263	131	70	329	246	210	159	95
5.50	27.61	1229.4	597	346	275	142	70	336	254	219	168	103

Experiment No. H-12 p_a = 737.4 mm Hg

L/D = 800 T_a = 70 °F

Nominal Rey_a = 858.7 Nominal T_1 = 624 °F

Time (min)	Δp_1 (psi)	Rey_a	T_1	T_{g_1}	T_{g_2}	T_{g_3}	T_{g_4}	T_{w_1}	T_{w_2}	T_{w_3}	T_{w_4}	T_{w_5} °F
0.25	17.76	858.7	608	166	104	74	71	173	100	78	75	71
0.50	17.76	858.7	-	204	126	77	71	209	131	90	79	71
0.75	17.65	840.0	608	230	145	80	71	225	154	108	84	72
1.00	17.65	849.4	-	247	161	82	71	239	170	121	90	72
1.25	18.60	868.0	615	263	178	85	71	255	185	135	97	73
1.75	18.50	868.0	617	283	198	92	71	259	197	155	108	75
2.50	18.81	868.0	620	303	220	101	71	289	224	176	125	79
3.50	19.02	868.0	624	310	233	110	71	293	230	191	137	84
5.50	19.34	858.7	629	322	244	121	71	303	239	201	147	90

Table A-2. Continued

Experiment No. H-13 p_a = 737.4 mm Hg

L/D = 800 T_a = 70 °F

Nominal Rey_a = 1232.7 Nominal T_1 = 816 °F

Time (min)	Δp_1 (psi)	Rey_a	T_1	T_{g_1}	T_{g_2}	T_{g_3}	T_{g_4}	T_{w_1}	T_{w_2}	T_{w_3}	T_{w_4}	T_{w_5} °F
0.25	26.36	1232.7	793	237	137	79	70	245	132	96	80	76
0.50	26.36	1232.7	-	300	180	85	70	300	181	123	88	77
0.75	26.86	1223.4	793	340	215	90	70	334	223	153	100	80
1.00	26.86	1195.3	-	369	242	96	70	354	252	180	113	82
1.25	27.61	1223.4	800	394	268	105	71	368	276	205	125	85
1.75	28.37	1232.7	805	418	300	118	70	389	302	236	150	89
2.50	28.87	1232.7	811	443	332	136	71	405	329	263	178	98
3.50	29.12	1232.7	816	457	350	153	71	416	336	273	196	107
5.50	29.87	1242.0	826	472	364	170	71	429	349	291	207	123

Experiment No. H-14 p_a = 737.4 mm Hg

L/D = 800 T_a = 71 °F

Nominal Rey_a = 873.1 Nominal T_1 = 815 °F

Time (min)	Δp_1 (psi)	Rey_a	T_1	T_{g_1}	T_{g_2}	T_{g_3}	T_{g_4}	T_{w_1}	T_{w_2}	T_{w_3}	T_{w_4}	T_{w_5} °F
0.25	18.39	873.1	807	214	116	75	72	233	117	87	75	72
0.50	18.39	873.1	-	272	146	77	72	287	166	107	82	72
0.75	18.50	873.1	807	311	173	80	72	311	198	126	89	73
1.00	18.60	863.8	-	336	199	84	72	335	221	146	96	74
1.25	19.02	873.1	808	355	221	89	72	345	243	167	107	76
1.75	19.24	873.1	808	385	251	97	72	366	270	194	124	79
2.50	19.55	854.5	811	400	274	108	72	379	286	217	144	82
3.50	20.08	873.1	815	414	292	121	72	396	303	235	161	88
5.50	20.40	873.1	820	434	310	137	72	406	317	243	173	99

Table A-2. Continued

Experiment No. H-15 p_a = 733.1 mm Hg

L/D = 1000 T_a = 70 °F

Nominal Rey_a = 1192.5 Nominal T_1 = 603 °F

Time (min)	Δp_1 (psi)	Rey_a	T_1	T_{g_1}	T_{g_2}	T_{g_3}	T_{g_4}	T_{w_1}	T_{w_2}	T_{w_3}	T_{w_4}	T_{w_5} °F
0.25	31.01	1183.4	601	218	113	86	70	202	123	90	77	72
0.50	31.01	1183.4	-	256	141	94	70	252	170	112	85	73
0.75	31.01	1183.4	601	283	167	100	71	279	202	133	93	75
1.00	31.01	1174.3	-	298	187	107	70	303	228	153	102	77
1.25	32.02	1201.6	603	315	207	116	71	317	245	170	112	79
1.75	32.02	1192.5	602	340	228	127	71	330	267	193	129	85
2.50	32.52	1192.5	602	349	246	139	71	337	281	208	146	91
3.50	32.77	1192.5	603	359	257	153	71	251	293	224	159	100
5.50	33.28	1192.5	605	367	266	153	71	358	301	232	169	111

Experiment No. H-16 p_a = 733.1 mm Hg

L/D = 1000 T_a = 71 °F

Nominal Rey_a = 860.1 Nominal T_1 = 612 °F

Time (min)	Δp_1 (psi)	Rey_a	T_1	T_{g_1}	T_{g_2}	T_{g_3}	T_{g_4}	T_{w_1}	T_{w_2}	T_{w_3}	T_{w_4}	T_{w_5} °F
0.25	22.51	851.1	603	193	98	78	71	184	110	81	74	72
0.50	22.51	851.1	-	231	118	80	71	226	149	97	80	72
0.75	22.62	851.1	603	255	138	81	71	256	176	114	86	73
1.00	22.72	851.1	-	272	157	84	71	270	196	126	91	74
1.25	22.83	860.1	604	286	173	86	71	287	213	142	99	74
1.75	22.93	860.1	605	303	192	90	71	304	232	161	110	77
2.50	23.15	860.1	607	316	207	96	71	314	250	179	124	88
3.50	23.57	851.1	612	323	218	100	71	324	258	188	134	94
5.50	23.99	860.1	616	333	229	109	71	331	268	198	144	92

Table A-2. Continued

Experiment No. H-17 p_a = 733.1 mm Hg

L/D = 1000 T_a = 72 °F

Nominal Rey_a = 1198.9 Nominal T_1 = 811 °F

Time (min)	Δp_1 (psi)	Rey_a	T_1	T_{g_1}	T_{g_2}	T_{g_3}	T_{g_4}	T_{w_1}	T_{w_2}	T_{w_3}	T_{w_4}	T_{w_5} °F
0.25	33.53	1198.9	807	282	130	89	72	260	150	102	84	74
0.50	33.53	1198.9	-	346	173	103	72	335	218	137	95	77
0.75	33.78	1189.9	807	386	213	111	72	370	267	168	108	79
1.00	34.03	1180.9	-	410	244	122	72	401	304	195	123	82
1.25	34.79	1180.9	807	-	-	-	-	-	-	-	-	-
1.75	35.54	1189.9	807	454	302	150	72	431	358	253	165	92
2.50	36.05	1198.9	809	474	329	172	72	458	382	283	188	103
3.50	36.55	1198.9	811	483	343	183	72	465	392	297	208	114
5.50	37.31	1198.9	812	493	352	202	72	475	415	295	219	130

Experiment No. H-18 p_a = 733.1 mm Hg

L/D = 1000 T_a = 72 °F

Nominal Rey_a = 819.9 Nominal T_1 = 814 °F

Time (min)	Δp_1 (psi)	Rey_a	T_1	T_{g_1}	T_{g_2}	T_{g_3}	T_{g_4}	T_{w_1}	T_{w_2}	T_{w_3}	T_{w_4}	T_{w_5} °F
0.25	23.04	819.9	809	239	112	83	72	244	131	92	73	73
0.50	23.04	819.9	-	297	147	87	72	312	192	115	79	73
0.75	23.36	819.9	809	332	160	94	72	343	231	139	86	73
1.00	23.46	810.9	-	361	204	100	72	370	261	162	93	75
1.25	23.99	819.9	809	381	226	105	72	387	287	185	101	76
1.75	24.20	819.9	810	401	257	116	72	401	311	210	113	80
2.50	24.63	828.9	812	420	279	131	72	424	335	236	135	84
3.50	24.73	828.9	814	430	297	146	72	438	351	255	149	93
5.50	25.15	819.9	817	444	311	161	72	445	362	263	160	104

Table A-2. Continued

Experiment No. H-19 p_a = 733.1 mm Hg

L/D = 1000 T_a = 72 °F

Nominal Rey_a = 1189.9 Nominal T_1 = 956 °F

Time (min)	Δp_1 (psi)	Rey_a	T_1	T_{g_1}	T_{g_2}	T_{g_3}	T_{g_4}	T_{w_1}	T_{w_2}	T_{w_3}	T_{w_4}	T_{w_5} °F
0.25	34.79	1189.9	946	337	147	98	72	301	165	108	82	72
0.50	34.79	1189.9	-	415	200	109	72	393	252	148	95	75
0.75	35.04	1180.9	946	459	248	122	72	439	312	190	113	78
1.00	36.05	1189.9	-	493	284	135	72	469	353	226	130	81
1.25	36.30	1189.9	946	517	311	146	72	494	383	256	147	86
1.75	37.06	1189.9	948	541	348	165	72	514	418	293	174	93
2.50	37.56	1189.9	951	560	379	187	72	534	443	323	204	104
3.50	38.32	1198.9	956	574	398	206	72	549	453	344	225	116
5.50	39.08	1189.9	956	584	416	230	72	563	473	357	247	137

APPENDIX B

EXPERIMENTAL REYNOLDS NUMBERS AND FRICTION FACTORS

For the tube flow experiments, the Reynolds number based on ambient conditions is defined as

$$Rey_a = \frac{GD_i}{\mu_a} \tag{B.1}$$

The friction factor for the calibrated Poiseuille tube is given for fully developed flow as

$$4f_p = \frac{64\mu_a}{G_p D_p} = \frac{2\rho_3 \Delta p_2}{G_p{}^2 (L/D)_p} \tag{B.2}$$

where G_p and Δp_2 denote the mass flux and pressure drop, respectively, of the Poiseuille tube. Equating the total mass flow rates through both tubes gives

$$G = \frac{G_p D_p{}^2}{D_i{}^2} \tag{B.3}$$

and substituting for G_p from equation (B.2) gives the mass flux in the test tube as

$$G = \frac{\rho_3 \Delta p_2}{\mu_a} \left[\frac{D_p{}^2}{D_i{}^2} \frac{D_p}{32(L/D)_p} \right] \tag{B.4}$$

Then from equation (B.1) and (B.4) the Reynolds number for the flow in the test tube is given as

$$Rey_a = K \frac{\rho_3 \Delta p_2}{\mu_a^2} \tag{B.5}$$

with

$$K = \frac{D_p^4}{32 D_i L_p}$$

The Poiseuille tube used in these experiments had a length of 100.00 inches and an internal diameter of 0.198 inches, which together with the test tube diameter, given in Table I, yields

$$K = 2.85077 \times 10^{-8} \text{ ft}^2 \tag{B.6}$$

Finally, the viscosity coefficient is found from the linear formula

$$\mu_a = (340.0 + 0.57\ T_a) 10^{-9} \tag{B.7}$$

The friction factor is defined in terms of the mass flux in the test tube as

$$4f = \frac{2\rho_1 \Delta p_1}{G^2\ L/D} \tag{B.8}$$

which is readily found from the measured test tube pressure drops and equation (B.4).

In all of the tube flow experiments of the present work the flow in the Poiseuille tube is cold, that is, the temperature corresponds to

ambient or room temperature. Consequently the density ρ_3 is for all practical purposes the same as the ambient density ρ_a. Likewise, for cold flow in the test tube, the density ρ_1 is the same as ρ_a. Thus equations (B.5) and (B.8) for the Reynolds number based on ambient temperature and the cold flow friction factor may be utilized in the present work in the following forms:

$$Rey_a = K \frac{\rho_a \Delta p_2}{\mu_a^2} \tag{B.9}$$

$$4f = \frac{2\rho_a \Delta p_1}{G^2 \, L/D} \tag{B.10}$$

APPENDIX C

INTEGRAL TUBE FLOW GOVERNING EQUATIONS

The governing equations for the flow of a viscous, heat conducting, compressible fluid through a tube are the statements of conservation of mass, momentum, and energy together with an equation of state. Inasmuch as these statements may be found in the literature in a variety of different forms, often subjected to some restrictions, it is considered appropriate to present here a brief development of the equations from first principles to a general form appropriate to the present problem.

Integral Equations

The general formulation of the conservation laws may be referenced to a stationary control volume V with enclosing surface A. An element of area of A is given by $n_i dA$ where n_i, the unit normal to A, is taken positive outward. The surface force acting on this area element is $P_i dA$ with P_i, the stress vector, conventionally defined by

$$P_i = (-p\,\delta_{ik} + \tau_{ik})n_k \qquad (C.1)$$

The heat flux through the area element is likewise given as $q_i n_i dA$ where q_i represents the heat flux vector.

The conservation laws as referenced to the control volume may then be stated in terms of integral equations (26) as follows by utilizing the definition (C.1):

$$\int_V \frac{\partial \rho}{\partial t}\, dV + \int_A \rho\, u_j n_j\, dA = 0 \tag{C.2}$$

$$\int_V \frac{\partial}{\partial t}(\rho\, u_i)dV + \int_A \rho\, u_i u_j n_j\, dA = \int_V \rho\, f_i\, dV \tag{C.3}$$

$$-\int_A p\, n_i\, dA + \int_A \tau_{ik}\, n_k\, dA$$

$$\int_V \frac{\partial}{\partial t}\left[\rho\,(e+\frac{1}{2}\, u_k u_k)\right]dV + \int_A \rho\,(e+\frac{1}{2}\, u_k u_k) u_j n_j dA \tag{C.4}$$

$$= \int_V \rho\, f_k u_k dV - \int_A p\, u_k n_k dA$$

$$+ \int_A \tau_{jk} u_j n_k dA - \int_A q_j n_j dA$$

The energy equation (C.4) is commonly referred to as the total energy equation as opposed to the thermal energy equation which is more suitable for problems, like the present one, involving heat transfer. The thermal energy equation is formulated in a conventional way by obtaining the mechanical energy equation from the momentum equation (C.3) and subtracting this result from the total energy equation (C.4). First it is convenient to rewrite equations (C.3) and (C.4) after transforming the surface integrals into their corresponding volume integrals with the aid of the divergence theorem to yield

$$\int_V \frac{\partial}{\partial t}(\rho\, u_i)dV + \int_V \frac{\partial}{\partial x_j}(\rho\, u_i u_j)dV = \int_V \rho\, f_i dV \tag{C.5}$$

$$-\int_V \frac{\partial p}{\partial x_i}\, dV + \int_V \frac{\partial}{\partial x_k}(\tau_{ik})dV$$

$$\int_V \frac{\partial}{\partial t}\left[\rho\left(e+\frac{1}{2}u_k u_k\right)\right]dV + \int_V \frac{\partial}{\partial x_j}\left[\rho\left(e+\frac{1}{2}u_k u_k\right)u_j\right]dV \qquad (C.6)$$

$$= \int_V \rho f_k u_k dV - \int_V \frac{\partial}{\partial x_k}(p u_k)dV$$

$$+ \int_V \frac{\partial}{\partial x_k}(\tau_{jk} u_j)dV - \int_V \frac{\partial q_j}{\partial x_j} dV$$

The mechanical energy equation is then obtained from the momentum equation (C.5) by dotting it with the velocity vector u_i which gives

$$\int_V \frac{\partial}{\partial t}\left(\rho \frac{u_i u_i}{2}\right)dV + \int_V \frac{\partial}{\partial x_j}\left(\rho \frac{u_i u_i}{2} u_j\right)dV = \int_V \rho u_i f_i dV \qquad (C.7)$$

$$- \int_V \frac{\partial}{\partial x_i}(p u_i)dV + \int_V p \frac{\partial u_i}{\partial x_i} dV$$

$$+ \int_V \frac{\partial}{\partial x_k}(u_i \tau_{ik})dV - \int_V \tau_{ik} \frac{\partial u_i}{\partial x_k} dV$$

and finally the mechanical energy equation (C.7) is subtracted from the total energy equation (C.6) to leave

$$\int_V \frac{\partial}{\partial t}(\rho e)dV + \int_V \frac{\partial}{\partial x_j}(\rho e u_j)dV$$

$$= \int_V p \frac{\partial u_j}{\partial x_j} dV - \int_V \frac{\partial q_j}{\partial x_j} dV$$

This equation, termed the thermal energy equation, may be expressed in a more convenient form by utilizing the divergence theorem again to transform the last integral on each side of the equation back into its corresponding area integral. This gives

$$\int_V \frac{\partial}{\partial t}(\rho e)dV + \int_A \rho e\, u_j n_j dA \qquad (C.8)$$

$$= -\int_V p \frac{\partial u_j}{\partial x_j} dV - \int_A q_j n_j dA$$

The continuity, momentum, and thermal energy equations (C.2), (C.3), and (C.8), respectively, together with the equation of state constitute the general governing laws as applied to the tube flow problem by specification of a control volume, use of appropriate nomenclature for the tube flow, and incorporation of the assumption of an essentially boundary-layer-like flow.

Tube Flow Integral Equations

The method of approximate treatment of viscous flow problems as applied to tube flow requires the governing laws for conservation of mass, momentum, and energy to be satisfied with reference to the simple cylindrical tube control volume shown in Figure C-1. The volume so chosen is enclosed by two cross-sectional area elements A_1 normal to the tube axis and the differential area element dA_2 comprising a length dx of the tube inner wall. This choice of control volume is obviously consistent with physical reasoning aimed at maximum simplification of the governing equations utilizing the approximately parallel character of the tube flow.

The boundary-layer-like character of the flow is essentially an approximation which is incorporated, as in the derivation of the Prandtl boundary layer equations, to delete the longitudinal transport of momentum and energy by the diffusion processes associated with viscosity and

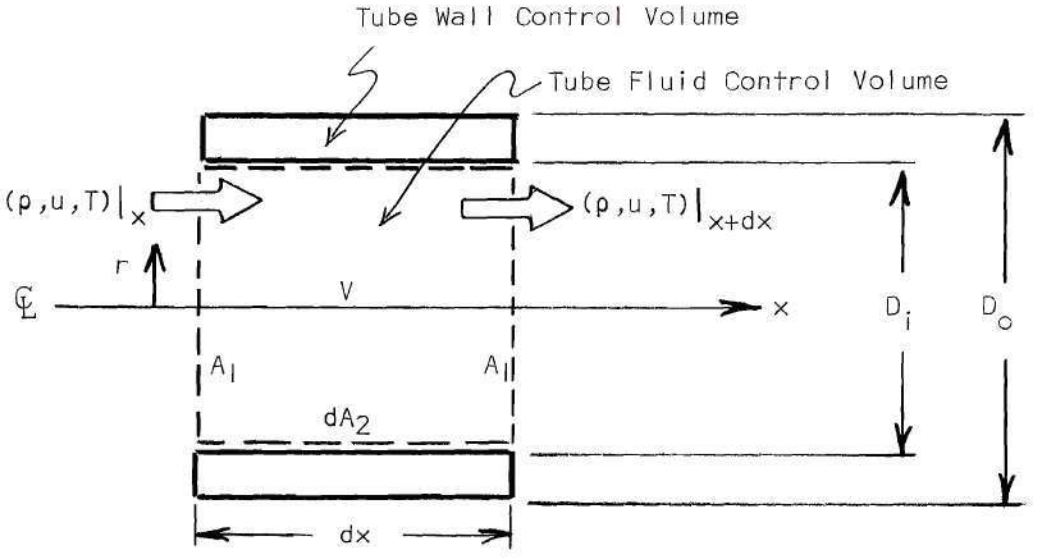

$$A_I|_x = A_I|_{x+dx} = \frac{\pi D_i^2}{4}$$

$$dA_2 = \pi D_i dx$$

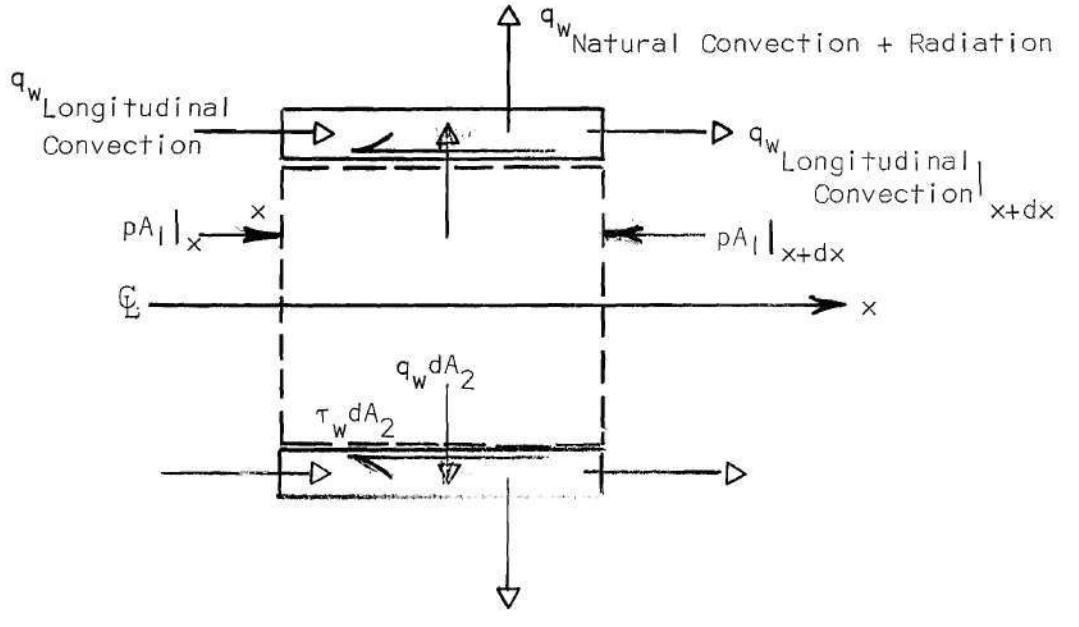

Figure C-1. Tube Control Volume

thermal conductivity. This characteristic of the flow together with the neglect of body forces allows one to simplify the general integral equations (C.2), (C.3), and (C.8) by considering that only the forces and heat fluxes shown in Figure C-1 are significant. Under these assumptions the transverse momentum equations are of higher order, the radial variation of pressure is negligible, and the governing equations reduce to

$$\int_V \frac{\partial \rho}{\partial t}\, dV + \int_{A_1 A_1} \rho\, u\, dA_1 = 0 \tag{C.9}$$

$$\int_V \frac{\partial}{\partial t}(\rho u) dV + \int_{A_1 A_1} \rho\, u^2\, dA_1 = \int_{A_1 A_1} p\, dA_1 + \int_{A_2} \tau_w\, dA_2 \tag{C.10}$$

$$\int_V \frac{\partial}{\partial t}(\rho e) dV + \int_{A_1 A_1} \rho e u\, dA_1 = -\int_V p\, \frac{\partial u}{\partial x}\, dV - \int_{A_2} q_w\, dA_2 \tag{C.11}$$

These equations constitute a one-dimensional representation of unsteady tube flow inasmuch as the integrals may be regarded as the dependent variables and are functions of the independent variables x and t alone. The dependence of the cross-section area integrals on x may be demonstrated by expansions in Taylor's series and the resulting equations, after neglecting higher order terms, are the corresponding

differential equations governing the integral-variables. These equations are examined individually in the following sections.

Conservation of Mass

The conservation of mass principle, equation (C.9), applied to the tube control volume of Figure C-1 may be expanded to yield

$$2\pi \frac{\partial}{\partial t}\int_o^R \rho r\, dr\, dx + \frac{\partial}{\partial x}\left[2\pi\int_o^R \rho u r\, dr\right] dx = 0 \qquad (C.12)$$

Interpretation of the integral quantities in equation (C.12) as the dependent variables is consistent with the definition of their equivalent cross-section average values given by

$$\overline{\rho u}\, A_1 = 2\pi\int_o^R \rho u r\, dr \qquad (C.13)$$

and

$$\overline{\rho}\, A_1 = 2\pi\int_o^R \rho r\, dr \qquad (C.14)$$

so that equation (C.12) may be expressed as

$$\frac{\pi D_1^2}{4}\frac{\partial \overline{\rho}}{\partial t} + \frac{\pi D_1^2}{4}\frac{\partial}{\partial x}\overline{\rho u} = 0 \qquad (C.15)$$

Conservation of Momentum

The principle of conservation of longitudinal momentum, given by equation (C.10), when expanded in terms of the momentum fluxes, the longitudinal pressure gradient, and the wall shear stress corresponding

to the tube control volume becomes, after neglecting higher order terms,

$$2\pi \frac{\partial}{\partial t}\int_o^R \rho u r \, dr \, dx + \frac{\partial}{\partial x}\left[2\pi \int_o^R \rho u^2 \, r dr\right] dx \qquad (C.16)$$

$$= \left(-\frac{\partial p}{\partial x} dx\right) \frac{\pi D_l^2}{4} - \tau_w \pi D_l \, dx$$

The cross-section average momentum flux defined as

$$\overline{\rho u^2} A_l = 2\pi \int_o^R \rho u^2 \, r dr \qquad (C.17)$$

together with equation (C.13), then allows equation (C.16) to be expressed as

$$\frac{\pi D_l^2}{4} \frac{\partial}{\partial t} \overline{\rho u} + \frac{\pi D_l^2}{4} \frac{\partial}{\partial x} \overline{\rho u^2} + \frac{\pi D_l^2}{4} \frac{\partial p}{\partial x} + \pi D_l \tau_w = 0 \qquad (C.18)$$

Conservation of Energy

The energy conservation principle, equation (C.11), for the tube control volume, following the expansion procedure for the previous equations, similarly yields

$$2\pi \frac{\partial}{\partial t}\int_o^R \rho e r \, dr \, dx + \frac{\partial}{\partial x}\left[2\pi \int_o^R \rho e u r \, dr\right] dx \qquad (C.19)$$

$$= -2\pi \int_o^R p \frac{\partial u}{\partial x} r dr \, dx - q_w \pi D_l \, dx$$

or

$$\frac{\pi D_I^2}{4} \frac{\partial}{\partial t} \overline{\rho e} + \frac{\pi D_I^2}{4} \frac{\partial}{\partial x} \overline{\rho e u} + \frac{\pi D_I^2}{4} p \frac{\partial \bar{u}}{\partial x} \tag{C.20}$$

$$+ \pi D_I q_w = 0$$

with appropriate averages defined by

$$\overline{\rho e} A_I = 2\pi \int_o^R \rho e r \, dr \tag{C.21}$$

$$\overline{\rho e u} A_I = 2\pi \int_o^R \rho e u r \, dr \tag{C.22}$$

$$\bar{u} A_I = 2\pi \int_o^R u r \, dr \tag{C.23}$$

Governing Equations

The governing equations (C.15), (C.18), and (C.20) provide a description of tube flow in terms of the one-dimensional variables $\bar{u}$, $\bar{\rho}$, $\overline{\rho u}$, $\overline{\rho u^2}$, $\overline{\rho e}$, $\overline{\rho e u}$, p, τ_w, and q_w which in general are dependent on longitudinal position and time. From the one-dimensional viewpoint, the equation of state is also averaged over the cross-section, thus introducing the additional variable $\overline{\rho T}$. For reference purposes these equations are collected together and given as follows after division by the cross-sectional area A_I:

$$\frac{\partial \bar{\rho}}{\partial t} + \frac{\partial}{\partial x} \overline{\rho u} = 0 \tag{C.24}$$

$$\frac{\partial}{\partial t} \overline{\rho u} + \frac{\partial}{\partial x} \overline{\rho u^2} + \frac{\partial p}{\partial x} + \frac{4}{D_I} \tau_w = 0 \tag{C.25}$$

$$\frac{\partial}{\partial t}\overline{\rho e} + \frac{\partial}{\partial x}\overline{\rho e u} + p\frac{\partial \bar{u}}{\partial x} + \frac{4}{D_I}q_w = 0 \qquad \text{(C.26)}$$

$$p = \overline{\rho T}\,R \qquad \text{(C.27)}$$

LITERATURE CITED

1. Hagen, G., "On the Motion of Water in Narrow Cylindrical Tubes," Poggendorff's Annalen der Physik und Chemie, 46, p. 423 (1839).

2. Poiseuille, J. L. M., Comptes Rendus, 11, p. 961 (1840); 12, p. 112 (1841); Memoires des Savants Etrangers, 9, p. 433 (1846).

3. Reynolds, O., "An Experimental Investigation of the Circumstances Which Determine whether the Motion of Water Will Be Direct or Sinuous, and of the Law of Resistance in Parallel Channels," Philosophical Transactions of the Royal Society of London, 174, p. 935 (1883).

4. Goldstein, S., Modern Developments in Fluid Mechanics (Dover Publications, Inc., New York, 1965), Vol. I, pp. 298-309.

5. Boussinesq, J., Comptes Rendus, 113, p. 9 (1891).

6. Schiller, L., "Investigations on Laminar and Turbulent Flow (German)," Zeitschrift fuer Angewandte Mathematik und Mechhanik, 2, p. 96 (1922).

7. Prandtl, L. and Tietjens, O. G., Applied Hydro- and Aeromechanics (Dover Publications, Inc., New York, 1957), pp. 14-29.

8. Langhaar, H. L., "Steady Flow in the Transition Length of a Straight Tube," Journal of Applied Mechanics, 9, p. 55 (1942).

9. Hornbeck, R. W., "Laminar Flow in the Entrance Region of a Pipe," Applied Scientific Research, A13, p. 224 (1964).

10. Graetz, L., Annalen der Physik, 18, p. 79 (1883); 25, p. 337 (1885).

11. Nusselt, W., Zeitschrift des Vereines deutscher Ingenieure, 54, p. 1154 (1910).

12. Jakob, M., Heat Transfer (John Wiley and Sons, Inc., New York, 1949), Vol. I, pp. 451-464, 543-547.

13. Sellars, J. R., Tribus, M., and Klein, J. S., "Heat Transfer to Laminar Flow in Round Tube or Flat Conduit," Transactions of the A. S. M. E., 78, p. 441 (1956).

14. Kays, W. M., "Numerical Solutions for Laminar-Flow Heat Transfer in Circular Tubes," Trans. ASME, 77, p. 1265 (1955).

15. Kays, W. M. and London, A. L., "Convective Heat-Transfer and Flow-Friction Behavior of Small Cylindrical Tubes - Circular and Rectangular Cross Sections," Trans. ASME, 74, p. 1179 (1952).

16. Ulrichson, D. L. and Schmitz, R. A., "Laminar-Flow Heat Transfer in the Entrance Region of Circular Tubes," International Journal of Heat and Mass Transfer, 8, p. 253 (1965).

17. Tribus, M. and Klein, J., "Forced Convection from Nonisothermal Surfaces," Heat Transfer, A Symposium (Univ. of Mich. Press, Ann Arbor, Mich., 1953), p. 211.

18. Deissler, R. G., "Analytical Investigation of Fully Developed Laminar Flow in Tubes with Heat Transfer with Fluid Properties Variable Along the Radius," NACA TN 2410 (1951).

19. Sze, B. C., "The Effect of Temperature-Dependent Fluid Properties on Heat Transfer and Flow Friction for Gas Flow," Ph.D. Dissertation, Stanford University (1957).

20. Davenport, M. E., and Leppert, G., "The Effect of Transverse Temperature Gradients on the Heat Transfer and Friction for Laminar Flow of Gases," Trans. ASME, 87, p. 191 (1965).

21. Dusinberre, G. M., "Calculation of Transient Temperatures in Pipes and Heat Exchangers by Numerical Methods," Trans. ASME, 76, p. 421 (1954).

22. Rooks, W. M., "A Theoretical Analysis of Unsteady Laminar Flow of Air in Tubes Subjected to Elevated Inlet Temperatures," M.S. Thesis, Georgia Institute of Technology, Atlanta, Georgia (1962).

23. Ducoffe, A. L. and White, F. M., Jr., "A Theoretical and Experimental Study for the Prediction of Pneumatic Pressure Lag Inherent in Typical Ballistic Missile Plumbing Systems," Army Ballistic Missile Agency, DA-01-009-ORD-595 (1959).

24. Ducoffe, A. L. and White, F. M., Jr., "An Analytical and Experimental Investigation of Steady and Unsteady Flow in Tubing, with Special Application to Simulated Missile Pressure-Sensing Systems," Sandia Corporation Research Report SC-4544 (RR) (1961).

25. Eckert, E. R. G., Heat and Mass Transfer (McGraw-Hill Book Co., Inc., New York, 1959), 2nd ed., p. 190.

26. Moore, F. K. (Edt.), Theory of Laminar Flows, High Speed Aerodynamics and Jet Propulsion, Vol. IV (Princeton University Press, Princeton, 1964), pp. 26-27, 187.

27. Bird, R. B., Stewart, W. E., and Lightfoot, E. N., Transport Phenomena (John Wiley and Sons, Inc., New York, 1960), p. 413.

28. Fox, L., Numerical Solution of Ordinary and Partial Differential Equations (Addison-Wesley Publishing Co., Inc., Reading, Massachusetts, 1962), p. 20.

29. Richtmeyer, R. D., Difference Methods for Initial-Value Problems (Interscience Publishing Co., New York, 1957), p. 101.

VITA

Arthur Chilton Bruce was born in Greensboro, North Carolina, on February 28, 1933. He attended public schools in Greensboro and in Bluefield, West Virginia, completing high school in 1951. In 1955 he received the Bachelor of Science degree in Aeronautical Engineering from the Virginia Polytechnic Institute and accepted a position there as Instructor of Aeronautical Engineering while completing requirements for the Master of Science degree which was awarded in 1957. After initiating graduate work leading to a doctoral degree at the Massachusetts Institute of Technology in 1958, he transferred to the Georgia Institute of Technology in 1961 to complete his graduate work. In September of 1964 he accepted a position as Assistant Professor of Aerospace Engineering at The Georgia Institute of Technology, a position which he held until September of 1967. At that time he joined the faculty of Louisiana Polytechnic Institute as an Associate Professor of Mechanical Engineering, a position which he holds at the present time.

In October, 1957, he married the former Joyce Clementine Stallard of Bluefield, West Virginia. They have three children, Kimberly Elizabeth, John Reeve, and Catherine Rachelle Bruce.